eman ta zabal zazu

Universidad del País Vasco

Euskal Herriko Unibertsitatea

EFFECTS OF ACUTE AND CHRONIC RESTRAINT STRESS DURING ADOLESCENCE ON ENDOCANNABINOID-MEDIATED SYNAPTIC PLASTICITY IN THE MOUSE HIPPOCAMPAL DENTATE GYRUS

DOCTORAL THESIS

Naiara Royo Zubillaga

Leioa 2019

eman ta zabal zazu

Universidad del País Vasco

Euskal Herriko Unibertsitatea

NEUROZIENTZIAK SAILA
DEPARTAMENTO DE NEUROCIENCIAS
MEDIKUNTZA ETA ERIZAINTZA FAKULTATEA
FACULTAD DE MEDICINA Y ENFERMERÍA

Doctoral Thesis presented by Lda.

NAIARA ROYO ZUBILLAGA

Financed by Predoctoral (PhD) contract for training of researchers from Universidad del País Vasco/Euskal Herriko Unibertsitatea (UPV/EHU)

Supervised by:

Prof. Dr. PEDRO ROLANDO GRANDES MORENO

Prof. Dra. NAGORE PUENTE BUSTINZA

Department of Neurosciences

Faculty of Medicine and Nursing

University of the Basque Country UPV/EHU

Achucarro Basque Center of Neurosciences, Scientific Park of UPV/EHU

Leioa, 2019

0. AGRADECIMIENTOS

Dicen que lo más sencillo de la tesis son los agradecimientos, sin embargo a mí no me lo parece. Seré escueta, ya que como sabéis no soy persona de mucha verborrea, y además por muy rico que pueda ser nuestro lenguaje hay cosas que no se pueden explicar con palabras.

Después de cinco años, lo que parecía una cosa lejana ya está terminando: la etapa de la tesis llega a su fin. Por suerte, o al menos así lo veo yo, esta parte de mi vida nunca se cerrará del todo, porque ha sido tanto lo aprendido y vivido a nivel personal y profesional, que me acompañará el resto de mis días.

En primer lugar, quisiera agradecer a mis directores de tesis, el Dr. Pedro Grandes y la Dra. Nagore Puente. Pedro, gracias por darme la oportunidad, sin apenas conocerme, de realizar la tesis bajo tu tutela y formar parte de este grupo de profesionales que diriges. Gracias también por facilitarme el poder realizar mi estancia en la University British Columbia, donde viví una de las mejores experiencias de mi vida en todos los aspectos. Nagore, gracias por adentrarme en el mundo de la electrofisiología que tanto me apasiona. Gracias por estar ahí, dispuesta a escuchar y ayudarme en este camino. Gracias a los dos, por vuestras sugerencias que siempre han sido constructivas, y esto no todo el mundo lo puede decir.

Gracias a los doctores Izaskun, Juan, Sonia, Edgar y Leire por vuestros ánimos y ayuda cuando os la he pedido. Izas, gracias por tus ideas en las reuniones.

Gracias a las post-doc Iran, Iani, Ana y Sara. Por vuestros conocimientos, ayuda, apoyo y cariño dentro del labo pero especialmente fuera. Gracias, por vuestras risas y hombros donde apoyarme cuando algo no iba tan bien. Seguiremos en contacto, no creáis que os habéis librado de mí.

Gracias a las técnicas Elsa y Yolanda. Elsa, gracias por tus cuidados y apoyo. Yolanda, quiero agradecerte especialmente tu ayuda en la experimentación, gracias por facilitarme el trabajo.

Mucho ánimo, suerte y a seguir trabajando duro como hasta ahora a todos los doctorandos: Itzi T, Jon, Itzi B, Svein y María.

También quiero agradecer al grupo del Dr. Joan Sallés, y al propio Dr. Sallés, por su colaboración en esta tesis y su disponibilidad para responder a cualquier tipo de duda.

On the other hand, I want to express my gratitude to Dr. Brian Christie, for opening the doors of his group to do my international internship. Thank you for your knowledge of electrophysiology, but especially for treating me like a member of your group, both inside and outside of the lab. I also want to give thanks to all my Canadian colleagues: Cris, Scott, Juantxo, Christine, Katie, Melissa, Wesley and Angela. From the first day, I felt like a regular member of your group. Thank you for making me feel valued and loved. Scott, thanks for teaching me your knowledge of patch clamp, and for trying to make difficult explanations easier to understand. Cris and Juantxo, I want to express my gratitude for all your help before I arrived in Victoria, but especially your support there. Thank you for all the good moments outside the lab.

My experience abroad would have been totally different If I had not met my Canadian family (Majo, I.K, Bea, Nóirín, Jannet, Josefine, María, Cristina and Olena). Thanks for taking care of me and making me not feeling foreign. Thank you for all the great little gestures that have made me feel so loved. We will keep in touch like so far up to now.

Siempre he pensado que recorrer tu camino acompañado de buenos amigos es fundamental en esta vida, y una vez más así lo he podido comprobar. Todo este recorrido hubiese sido mucho más arduo si no hubiese contado con mi gente ("Pamplonicas" y Bilbaínas). Esos amigos que te hacen reír, te escuchan, te echan un cable o que simplemente están ahí. Sandra, Estefi y Susi a vosotras tengo que daros especialmente las gracias por compartir "mis locuras". Zulu, Sandra, Lu y Majo: Gracias

por todas esas horas en las que me habéis escuchado hablar ilusionada sobre este trabajo, aunque os pareciese que hablara en chino, pero gracias especialmente por todos vuestros pequeños grandes detalles de cariño.

Y por último, quiero dar las gracias con mayúsculas, a las dos personas que más han creído en mí y han tenido que soportar en este proceso: mis padres. Sin vosotros, sin vuestro amor y apoyo incondicional, ánimo inquebrantable y paciencia infinita, esta tesis no hubiese sido posible. Gracias por todo lo que me habéis dado y enseñado.

A todos, MUCHAS GRACIAS.

INDEX

1. SUMMARY

Our society lives embedded in stress. This causes numerous environmental factors that precipitate and exacerbate psychiatric disorders, such as anxiety and depression. In all organisms, stress is recognized as an adaptive response and is essential for survival to re-establish homeostasis. The brain is the most sensitive organ to stress and responsible for generating an adaptation to stressors, both social and physical. In mammals, multiple brain areas, such as the hippocampus, amygdala, prefrontal cortex and hypothalamus are activated in response to the threat of homeostasis disruption. In particular, the hippocampus is critically involved in many forms of learning and memory, as well as emotional processing and stress.

Despite adolescence being a vital stage where numerous changes occur, research on changes in stress-related synaptic plasticity and the brain has been focused more on childhood and adulthood.

The endocannabinoid (eCB) system is widely distributed in the central nervous system and participates in many brain functions. To better understand the role of the eCB system in the context of anxiety and how to cope stress is necessary an integrated view of the endocannabinoid-mediated control in brain regions involved in stress processing and regulation.

In this Doctoral Thesis, adolescent Swiss male mice were used to investigate the localization and function of the CB_1 receptor at the excitatory medial perforant path (MPP) synapses in the dentate molecular layer (DML) of the hippocampus in control, acute and chronic restraint stress condition. The rational behind is that these synapses show high efficiency in neuronal activation and contribute to the excitatory tri-synaptic circuit related to learning and memory in the hippocampus. Furthermore, restraint stress damages the entorhinal cortex and dentate gyrus affecting the entorhino-dentate (perforant) pathway. We studied in the Thesis the effect of acute and chronic restraint stress to adolescent mice on synaptic transmission and in particular on CB_1 receptor-dependent long-term depression at the excitatory MPP-granule cell synapses (eCB-eLTD).

2. INTRODUCTION

2.1 The stress

Daily life is very stressful and exhibits numerous environmental factors that precipitate and exacerbate psychiatric disorders such as depression and anxiety. Indeed, homotypic stressors (repeated exposure to the same stressor) that occur on a daily basis are associated with increased depressive symptoms (Robertson Blackmore *et al*., 2007; Patel and Hillard, 2008).

In all organisms, the stress is a biological cascade of events that occurs in a real or perceived threat and is vital for the survival, impacting on energy homeostasis that is profoundly affected by acute and chronic stress (Ulrich-Lai and Ryan, 2014; Razzoli and Bartolomucci, 2016; Sticht *et al*., 2018).

Stress and adaptation to social and physical stressors depend on the brain. It determines the threats, stores memories and regulates physiology as well as behavior (McEwen, 2006; McEwen *et al*., 2015). Specifically, some brain areas (hippocampus, amygdala, prefrontal cortex, and hypothalamus) are activated in mammals in response to threats to homeostasis switching on a cascade of neural, neuroendocrine and behavioral responses (Senst and Bains, 2014).The amygdala elaborates a preconscious threat detection and attributes an emotional value in the context of previous experiences through a crosstalk with the medial prefrontal cortex and the hippocampus (Bishop, 2008; Hermans *et al*., 2014; Likhtik and Paz, 2015; Roozendaal *et al*., 2009).

Stressful conditions change the eCB signaling and increase the susceptibility to psychiatric disorders (Hill *et al*., 2010; Hillard, 2014). The impact of stress over the eCB system is complex and depends on factors such as duration, intensity, stressor type and brain region (Patel *et al*., 2004; Rubino *et al*., 2008; Campos *et al*., 2010; Hill *et al*., 2010; Razzoli *et al*., 2017; Sticht *et al*., 2018).

2.1.1 Stress and adolescent brain

Adolescence is a period of significant psychological and physiological vulnerabilities. Depression, anxiety, schizophrenia and drug abuse increase in the adolescence (Dahl, 2004; Patton and Viner, 2007; Eiland and Romeo, 2013) and some authors have proposed that exposure to stressors during this period plays a significant role in the development of the disorders (Charil *et al.,* 2010; McCormick and Mathews *et al.,* 2010; Romeo, 2017). Moreover, the negative effects of stress are exacerbated when they happen during the prenatal or neonatal stages of significant brain maturation (McEwen, 2008; Charil *et al*., 2010).

The vast majority of research has been focused on the effects of stress in childhood and adulthood; however there is an increasing interest in investigating brain structure and plasticity under stress conditions during the adolescence (McCormick and Mathews, 2010; Eiland and Romeo, 2013), in particular in the hippocampal formation which is critically involved in learning and memory, emotional processing and stress reactivity (Fanselow and Dong, 2010; Romeo, 2017).

2.2 The Endocannabinoid System

The Cannabis plant (*cannabis sativa)* has been used for therapeutic (antiemetic, analgesic, antispasmodic effects) and recreational purposes since ancient times (Piomelli, 2003; Freund *et al*., 2003; Mechoulam and Parker, 2013). The Cannabis plant contains more than 400 different chemical compounds. In the1960s, the Mechoulam team isolated and described more than 60 cannabinoids among which delta (9) - tetrahydrocannabinol (Δ9-THC or THC) is the main psychoactive compound (Gaoni and Mechoulam, 1964). In the 1990s, the THC receptors were cloned and termed cannabinoid CB_1 receptor (CB_1R) (Matsuda *et al*., 1990) and cannabinoid CB_2 receptor (CB_2R) (Munro *et al*., 1993).

In parallel with these discoveries, endogenous ligands for the cannabinoid receptors were identified and named endocannabinoids (Devane *et al*., 1992; Mechoulam *et al*., 1995). The most studied eCBs are derived from membrane phospholipids, particularly arachidonoyl ethanolamide or anandamide (AEA), and 2-arachidonoyl glycerol (2-AG) (Maccarrone *et al*., 2014; Scarante *et al*., 2017). Both AEA and 2-AG have been regarded as the two main eCBs in animal´s tissue. Altogether, the eCB system composed of the cannabinoid receptors, eCBs, their synthesizing and degrading enzymes, the intracellular signaling pathways and transport systems, provides the basis for the endogenous modulation of many functions in the nervous system and peripheral organs.

2.2.1 Endocannabinoid Receptors

CB_1R and CB_2R are seven transmembrane receptors coupled to $G_{i/o}$ protein (Figure 1). They operate functionally inhibiting adenylyl cyclase activity, activating potassium channels and inhibiting voltage-gated calcium channels (Howlett *at al.*, 2002; Kano, 2014).

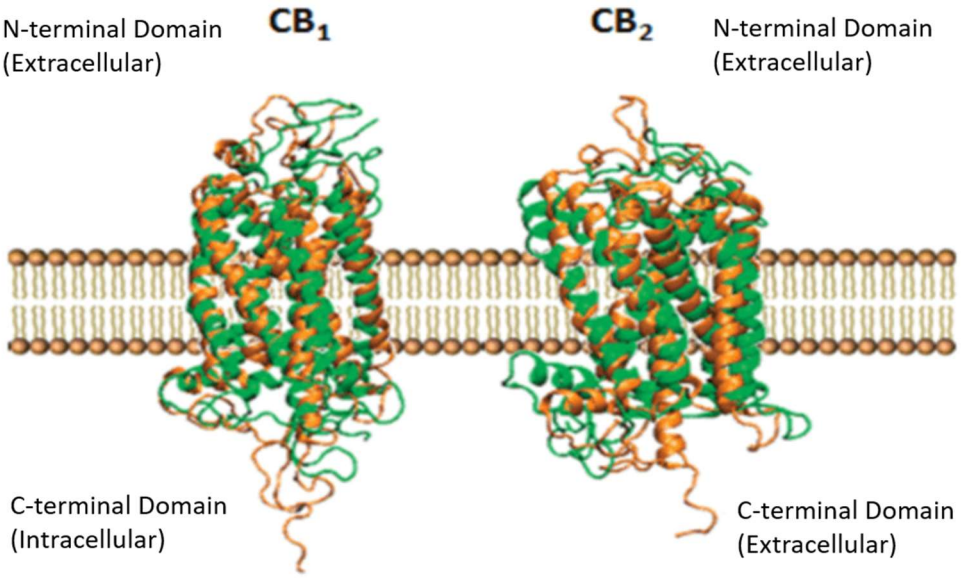

Figure 1: Three-dimensional structure of CB_1R and CB_2R. Modified from Fraguas-Sánchez *et al*., 2014.

2.2.1.1 CB_1 Receptor

CB_1R is highly expressed in the central nervous system (CNS) and is present in neuronal and non-neuronal cells and also intracellularly throughout the brain. In neurons, the CB_1R expression is very high in the prefrontal cortex (PFC), cingulate gyrus, hippocampus, basal ganglia, substantia nigra and cerebellum (Mackie, 2005; Hillard, 2014; Gutiérrez-Rodríguez *et al*., 2017). Also, astrocytes (Salio, 2002; Navarrete and Araque, 2008, 2010; Han *et al*., 2012; Bonilla-Del Río *et al*., 2017; Gutiérrez-Rodríguez *et al*., 2018), oligodendrocytes (Moldrich and Wenger, 2000) and cells of the cerebral vasculature (Gebremeghin *et al*., 1999; Golech *et al*., 2004) express CB_1R. Moreover, CB_1 receptor is localized to the outer mitochondrial membrane at both presynaptic and postsynaptic terminals and astrocytes (Bernard *et al*., 2012; Hebert-Chatelain *et al.,* 2014a, 2014b, 2016; Koch *et al.,* 2015; Lutz *et al*., 2015; Gutiérrez-Rodríguez *et al*., 2018). The stimulation of the mitochondrial CB_1R leads to inhibition of oxidative phosphorylation and ATP production modulating energy metabolism, neurotransmitter

release (Bernard *et al*., 2012; Lutz *et al*., 2015) and memory (Hebert-Chatelain *et al.,* 2016). The CB_1Rs are mostly localized to presynaptic terminals; their activation results in suppression of neurotransmitter release into the synapse (Kano *et al.,* 2009). In the brain, CB_1Rs are expressed in GABAergic, glutamatergic, serotonergic, dopaminergic and noradrenergic neurons, suggesting that the eCB system is involved in the suppression of the release of these neurotransmitters (Hermann *et al*., 2002; Oropeza *et al*., 2007; Haring *et al*., 2007; Azad *et al*., 2008; Kano *et al*., 2009; Morozov *et al*., 2009; Lutz *et al*., 2015; Morena *et al*., 2016; Gutierrez-Rodriguez *et al.,* 2017) with the predominant effects of the eCB signaling taking place at GABAergic and glutamatergic synapses (Katona and Freud, 2012).

The CB_1 receptors are also localized in peripheral organs and tissues, like adipose tissue, muscle, liver, heart, gastrointestinal tract, pancreas, spleen, tonsils, prostate, testicle, uterus, ovary, skin, eye, or peripheral presynaptic sympathetic nerve terminals (Galiègue *et al.,* 1995; Ishac *et al.,* 1996; Pertwee, 2001; Maccarone *et al.,* 2016; Zou and Kumar, 2018). They are also in mitochondria of skeletal muscles (gastrocnemius and rectus abdominis) and myocardium (Mendizabal-Zubiaga *et al.,* 2016) whose activation by THC reduces mitochondria-coupled respiration (Mendizabal-Zubiaga *et al.,* 2016).

The eCB system through CB_1 receptors activation exerts important functions in the CNS. For instance, retrograde inhibition of neurotransmitter release (Alger, 2002; Chevaleyre *et al*., 2006; Marsicano and Lutz, 2006; Heifets and Castillo, 2009; Kano *et al*., 2009), control of neuronal excitability (Marsicano *et al*., 2003), regulation of various forms of short and long term synaptic plasticity (Gerdeman and Lovinger, 2003; Chevaleyre *et al*., 2006; Marsicano and Lutz, 2006; Heifets and Castillo, 2009; Kano *et al*., 2009, Puente *et al*., 2011), neuron-astrocyte communication (Navarre and Araque, 2008, 2010), proliferation of neuronal progenitors and neurogenesis induced by

excitotoxic insults (Aguado *et al*., 2005, 2007), control of neuronal survival (Galve-Roperh *et al*., 2008, 2009).

2.2.1.2 CB_2 Receptor

The CB_2R is mostly expressed in immune system and modulates immune cell migration and cytokine release both outside and within the brain (Pertwee, 2005). Furthermore, CB_2Rs are also expressed in the heart, bone, endothelium, pancreas, liver and testicle (Zou and Kumar, 2018).

2.2.1.3 Other endocannabinoid receptors

There are another receptors mediating the effects of eCBs (Pertwee, 2015), such as the Transient Receptor Potential (TRP) Vanilloid 1 (TRPV1) activated by AEA (Maccarrone *et al*., 2008; De Petrocellis and Di Marzo, 2009b; Tóth *et al*., 2009; Alhouayek *et al*., 2014; Rossi *et al*., 2015). Many of the TRP channels can be regulated by phospholipase C (PLC)-generated products such as diacylglycerol (DAG) (Hardie, 2007; Zygmunt *et al*., 2013), which is metabolized by DAG lipase (DAGL) leading to 2-AG production (Freund *et al*., 2003). When 2-AG suffers a spontaneous acylmigration to yield 1-arachidonoylglycerol (1-AG), the balance between the effects on TRPV1 and CB_1R change in systems that contain both receptors. This fact occurs because the CB_1R, in contrast to TRPV1, is not activated by 1-AG (Sugiura *et al*., 2006; Zygmunt *et al*., 2013) (Figure 2). Other receptors are the Transient Receptor Potential Ankyrin 1 (TRPA1) (De Petrocellis *et al*., 2008), Peroxisome Proliferator-Activated Receptor α (PPAR-α)((Sun *et al*., 2006; Alhouayek *et al*., 2014) and the non CB_1/CB_2 G protein-coupled receptor 55 (GPR55) (Ryberg *et al*., 2007).

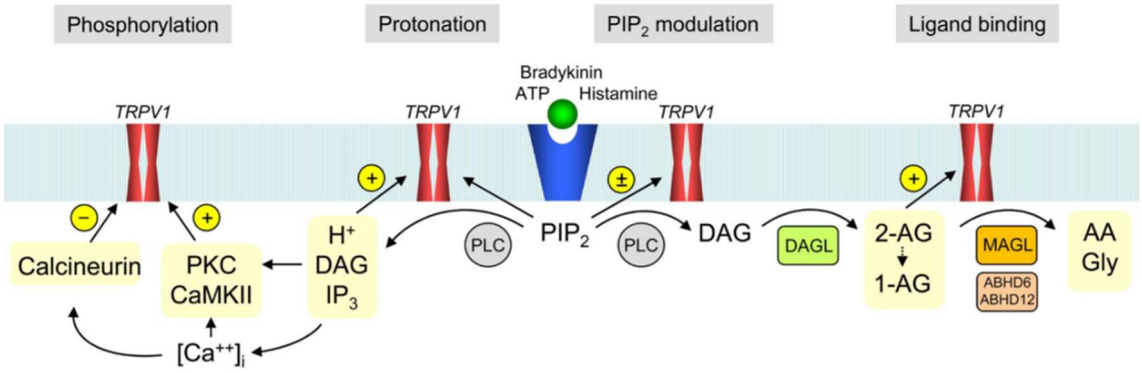

Figure 2: Illustration of the contribution of 2-AG and 1-AG to PLC-dependent activation of TRPV1. Collected from Zygmunt *et al*., 2013.

2.2.2 Compounds and metabolism of endocannabinoids

The two best characterized endocannabinoids are AEA and 2-AG. Both eCBs are synthesized and released on demand (Alger, 2012; Castillo *et al*., 2012). Hence, their endogenous levels determine the magnitude and duration of CB_1R stimulation (Guggenhuber *et al*., 2016). These eCBs are synthesized from phospholipid precursors, such as phosphatidylethanolamine (PE) for AEA and phosphatidylinositol (PI) for 2-AG, in the postsynaptic membrane and generate a retrograde eCB signaling. This retrograde signaling activates presynaptic CB_1Rs to reduce neurotransmitter release. The biosynthesis of AEA and 2-AG could be Ca^{2+}-dependent and independent (Kano *et al*., 2009; Castillo *et al*., 2012; Ohno-Shosaku and Kano, 2014). Furthermore, the main enzymes that degrade AEA (fatty acid amide hydrolase, FAAH) and 2-AG (monoacylglycerol lipase, MAGL) are localized in different subcellular sites, suggesting different signaling mechanisms for AEA and 2-AG (Cravatt *et al*., 1996; Cristino *et al*., 2008; Kano *et al*., 2009).

The AEA is a partial agonist of CB_1R and CB_2R, and a full agonist of TRPV1. N-arachidonoyl phosphatidylethanolamine-hydrolyzing phospholipase D (NAPE-PLD) is

the principal biosynthesis enzyme for AEA (Kano, 2014). However, AEA can also be produced in a NAPE-PLD-independent manner (Okamoto *et al*., 2007; Kano, 2014).

The 2-AG is a full agonist of CB_1R and CB_2R having a brain concentration higher than AEA (Sugiura *et al*., 2006; Kano, 2014). 2-AG acts in concert with protein kinase C (PKC) and other PLC-dependent signaling pathways to fine-tune TRPV1 channel activity (Zygmunt *et al*., 2013). As already mentioned briefly, the main biosynthetic pathway for 2-AG is the formation from membrane PI through the PLC-β and DAGL. The PLC-β can be activated by various G protein-coupled receptors, such as type-1 metabotropic glutamate receptors (mGluR1 and mGluR5). The PLC-β synthesizes DAG from PI. This new messenger regulates PKC activity but is also the substrate of diacylglycerol kinase (Piomelli, 2013). There are two DAGL isoforms, $DAGL_\alpha$ and $DAGL_\beta$ (Bisogno *et al*., 2003). $DAGL_\alpha$ is expressed postsynaptically, in particular at the spine head and neck, as well as in dendrites (Katona *et al*., 2006; Uchigashima *et al*., 2007; Kano, 2014; Reguero et al., 2014). The MAGL enzyme is presynaptic and hydrolyzes 2-AG to arachidonic acid and glycerol (Ahn *et al*., 2008; Piomelli, 2013). Additionally, there are other 2-AG hydrolyzing enzymes (ABHD6 and ABHD12) localized in postsynaptic loci (Figure 3).

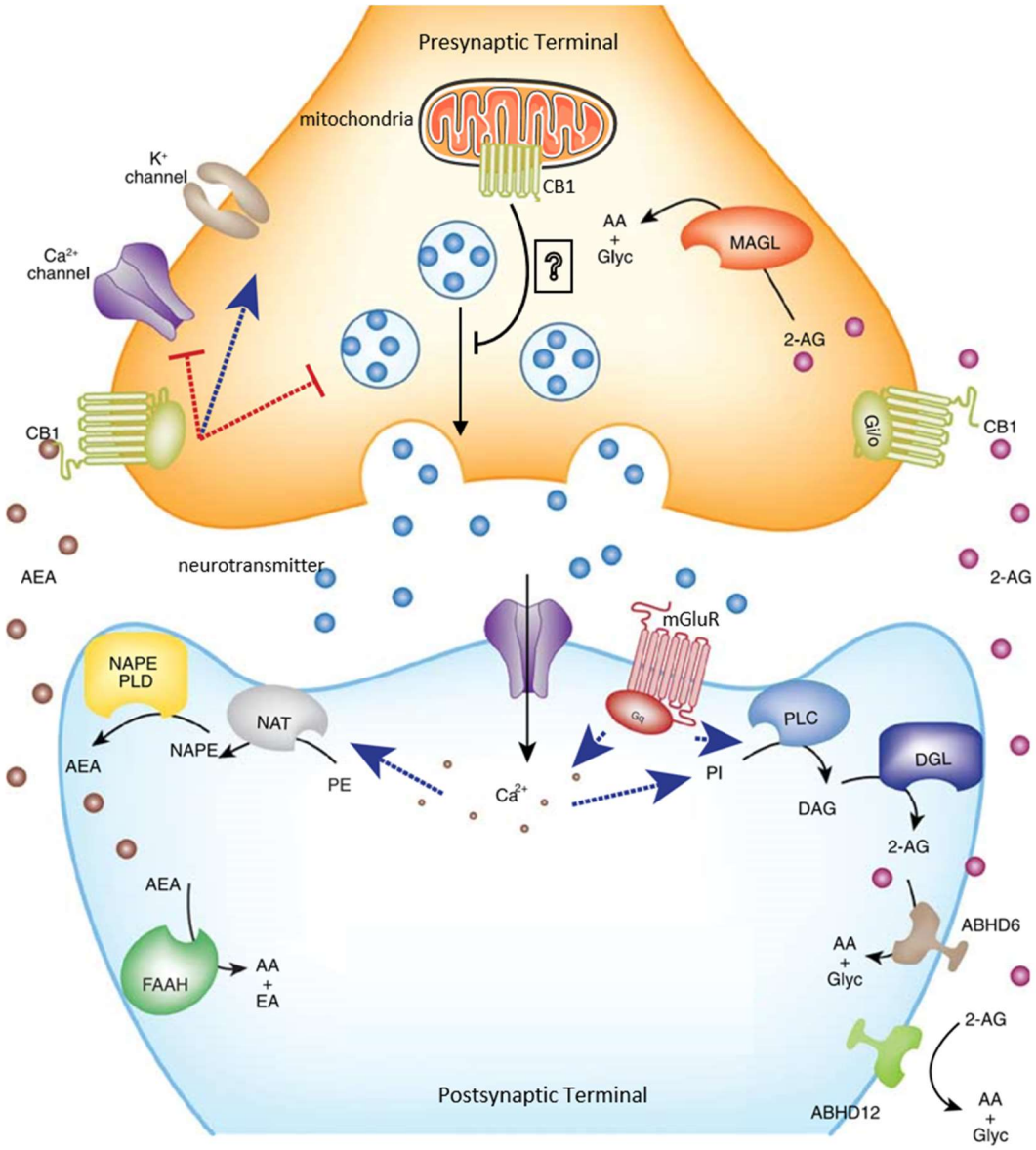

Figure 3: Illustration of retrograde endocannabinoid system. The neurotransmitter release (i.e: glutamate and GABA) causes a postsynaptic depolarization. This fact generated an increase of the intracellular Ca^{2+} levels through activation of AMPA, NMDA receptors and/or Gq-coupled receptors (i.e mgluR1/5) and voltage-gated Ca^{2+} channels. The elevation of intracellular Ca^{2+} increases the eCB biosynthesis. The eCBs as retrograde messengers activate the CB_1R presynaptic. This fact leads to the suppression of neurotransmitter release from the presynaptic terminal, the inhibition of postsynaptic Ca^{2+} Channels and the activation of postsynaptic K^+ Channels. Red line: Inhibitory process. Blue line: Activation process. Black line: Enzymatic process. Question mark: Unknown process. Modified from Morena *et al*., 2016.

The eCB system participates in the short-term regulation of inhibitory and excitatory synapses through retrograde signaling mechanisms. This phenomenon is named depolarization-induced suppression of inhibition (DSI) and depolarization-

induced suppression of excitation (DSE) that are mediated by the release of GABA and glutamate, respectively (Chevaleyre *et al*., 2006; Kodirov *et al*., 2010; Senst and Bains, 2014). Moreover, the eCB system also participates in long-term synaptic plasticity. Thus, retrograde signaling mediated by eCBs has been related to the phenomenon named long-term depression (LTD). LTD requires postsynaptic activation of mGluR5 and increase in postsynaptic calcium (Robbe *et al*., 2002). The DSI, DSE and LTD induced by eCBs have been characterized in different brain areas (hippocampus, amygdala, cortex, nucleus accumbens, bed nucleus stria terminalis (BNST) or cerebellum) and play a role in memory formation associated with experience (Chevaleyre *et al*., 2006; Heifets and Castillo, 2009; Kano *et al*., 2009; Puente *et al*., 2011).

2.3 Stress and endocannabinoid signaling in the hippocampus

Stress is an adaptive response of the organism to real or perceived threat in the environment (i.e. stressful stimuli) aimed at restoring the homeostasis (McEwen, 2007). Physiological and psychological stressors are identified; the latter could also result in physical demands such as release of energy reservoirs to provide survival, explaining why both stressors could elicit similar stress responses (Micale and Drago, 2018). Furthermore, the earliest responses to stress are neural, occur within seconds of the stress and involve many neurotransmitters such as serotonin, adrenaline, noradrenaline, glutamate and GABA (Lutz *et al.,* 2015).

There are two types of response to stressors: activation of the hypothalamic-pituitary-adrenocortical (HPA) axis (see 1.3.1 below), and activation of the sympathetic-adrenergic system. The latter system leads to the release of epinephrine and norepinephrine into the blood stream that is taken as an index of the autonomic response (Micale and Drago, 2018). The brain regions implicated in the integration and processing of distinct stressors are different. Thus, limbic areas such as the prefrontal cortex (PFC),

amygdala and hippocampus are strongly involved in the interpretation of psychological stressors (Herman *et al*., 2005), while mid-hindbrain regions (raphe nuclei and locus coeruleus), seem to participate in responses to physiological stressors (Herman *et al*., 2003; Micale and Drago, 2018).

2.3.1 Stress and HPA axis

Responses to stressors involve the activation of the HPA system. The HPA system is the primary neuroendocrine axis responsible for mediating the hormonal response to stressors (Sapolsky *et al*., 2000; Herman *et al*., 2003). Several studies suggest that the eCBs reduce the HPA axis activation and facilitate appropriate stress recovery (Patel *et al*., 2004, 2009; Balsevich *et al*., 2017).

During stress exposure, neurons in the paraventricular nuclei (PVN) of the hypothalamus secrete corticotrophin-release-hormone (CRH) which stimulates the secretion of adreno-corticotropin hormone (ACTH) from the pituitary gland to the blood stream. In turn, ACTH stimulates the production and secretion of glucocorticoids in the adrenal cortical gland (cortisol in humans and corticosterone in rodents) (Scarante *et al*., 2017; Micale and Drago, 2018) (Figure 4).

Although the fast-feedback mechanisms of corticosterone are not fully understood, it seems that endocannabinoids are involved in the HPA regulation through G-protein coupled glucocorticoid receptors in the PVN (Di *et al*., 2003; Malcher-Lopes *et al*., 2006).

2.3.2 Endocannabinoid system and the HPA axis

The hippocampal projections to the PVN participate in the negative feedback regulation of the HPA axis. The CB_1R-mediated reduction in glutamate release is responsible for the glucocorticoid-feedback regulation of the HPA axis (Di *et al*., 2003). In stress conditions, the 2-AG synthesis elicited by hippocampal glucocorticoid receptors

leads to a glutamatergic disinhibition through the activation of CB_1Rs located in GABAergic interneurons (Hill *et al*., 2010; Balsevich *et al*., 2017; Scarante *et al*., 2017).

The CB_1R expression is high in limbic regions (i.e. hippocampus, amygdala and PFC) and low in subcortical regions (i.e. the BNST, PVN, mid-hindbrain regions) involved in HPA axis regulation (Herkenham *et al*., 1990, 1991; Wittmann *et al*., 2007; Senst and Bains, 2014; Puente *et al*., 2011). Both CB_1R and CRH mRNAs co-localize in the PVN (Cota *et al*., 2003) as well as in the amygdala, PFC and BNST (Cota *et al*., 2007). Thus, the presynaptic CB_1R receptor signaling might regulate the CRH release in limbic structures. In addition, CB_1Rs and both 2-AG and AEA are present in the intermediate and anterior lobes of the pituitary gland (Herkenham *et al*., 1991; Pagotto *et al*., 2001; Wittmann *et al*., 2007); CB_1Rs are also expressed in the adrenal gland (Ziegler *et al*., 2010).

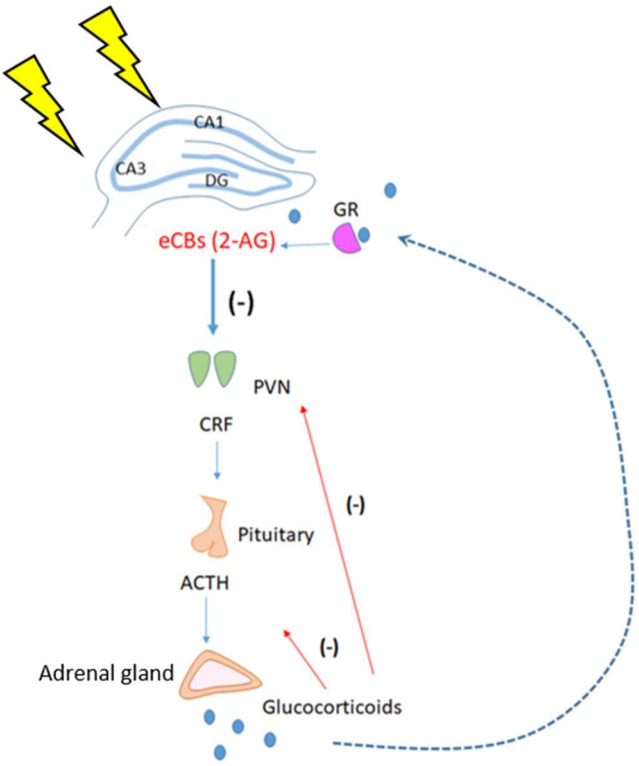

Figure 4: Scheme of the HPA axis. Hippocampal endocannabinoid-mediated signaling participates in the negative feedback of HPA axis. The secretion of corticotrophin-released-hormone (CRH) by the hypothalamic paraventricular nuclei (PVN) under stressful conditions, stimulates adrenocorticotropic hormone (ACTH) production in the pituitary which in turn elicits glucocorticoid (i.e. corticosterone) release from the adrenal gland. The PVN receives projections the hippocampus that participates in the glucocorticoid-mediated negative feedback inhibition of the HPA axis. The activation of glucocorticoid receptors in the hippocampus induces 2-AG synthesis which activates CB_1R in GABAergic interneurons leading to disinhibition of glutamatergic neurons. These neurons excite GABAergic neurons in the PVN inhibiting CRH release and stopping the stress response. Modified from Scarante *et al*., 2017.

The CB_1 receptor antagonism leads to corticosterone increase indicating that the eCB system controls basal HPA activity (Patel *et al.*, 2004; Sens and Bains, 2014). Furthermore, the enhancement of the eCB signaling decreases the corticosterone secretion induced by stress, as a result of the eCB effect on CRH neurons to dampen neurotransmitter release. Likewise, CB_1R blockade causes a potentiation of corticosterone release following HPA activation (Evanson *et al*., 2010). Moreover, the HPA stimulation and the subsequent corticosterone release directly influences eCB-

mediated retrograde signaling; thus, acute and chronic stress factors facilitate or inhibit different eCB-mediated outcomes in adolescent rodents (Wamsteeker *et al*., 2010; Crosby and Bains, 2012). Also, eCB synthesis triggered by glucocorticoid receptors activation in PNCs following acute stress or glucocorticoid administration (i.e. corticosterone) decreases HPA axis hyperactivity (Di *et al*., 2003; Hill *et al*., 2010; Sens and Bains, 2014). Overall, the state-of-the-art of this Thesis work shows the decisive role of the endocannabinoids and CB_1 receptors in the regulation of HPA axis.

2.4 Hippocampal formation

The hippocampal formation (HF) in rodents is a C-shaped structure positioned in the posterior half of the hemisphere. The HF features the dentate gyrus (DG), the Ammon´s horn (which is subdivided into CA1, CA2 and CA3-CA4) and the subiculum. The parahippocampal region lies adjacent to the hippocampal formation and comprises five sub-regions: perirhinal cortex, entorhinal cortex (EC), postentorhinal cortex, presubiculum and parasubiculum (Schultz and Engelhardt, 2014; Boccara *et al*., 2015; Cappaert *et al*., 2015) (Figure 5).

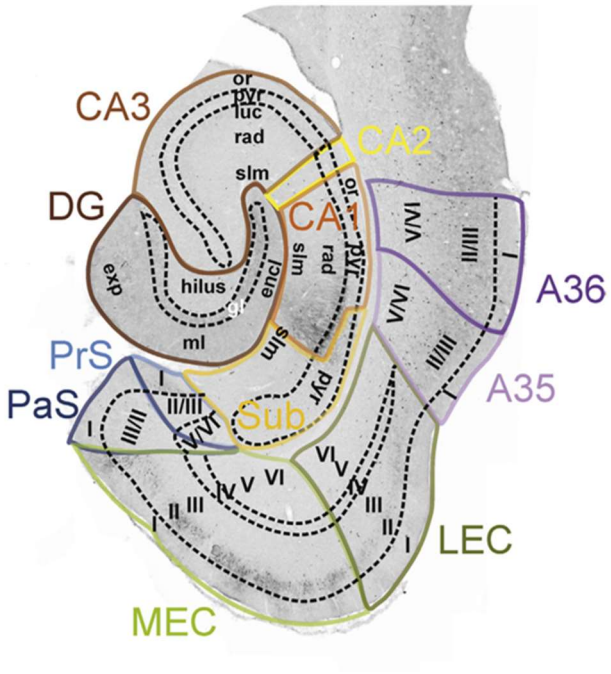

Figure 5: Illustration of the hippocampal formation and the parahippocampal gyrus. DG: Dentate gyrus. CA1-3: Hippocampus (Ammon´s horn). Sub: Subiculum. PrS: Presubiculum. PaS: Parasubiculum. MEC: Medial entorhinal cortex. LEC: Lateral entorhinal cortex. A35 and A36: Perirhinal cortical area. The cortical layers are indicated by Roman numerals. dist: distal. encl: enclosed blade of the DG. exp: exposed blade of the DG. gl: granule cell layer. luc: stratum lucidum. ml: molecular layer. or: stratum oriens. pyr: pyramidal cell layer. rad: stratum radiatum. slm: stratum lacunosum-moleculare. Collected from Cappaert *et al*., 2015.

The HF is part of the limbic system controlled by hormonal influence (McEwen and Alves, 1999; McEwen, 2002) and plays an essential role in learning, memory and mood regulation. Moreover, mood disorders (depression and anxiety) and Alzheimer´s disease relate to alterations in the HF.

2.4.1 Dentate gyrus and perforant path

The dentate gyrus is an integral portion of the HF. This region comprises three layers: molecular layer, granule cell layer and hilus or polymorph layer (Amaral *et al*., 2007; Boccara *et al*., 2015; Cappaert *et al*., 2015).

Many of the connections of the HF are unidirectional. The hippocampus has a tri-synaptic circuit consisting of three glutamatergic connections between the DG and the

fields CA3 and CA1 of the Ammon´s horn (Amaral and Witter, 1989). The EC provides the mayor excitatory input to the DG through the perforant pathway composed of the axons of layer II stellate cells and layer III pyramidal neurons. This glutamatergic projection innervates the granule cell dendritic spines distributed in the outer two-thirds of the DML; namely, the lateral and medial EC innervate the outer 1/3 and the middle 1/3 in a highly topographied fashion forming the lateral perforant path (LPP) and the medial perforant path (MPP), respectively (Amaral *et al.,* 2008). The dentate granule cells in turn give rise to their axons, the mossy fibers which send collaterals onto the mossy cells in the dentate polymorphic layer. Mossy fibers terminate in the stratum lucidum innervating the CA3 pyramidal neurons. In turn, the axons of the CA3 pyramidal neurons form the Schaffer collaterals that innervate the ipsilateral CA1 pyramidal neurons (Amaral *et al.,* 2008) whose axons project into the subicular complex and then back to the EC, thus completing the local excitatory loop (Figure 6).

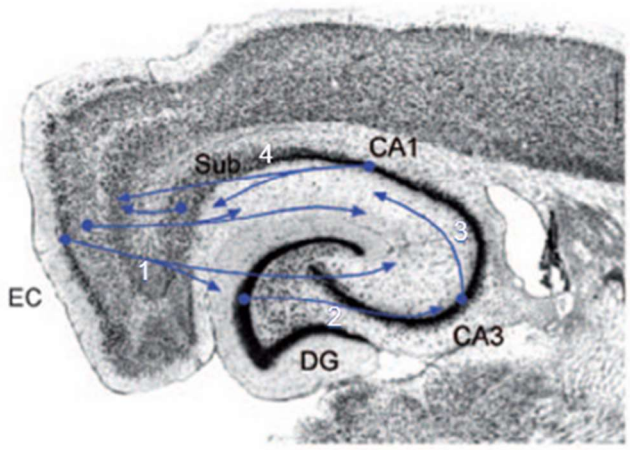

Figure 6: The hippocampal formation in the mouse. Perforant path scheme. 1: Axonal projections from layer II of the entorhinal cortex (EC) go to the dentate molecular layer and to the CA3 stratum lacunosum-moleculare. Layer III projections terminate in the CA1 and the subiculum. 2: The granule cell axons from the mossy fibers that terminate in the dentate polymorphic layer and in the CA3 stratum lucidum. 3: The CA3 pyramidal neurons send the Schaffer collaterals to the ipsilateral CA1. 4: CA1 pyramidal neurons project to the subiculum. Modified from Amaral *et al*., 2008.

3. WORKING HYPOTHESIS AND OBJECTIVES

3.1 Working Hypothesis

The brain is the most sensitive organ to stress and is responsible for generating adaptations to social and physical stressors. In mammals, the amygdala, prefrontal cortex, hippocampus and hippothalamus are activated in response to the threat of homeostasis alteration. The activity of the eCB system participates in behavioral responses to stress, fear and anxiety in a highly specific and localized manner. Of particular importance is the transmission of stress information to the amygdala, where a reference to previous experiences takes place through the crosstalk with the medial prefrontal cortex (mPFC) and hippocampus (Bishop, 2008; Roozendaal *et al*., 2009; Hermans *et al*., 2014a; Likhtik and Paz, 2015; Lutz *et al*., 2015). The amygdala-cortical-hippocampal circuit is relevant for almost every neurobehavioral response to psychological stress (McEwen, 2012). Particularly, the hypocamppus is critically involved in many forms of learning and memory as well as emotional and stress processing (Fanselow and Dong, 2010; Romeo, 2017).

Sustained stress affects neuronal communication and alters neuronal circuits in an attempt to adapt these circuits to the changes caused. The adolescence is especially sensitive to stress. However, despite this period of life is a vital stage with numerous structural, functional and behavioral changes, research has mostly focused on the effects of stress in synaptic plasticity and brain circuits during earlier and later periods of life (McCormick and Mathews, 2010; Eiland and Romeo, 2013).

Based on this, we hypothesized that the acute and chronic stress during the adolescence should elicit important molecular, anatomical and physiological alterations in the eCB system, consequently disrupting synaptic plasticity that holds a negative impact on behavior.

3.2 Objectives

The general goal of my Doctoral Thesis was to investigate the effects of acute and chronic restraint stress during adolescence on the molecular organization of the eCB system, synaptic plasticity and behavior. To carry out this investigation, we developed an interdisciplinary strategy that combined biochemical, morphological, electrophysiological and behavioral techniques applied to the hippocampal dentate gyrus of healthy and stress mice.

The specific objectives of the Doctoral Thesis were to:

1. Determine the anatomical distribution of CB_1 receptors in the dentate MPP synapses after acute and chronic restraint stress.
2. Quantify the levels of 2-AG in the hippocampus of stressed mice relative to control.
3. Characterize the excitatory synaptic transmission after CB_1 receptor activation at the MPP synapses of adolescent mice exposed to acute and chronic restraint stress.
4. Investigate the excitatory long-term depression mediated by activation of MPP CB_1 receptors after acute and chronic restraint stress.
5. Compare the CB_1 receptor expression and receptor efficiency in hippocampi of stress versus control mice.
6. Study the effects of restraint stress on the adolescent behavior.

4. MATERIAL AND METHODS

4.1. Research animals and stress protocols

Male Swiss mice (35 to 42 days old) were used in all experiments. They were housed on a 12:12 light-dark cycle, with food and water *ad libitum* and were transferred to the behavioral testing room at least 30 minutes (min) before the test to acclimatize. The protocols for animal care and use were approved by the Committee of Ethics for Animal Welfare of the University of the Basque Country (CEEA M20-2015-093) and were in accordance to the European Communities Council Directive of 22nd September 2010 (2010/63/EU) and Spanish regulations (Real Decreto 53/2013, BOE 08-02-2013). Great efforts were made in order to minimize the number and suffering of the animals used.

4.1.1. Acute Restraint Stress Test

The acute stress procedure was performed between 9 and 11 am. The animals were restrained for 2 hours (h) during 1 day in well ventilated single bags (Ref: 629444, Harvard Apparatus Bags. USA) (Zimprich *et al*., 2014; Bali *et al*., 2015). They were anesthetized right after and processed for biochemical, anatomical or *ex vivo* electrophysiological experiments (Fig. 7A).

4.1.2. Chronic Restraint Stress Test

The procedure started between 9 to 11 am. The mice were restrained for 1h during 10 consecutive days in well ventilated single bags (Ref: 629444, Harvard Apparatus Bags. USA) (Patel, 2010; Sumislawski *et al*., 2011). They were anesthetized right after and processed for biochemical, anatomical or *ex vivo* electrophysiological experiments (Fig. 7B).

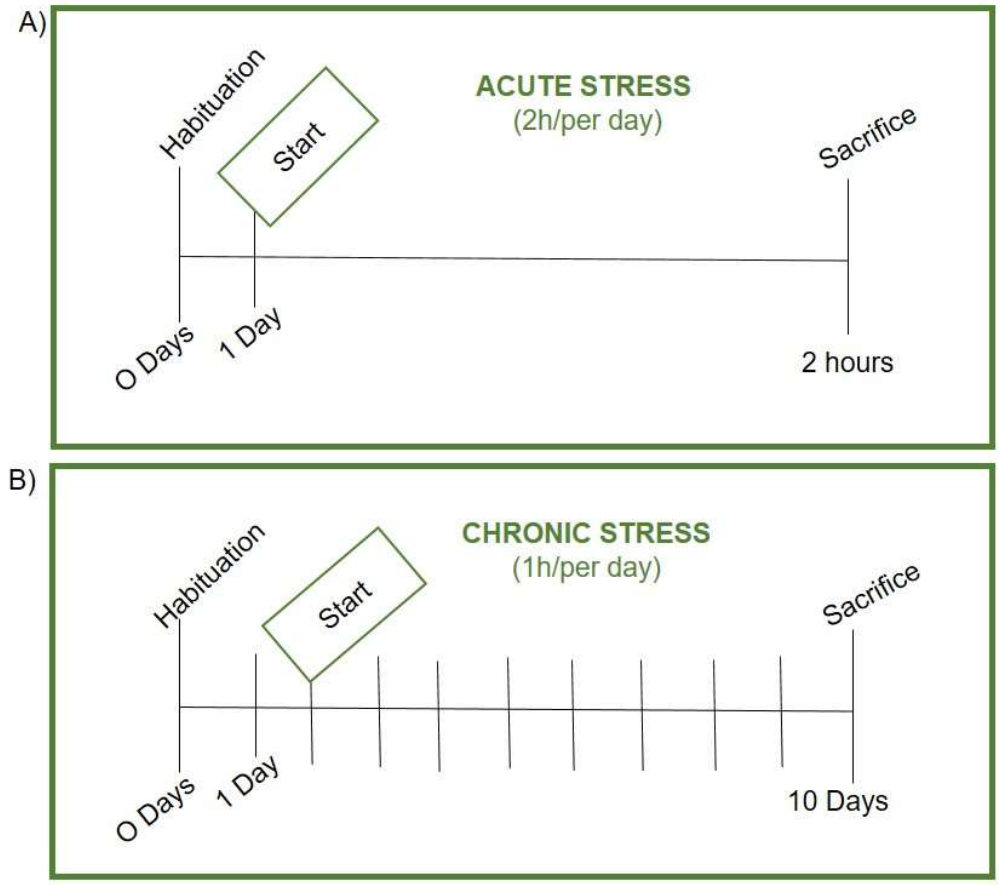

Fig 7: Graphical illustrations of the acute (A) and chronic (B) restraint stress protocols

4.2. Behavioral Test

4.2.1. Elevated plus-maze

The elevated plus-maze test assesses unconditioned anxiety-like behaviors in rodents (Lister 1987). The apparatus consisted of two open arms (30 X 5 cm), two enclosed arms (30 X 5 cm) and a connecting central platform (5 X 5 cm). The device was elevated 38.5 cm from the ground (Tordera *et al.,* 2007). The mouse was placed in the center of the maze with the head facing a close arm, and allowed to move freely for 5 min under dimly light conditions (10 lx). During the test, the following parameters were

recorded: time spent in open arms, time in crossroad and time of latency. The arm entry was defined as a mouse having entered with the four paws into it.

The test was as follows:

1. After stress in the behavioral room the animals rated 5 min before carrying out the test to avoid false negatives.
2. The mice were put in the cross of the maze facing to the enclosed arm and allowed to move freely for 5 min. The time latency was measured (time spent by the mice in the cross for the first time).
3. The apparatus was cleaned with ethanol and water after each test.

4.3 Antibodies and Drugs

4.3.1 Antibodies

Specific antibodies were used in combination with an immunoperoxidase method for light microscopy (LM) and a pre-embedding silver intensified immunogold technique for electron microscopy (EM). They were also applied for western blotting (WB).

The primary antibodies were:

- **Anti-CB_1:** The sequence of the immunizing peptide used to generate the antibody corresponded with the last 31 amino acids of the C-terminus of the mouse CB_1 receptor (NM007726), as provided by the manufacturer (NCBI Reference Sequence: NP_031752.1; 443-473 amino acid residues: MHRAAESCIKSTVKIAKVTMSVSTDTSAEAL) (Antibody´s data sheet, Frontier Science co. Ltd, USA). The specificity of the CB_1 receptor antibody was assessed

in previous publications (Reguero *et al*., 2011; Mendizabal-Zubiaga *et al*., 2016; Gutierrez-Rodriguez *et al.,* 2017, 2018; Bonilla-Del Río *et al*., 2017; Puente *et al*., 2019). Furthermore, a single protein band at 52KDa was detected by immunoblotting that corresponds with the predicted molecular weight of the CB_1 receptor.

- **Anti-TRPV1:** The sequence of the immunizing peptide used to generate the antibody was near the amino terminus of VR1 of rat origin (VR1 (P-19),sc-12498, Santa Cruz Biotechnology) (Antibody´s data sheet, Santa Cruz Biotechnology,USA). The specificity of the TRPV1 receptor antibody was validated in previous studies (Puente *et al*., 2015; Canduela *et al*, 2015).
- **Anti-DAGL-α**: The antibody recognizes a 105 or 120 KDa protein band in immunoblots from hippocampal and cerebellar membranes, respectively (Yoshida *et al*., 2006; Uchigashima *et al*., 2007; Puente *et al.*, 2011; Reguero *et al.,* 2014). (Antibody´s data sheet, Frontier Science co. Ltd, USA).
- **Anti-MAGL:** The sequence used to raise the antibody (C-QDLPHLVNADGQY) corresponded to the internal 17-29 amino acids of the human monoacylglycerol lipase sequence (NP_009214.1; NP_001003794.1). This antibody recognizes both reported isoforms (NP_009214.1 and NP_001003794.1) (Antibody´s data sheet, Abcam, USA).
- **Anti-PLCβ:** The sequence of the immunizing peptide corresponded with 4-159 amino acids of the rat phospholipase Cβ1 N-terminal. The antibody detects a single band of 150 KDa by immunoblotting (Antibody´s data sheet, BD Transduction Laboratories).
- **Anti-B-actin:** the monoclonal anti β-actin (mouse IgG1 isotype) was obtained from the AC-15 hybridoma. The antibody recognizes an epitope located on the N-terminal end of the actin β-isoform and specifically labels a β-actin band (42 KDa) in a wide variety of tissues and species (Antibody´s data sheet, Sigma Aldrich).

Antibody	Manufacturer	Host	Concentration/ Dilution	IHQ Method
CB_1	Frontier Science	Goat	2 µg/ml	LM, EM, WB
TRPV1	Frontier Science	Goat	1:50	LM
DGL-α	Frontier Science	Rabbit	1:1000	WB
MAGL	Abcam	Goat	1:1000	WB
PLCβ	BD Transduction Laboratories	Rabbit	1:8000	WB
Actin	Sigma Aldrich	Mouse	1:50000	WB

Table1: Primary antibodies used. LM: Light microscopy. EM: Electron microscopy. WB: Western Blot.

The secondary antibodies were:

- **Nano-gold anti-goat:** Fab' fraction of an IgG produced in rabbit and labeled with a 1.4nm-diameter gold particle (Nanoprobes Inc., Yaphank, NY, USA).
- **Biotinylated anti-goat:** biotinylated IgG (H + L) yielded in horse (Vector Laboratories, Burlingame, CA, USA).

Antibody	Manufacturer	Host	Concentration/ Dilution	IHQ Method
Nanogold anti-goat	Nanoprobes	Rabbit	1:100	EM
Biotinylated anti-goat	Vector Laboratories	Horse	1:200	LM

Table 2: Secondary antibodies used. LM: Light microscopy. EM: Electron microscopy.

4.3.2 Drugs

Agonists, antagonists and inhibitors of different compounds of the eCB system and calcium channel blockers were used for electrophysiology. All drugs were purchased from Tocris Bioscience (Table 2):

- **AM251:** N-(Piperidin-1-yl)-5-(4-iodophenyl)-1-(2,4-dichlorophenyl)-4-methyl-1 H-pyrazole-3-carboxamide is a potent CB_1 receptor antagonist. ($C_{22}H_{21}Cl_2N_4O$).
- **AMG9810:** (2*E*)-*N*-(2,3-Dihydro-1,4-benzodioxin-6-yl)-3-[4-(1,1-dimethylethyl)phenyl]-2-propenamide is a potent, selective and competitive TRPV1 receptor antagonist ($C_{21}H_{23}NO_3$).
- **CGP55845 hydrochloride:** (2*S*)-3-[[(1*S*)-1-(3,4-Dichlorophenyl)ethyl]amino-2-hydroxypropyl](phenylmethyl)phosphinic acid hydrochloride is a potent and selective $GABA_B$ receptor antagonist which prevents agonist binding and inhibits GABA and glutamate release ($C_{18}H_{22}Cl_2NO_3P.HCl$).
- **CP55,940:** The (-)-*cis*-3-[2- Hydroxy-4-(1,1-dimethylheptyl)phenyl]-trans-4-(3-hydroxypropyl)cyclohexanol is a cannabinoid receptor agonist which is considerably more potent than Δ^9-THC ($C_{24}H_{40}O_3.^{1/2}H_2O$).

- **D-APV:** The D-2 Amino-5-phosphonopentanoic acid is a potent NMDA antagonist ($C_5H_{12}NO_5P$).
- **JZL184:** The 4-[*Bis*(1,3-benzodioxol-5-yl)hydroxymethyl]-1-piperidinecarboxylic acid 4-nitrophenyl ester is a potent and selective MAGL inhibitor ($C_{27}H_{24}N_2O_9$).
- **MPEP hydrochloride (MPEP):** The 2-Methyl-6-(phenylethynyl) pyridine hydrochloride is a potent and highly selective non-competitive antagonist of the $mGlu_5$ receptor and a positive allosteric modulator of the $mGlu_4$ receptor ($C_{14}H_{11}N.HCl$).
- **Nimodipine:** T1,4-Dihydro-2,6-dimethyl-4-(3-nitrophenyl)-3,5-pyridinedicarboxylic acid 2-methyloxyethyl 1-methylethyl ester is a L-type Ca^{2+} channel blocker ($C_{21}H_{26}N_2O_7$).
- **Picrotoxin:** It is a $GABA_A$ receptor antagonist ($C_{30}H_{34}O_{13}$).
- **RHC80267:** *O,O´*-[1,6-Hexanediyl*bis* (iminocarbonyl)] dioxime cyclohexanone is a DAGL inhibitor and a weak phospholipases C and A_2 inhibitor ($C_{20}H_{34}N_4O_4$).
- **URB597:** The cyclohexylcarbamic acid 3´-(Aminocarbonyl)-[1,1´-biphenyl]-3-yl ester is a potent and selective FAAH inhibitor ($C_{20}H_{22}N_2O_3.^{1/4}H_2O$).

Drugs	Concentration	Property	Manufacturer
AM251	4 µM	CB_1R antagonist	Tocris Bioscience
AMG9810	3 µM	TRPV1 antagonist	Tocris Bioscience
CGP55845	5 µM	$GABA_B$ antagonist	Tocris Bioscience

CP55,940	10 µM	CB_1R agonist	Tocris Bioscience
DL-APV	100 µM	NMDA antagonist	Tocris Bioscience
JZL184	50 µM	MAGL inhibitor	Tocris Bioscience
MPEP	50 µM	$mGluR_5$ antagonist	Tocris Bioscience
Nimodipine	1 µM	L-type Ca^{2+} channel blocker	Tocris Bioscience
PTX	100 µM	$GABA_A$ antagonist	Tocris Bioscience
RHC80267	100 µM	DAGL inhibitor	Tocris Bioscience
URB597	2 µM	FAAH inhibitor	Tocris Bioscience

Table 3: List of drugs used in the study.

4.4. Biochemical Technique

4.4.1. Corticosterone Levels

Corticosterone is the aldosterone precursor produced in response to stimulation of the adrenal cortex by ACTH. Corticosterone is the major stress steroid produced in non-human mammals, therefore, it is one of the most effective indicators of stress.

Corticosterone levels were measured as follows:

1. Blood was collected (~ 500µl) from the trunk or the heart and kept into 1 mL tubes containing EDTA (BD Microtainer K2E Tubes, US).
2. Blood samples we centrifuged at 2000g for 10 min at 4ºC (Ota *et al*., 2015) in a Heraeus Fresco 21 centrifuge.
3. Plasma was collected in 1 mL eppendorfs.
4. The EIA Kit was used (KO14-H5, Arbor Assays, Michigan, USA) to measure corticosterone in plasma.
5. Measurement of the chemiluminescent signal was done with Synergy H4 Hybrid Reader, Biotek.
6. Final corticosterone concentration was calculated with MyAssays™ online tool.

4.4.2. Hippocampal membrane preparation and protein determination

Samples for western blots and [^{35}S] GTPγS binding assays were processed in the following way:

1. Mice were anesthetized with isofluorane and decapitated.
2. The hippocampi were removed and immediately were frozen with liquid nitrogen and stored at -80ºC until used.
3. Hippocampal membranes (P2 fraction) were used for western blotting and [^{35}S] GTPγS binding assays.
4. Hippocampal tissue was thawed in ice-cold 20 mMTris-HCl, pH 7,4, containing 1 mM EGTA (Tris/EGTA buffer) prior to homogenization.
5. Membranes were obtained by centrifugation at 40000g for 30 min at 4ºC. Next, the pellet was re-suspended and re-centrifuged under the same conditions.
6. The pellets were aliquoted in microcentrifuge tubes, centrifuged and stored at -75ºC prior to use. Protein content was determined using the Bio-Rad dye reagent with bovine γ-globulin as standard.

4.4.2.1. Western blot technique

Hippocampal concentration of CB_1R, G-protein α subunits, MAGL, DAGL and PLC was measured. The experiments were performed as previously described with minor modifications (Garro *et al*., 2001; López de Jesús *et al*., 2006a,b; Montaña *et al*., 2012):

1. P2 fractions of hippocampal membranes were boiled in urea-denaturing buffer 20 mM Tris-HCl, pH 8.0, 12% glycerol, 12% Urea, 5% dithiothreitol, 2% sodium dodecyl sulfate (SDS), 0.01% bromophenol blue] for 5 min.

2. Increasing amounts of denatured proteins were resolved by electrophoresis on SDS–polyacrylamide (SDS–PAGE) gels (10%) using the Mini Protean II gel apparatus (Bio-Rad, Hercules, CA, USA).

3. Proteins were transferred to polyvinylidene fluoride (PVDF) membranes (Amersham Bioscience, Buckinghamshire, UK) using the Mini TransBlot transfer unit (Bio-Rad, Hercules, CA, USA) at 90 V constant voltage for 1 h at 4ºC.

4. Blots were blocked in 5% non-fat dry milk/phosphate buffered saline containing 0.5% BSA and 0.2% Tween for 1 h, and incubated overnight at 4ºC with CB_1R antibodies, or antibodies against different Gαi/o subunits subtypes (sc-387 (Gαo), sc-391 (Gαi1), sc-7276 (Gαi2), sc-262 (Gαi3); Santa Cruz Biotechnology).

5. Blots were washed and incubated with specific horseradish peroxidase conjugated secondary antibodies diluted 1:10,000 in blocking buffer for 2 h at room temperature (RT).

6. Immunoreactive bands were incubated with the ECL system according to the manufacturer instructions (Amersham Bioscience, Buckinghamshire, UK).

4.4.2.2. [^{35}S] GTPγS binding assays

The [^{35}S] GTPγS binding assays were performed according to the procedure described elsewhere (Barrondo and Sallés, 2009; Casado *et al*, 2010):

1. Hippocampal membranes (25µg protein) were thawed, and incubated at 30ºC for 2 h in [^{35}S] GTPγS-incubation buffer (0.5 nM [^{35} S] GTPγS, 1 mM EGTA, 3 mM $MgCl_2$, 100 mM NaCl, 0,2 mM DTT, 50 µM GDP, and 50 mM Tris-HCl, pH 7.4).

2. Receptor-stimulated [^{35}S] GTPγS binding was determined by adding CP55940 at eight different concentrations between 10^{-11} – 10^{-5} M. Nonspecific binding was measured in the presence of 10 μM unlabeled GTPγS. Basal binding was established as the specific [^{35}S] GTPγS binding in the absence of agonist.
3. Rapid vacuum and filtration ended through Whatman GF/C glass fiber filters. The remaining bound radioactivity was measured by liquid scintillation spectrophotometry.

For data analysis, individual CP55940 concentration-response curves were fitted by nonlinear regression to the four parameter Hill equation:

$$\mathbf{E = Basal + Emax\text{-}Basal/1+ 10\ (LogEC50\text{-}Log\ [A])\ nH}$$

Where E is the effect, log [A] the logarithm of the concentration of agonist, nH the midpoint slope, LogEC50 the logarithm of the midpoint location parameter, and Emax and basal the upper and lower asymptotes, respectively. When required, simultaneous model-fitting with parameter-sharing across datasets was performed using PRISM 5.0.

4.4.2.3. Measurement of endogenous 2-AG by liquid chromatography tandem/mass spectrometry (LC-MS/MS) in the hippocampus

The determination of the endogenous 2-AG was carried out as described by Schulte *et al*. (2012) with minor modifications (Zhang *et al*., 2010; García del Caño *et al*., 2015):

1. Hippocampal samples were stored at -80ºC until extraction.
2. Samples (25mg wet weight) were put into borosilicate tubes. The tubes contained 0.5 mL ice-cold 0.1M formic acid.
3. They were homogenized with a 5 mm-steel ball using the Digital Sonifier (Model S250 Branson, USA) for 1 cycle of 10 s at 10% amplitude.
4. Aliquots with 50 µl of homogenate were placed into silized microcentrifuge tubes containing ice-cold 0.1M formic acid.
5. Homogenates were spiked with 20 µL acetonitrile containing the internal standard [deuterated 2-AG-d_5 (final concentration 100nM), deuterated 1-AG-d_5 (final concentration 100 nM) and 10 µL of 2-AG natural form at the adequate concentration, to give a final volume of 500 µL.
6. Hippocampal homogenates were extracted with ethylacetate/hexane (1000 µL; 9:1, v/v) and the aid of the digital sonifier for 1 cycle of 10 s at 10% amplitude.
7. The tubes were centrifuged at 10.000 g for 10 min at 4ºC and the upper (organic) phase was removed, evaporated to dryness under a gentle stream of nitrogen at 37ºC and re-dissolved in 500 µL acetonitrile.

The analysis was performed on a LC-MS/MS system based on Agilent technologies (Wilmington) consisting of a 6410 Triple Quad mass spectrometer equipped with an electrospray ionization source operating in positive ion mode and a 1200-series binary pump system, as previously described (Zhang *et al.*, 2010; Schulte

et al., 2012; García del Caño *et al.*, 2015). 2-AG was separated with a Phenomenex Luna 2.5 µm C18(2)-HST column, 100 x 2 mm, combined with a Security Guard pre-column (C18, 4x2 mm; Phenomenex) with solvents A (0.1% formic acid in 20:80 acetonitrile/water, v/v) and B (0.1% formic acid in acetonitrile), using the following gradient: 55-90% B (0-2 min), then held at 90% B (2-7.5 min) and re-equilibrated at 55% B (7.5-10 min). The column temperature was 25ºC, the flow rate was 0.3 mL/min, the injection volume was 10µL and the needle was rinsed for 60 seconds (s) using a flushport with water/acetonitrile (80:20) as the eluent. The electrospray ionization interface was operated using nitrogen as nebulizer and desolvation gas, and using the following settings: temperature 350 ºC, nebulizer pressure 40 psi, and capillary voltage + 4800 V. The following precursors to product ion transitions were used for multiple-reaction monitoring (MRM): 2-AG and 1-AG m/z 379.4→ 287; 2-AG-d_5 and 1-AG-d_5 m/z 384→ 287, respectively. Dwell times were 20 ms; pause between MRM transitions was 5 ms. Data acquisition and analysis were performed using Mass Hunter Software.

4.5. Immunohistochemical Procedures

4.5.1. Tissue processing

The stress protocols for animal care and use were approved by the appropriate Committee at the University of the Basque Country (M30-2015-094). Furthermore, the animal experimental procedures were carried out in accordance with the European Communities Council Directive 2010/63/UE and current Spanish legislation (RD 53/2013 and Ley 6/2013). Great efforts were done to minimize the number and suffering of the animals used.

4.5.2. Transcardially perfusion of the animals

1. Mice (at least 3 animals per group) were deeply anesthetized by intraperitoneal injection of ketamine/xylazine (80/10 mg/kg body weight).
2. They were transcardially perfused at RT (20-25ºC) with phosphate buffered saline (0.1 M PBS, pH 7.4) for 20 s, followed by the fixative solution made up of 4% formaldehyde (freshly depolymerized from paraformaldehyde), 0.2% picric acid, and 0.1% glutaraldehyde in phosphate buffer (0.1 M PB, pH 7.4) for 10-15 min.
3. Brains were carefully removed from the skull and post-fixed in the fixative solution for approximately 1 week at 4 ºC.
4. Then, brains were stored at 4 ºC in 1:10 diluted fixative solution plus 0.025% sodium azide at 4°C until processing.

4.5.3. Pre-embedding immunoperoxidase method for light microscopy: the avidin-biotin peroxidase method

The avidin-biotin complex (ABC) method is an indirect immunohistochemical technique which implies the use of a biotinylated secondary antibody against a primary antibody. The amplification of the signal is performed by the addition of the ABC complex. This complex consists of biotin associated with peroxidase and avidin mixture in a proportion that leaves free some of the avidin-biotin binding sites. The biotin of the secondary antibody binds to the free valencies of avidin in the ABC complex. The complex binds in succession to other ones. The chromogen used was 3,3'-diaminobenzidine (DAB) which oxidizes in a medium containing hydrogen peroxide. The

peroxidase in the ABC catalyzes the decomposition reaction of the hydrogen peroxide resulting in free oxygen formation that oxidizes the DAB. This DAB oxide is insoluble and gives a reddish-brown precipitate in the conventional light microscope.

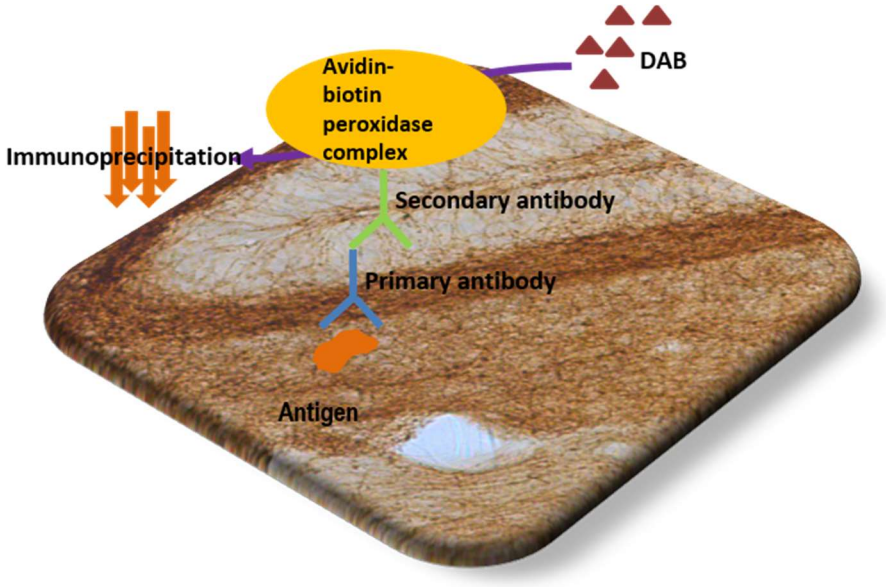

Fig 8: Pre-embedding immunoperoxidase method for light microscopy

Negative controls were run simultaneously to discard false positives.

The following protocol was applied:

1. Brain coronal vibrosections were cut at 50µm and collected in 0.1M PB at RT.
2. Pre-incubation of the hippocampal sections in a blocking solution of 10% bovine serum albumin (BSA), 0.1% sodium azide and 0.5% triton X-100 prepared in tris-hydrogen chloride buffered saline (TBS 1X, pH 7.4) for 30 min at RT.

3. Tissue incubation in the corresponding primary antibody (Table 1) prepared in the blocking solution was kept shaking gently for 2 days at 4ºC. Negative controls were only incubated in the blocking solution.
4. Several washes in 1% BSA and 0.5% triton X-100 in TBS 1X for 30 min to remove excess of the antibody.
5. Incubation with the biotinylated antibody (1:200) (Table 2) prepared in the washing solution for 1 h on a shaker at RT.
6. Several rinses in TBS 1X, 1% BSA and 0.5% triton X-100.
7. Incubation in avidin-biotin complex (1:50; avidin-biotin peroxidase complex, Elite, Vector Laboratories, Burlingame, CA, USA) prepared in the washing solution for 1h at RT.
8. Several washes in TBS 1X, 1% BSA and 0.5% triton X-100. Last wash was done with 0.1M PB and 0.5% triton X-100.
9. Tissue was incubated in 0.05% DAB and 0.01% hydrogen peroxide prepared in 0.1 M PB and 0.5% triton X-100.
10. Several rinses in 0.1M PB and 0.5% triton X-100.
11. Tissue sections were mounted on gelatinized slides.
12. Dehydration in graded alcohols (50º, 70º, 96º, 100º) for 5 min each.
13. Clearing in Xylol (3x5 min).
14. Sections were coverslipped with DPX.

15. Hippocampal tissue was studied and photographed with a Zeiss Axiocam light microscope coupled to Zeiss AxioCamHRc camera.

For the purpose of standardized the technique, the three animal groups under study (control, acute stress, chronic stress) were incubated in the same well. The proportion of the CB_1R immunoreactivity in the acute and chronic stress conditions versus controls was assessed by optical density analysis using the Image-J software.

4.5.4 Pre-embedding silver-intensified immunogold method for electron microscopy

This is an excellent technique for the ultrastructural localization of receptor proteins (Baude *et al*., 1993; Luján *et al*., 1997; Mateos *et al*., 1999; Elezgarai *et al*., 2003; Alonso-Espinaco *et al.*, 2008; Puente *et al.*, 2010a, 2010b; Reguero *et al.*, 2011, 2014; Gutiérrez-Rodríguez *et al*., 2016, 2018; Puente *et al*., 2019). The secondary antibody is a Fab' fraction conjugated to a 1.4nm gold particle that binds to primary antibodies. Its small size allows a greater penetration in the tissue, increasing the sensitivity of the method. Gold particles are then silver intensified to increase their size making them visible in the electron microscope. An advantage of the technique is that the antigen-antibody reaction is not altered by the exposure to osmium tetroxide and resin polymerization at high temperatures.

Negative controls were run simultaneously to discard false positives.

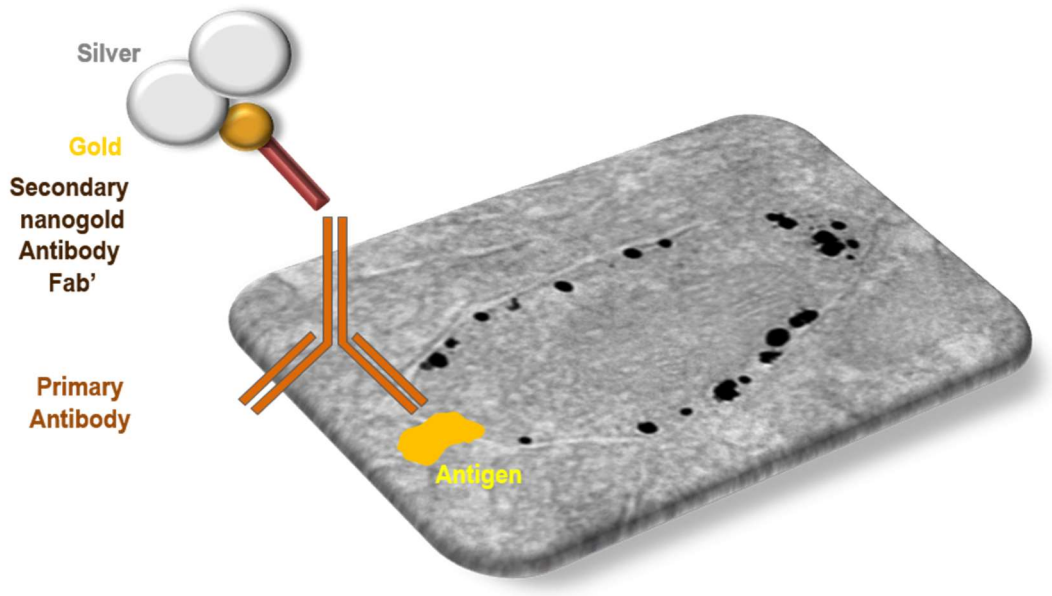

Fig 9: Pre-embedding immunogold method for electron microscopy

The following protocol was applied (Puente *et al.*, 2019):

1. Coronal hippocampal sections were cut at 50µm in a vibratome (Leica VT1000S) and collected in 0.1M PB (pH=7.4) at RT.
2. Pre-incubation in a blocking solution of 10% BSA, 0.1% sodium azide, and 0.02% saponin prepared in TBS 1X for 30 min at RT.
3. Tissue incubation in the primary goat polyclonal anti-CB_1 receptor antibody (1:100) prepared in the blocking solution containing 0.004% saponin on a shaker for 2 days at 4ºC. Negative controls were only incubated in the blocking solution.
4. Several washed in TBS 1X and 1% BSA for 30 min.

5. Incubation in a secondary nanogold antibody (Table 2) prepared in the same solution as the primary antibody for 3 h on a shaker at RT.
6. Various washes in TBS 1X and 1% BSA overnight on a shaker at 4ºC.
7. Post-fixation with 1% glutaraldehyde prepared in TBS 1X for 10 min at RT.
8. Several washes in double distilled water for 30 min.
9. Silver intensification of gold particles with a HQ Silver Kit (Nanoprobes Inc., Yaphank, NY, USA) for about 12 min in the dark.
10. Several washes in double distilled water for 10 min.
11. Various washes in 0.1M PB (pH 7.4) for 30 min.
12. Osmication with 1% osmium tetroxide in 0.1M PB (pH= 7.4) for 20 min at RT.
13. Several washes in 0.1M PB (pH=7.4) for 30 min.
14. Dehydration in graded alcohols (50º, 70º,96º and 100º) for 5 min each and 3 times of 5 min for 100º.
15. Clearing in propylene oxide 3x5 min each.
16. Embedding in a mixture of 1:1 propylene oxide and Epon resin 812 overnight on a shaker at RT.
17. Embedding in Epon resin 812.
18. Resin polymerization in a heater at 60ºC for 2 days.
19. Cutting 1µm semithin sections in the Reichert-Jung ultracut.

20. Collection of 60nm ultrathin sections on nickel mesh grids.
21. Counterstaining with 2.5% lead citrate for 20 min.
22. Examination in a Philips EM208S electron microscope. Tissue was photographed by using a digital Morada Camera from Olympus coupled to the electron microscope.

In order to maximizing the standard conditions, the pre-embedding immunogold method was systematically applied simultaneously to all the sections collected from three different animals (n=3 each condition). The immunogold-labeled hippocampal sections were observed in the light microscope and DML samples with good and reproducible CB_1R immunolabeling were selected. Moreover, to further standardize the conditions between the three different mice belonging to the same experimental group, only the first 1.5 μm from the surface of the tissue section was photographed. All the electron micrographs were taken at 22.00X from grids with 50nm-thick ultrathin sections containing silver-intensified gold particles in the DML. Sampling was always performed accurately in the same way for all the animals studied.

The glutamatergic terminals were identified for their typical ultrastructural features, i.e. asymmetric synapses with thick postsynaptic densities and presynaptic boutons containing abundant and spherical synaptic vesicles. Positive CB_1 receptor labeling was only considered if the identified excitatory synapses had at least one silver-intensified gold particle within 30nm from the synaptic terminal membrane. Image-J software was used to measure labeling density (particles/μm membrane) and the percentage of CB_1 receptor immunopositive excitatory terminals.

4.6. Electrophysiological Techniques

The following protocol was used:

Mice were deeply anesthetized with isoflurane inhalation before decapitation.

1. Brains were rapidly removed and placed in rich sucrose artificial cerebrospinal fluid (ACSF) (pH= 7.3) (Table 4) at 4ºC gassed with 95%O_2/5%CO_2.
2. Coronal hippocampal slices were cut at 300µm in a vibratome (Leica VT1000S) in rich sucrose ACSF (pH=7.3) at 4ºC gassed with 95%O_2/5%CO_2.
3. The slices were incubated in normal ACSF (pH=7,3) gassed with 95%O_2/5%CO_2 for 30 min at RT. Some drugs required pre-incubation for at least 1 h.
4. The hippocampal slices were transferred to an immersion recording chamber and superfused at 2ml/min with gassed normal ACSF and the drugs (Table 5). All recordings were taken at 30 ºC ±1ºC by using an automatic temperature controller (Puente *et al.*, 2011).
5. Extracellular electrodes filled with normal ACSF were used to record neuronal activity. The electrodes were manufactured with borosilicate glass capillaries in Sutter 97-B pipettor stretcher.
6. The stimulation electrode was placed in the MPP and the recording pipette in the inner 1/3 of the DML.
7. Transmission or tetanus protocol was applied at least 20 min after settled the slice in the immersion recording chamber.

4.6.1. Protocol for the study of the excitatory synaptic transmission

1. To evoke field excitatory postsynaptic potentials (fEPSPs), repetitive stimuli (100-150 μs duration) were applied at 0.1Hz (Stimulus isolater ISU165, Cibertek, Spain; controlled by Master-8 stimulator with an isolation unit (AMPI)).
2. A baseline of 10 min was set.
3. Drugs were superfused during 40 min (Puente *et al.*, 2011).

4.6.2. Protocol for the study of the long-term depression of the excitatory synaptic transmission

1. To evoke fEPSPs, stimuli (100-150 μs duration) were delivered at 0.1Hz (Stimulus isolater ISU165, Cibertek, Spain; controlled by Master-8 stimulator with an isolation unit (AMPI)).
2. A baseline of 10 min was set.
3. 10Hz frequency was applied during 10 min.
4. Repetitive control stimuli were applied at 0.1Hz and were recorded during 30 min (Puente *et al.*, 2011).

The inhibitory component was blocked by the $GABA_A$ antagonist picrotoxin (Table 3).

In both protocols, signal recordings were done using an Axopacth-200B (Axon Instruments/Molecular Devides, Union City, CA, USA). Signals were filtered at 1-2 kHz, digitized at 5 kHz on a DigiData 1200 interface (Axon Instruments/Molecular Devides, Union City, CA, USA) and gathered on a PC using Campex 9.2 (Axon Instruments/Molecular Devides, Union City, CA, USA). The area was analyzed with Clamfit 10.2 Package Program (Axon Instruments/Molecular Devides, Union City, CA, USA).

SUCROSE BUFFER

PRODUCT	MW	mM	Gr per 1000mL	Osmol
NaCl	58.44	87	5.08	174
Sucrose	342.3	75	25.67	75
Glucose	180.2	25	4.5	25
$MgCl_2$	203.3	7	1.4	21
KCl	74.55	2.5	0.18	5
$CaCl_2$	147.0	0.5	0.07	1.5
NaH_2PO_4	120.0	1.25	0.15	2.5

Table 4: Composition of the sucrose buffer

NORMAL BUFFER

Product	MW	mM	Gr per 1000mL	Osmol
$NaHCO_3$	84.01	23	1.93	46
NaCl	58.44	130	7.59	260
Glucose	180.2	11	1.98	11
KCl	74.55	2.5	0.18	2.5
$CaCl_2$	147.0	2.4	0.35	7.2
NaH_2PO_4	120.0	1.2	0.14	2.4
$MgCl_2$	203.3	1.2	0.24	2.4

Table 5: Composition of the normal buffer

4.7 Statistical Analysis

It was performed using the Statistical Program for Social Science (SPSS 22.0; IBM, Spain). The normality of the samples was studied by the Shapiro-Wilks test followed by the Levene´s test for the variance homoscedasticity. Depending on the technique, different statistical analysis (One-way ANOVA, Kruskal-Wallis test, unpaired two-tailed Student´s t-test or U-Mann Whitney test) was applied followed by the corresponding post-hoc test (Bonferroni with homogeneous variances or Tamhane T2 with heterogeneous variances). Western blots, [^{35}S]GTPγS binding and LC-MS/MS assays were analyzed using the statistical software package GraphPad Prism V.5 (GraphPad Software Inc, San Diego, USA). All data was expressed as mean ± S.E.M. Values of $p < 0.05$ were considered statistically significant.

5. RESULTS

5.1 Corticosterone Levels and Body Weight

We measured the plasma corticosterone concentration in the control and stress mice. Corticosterone levels were significantly higher in acute (1,182 ± 158.8 pg/ml; $p<0.01$; n=11) and chronic stress (1,296 ± 167.9 pg/ml; $p<0.001$; n=12) than in control (508 ± 77.21 pg/ml; n=20). Thus, plasma corticosterone concentration increased with the intensity and time of stress.

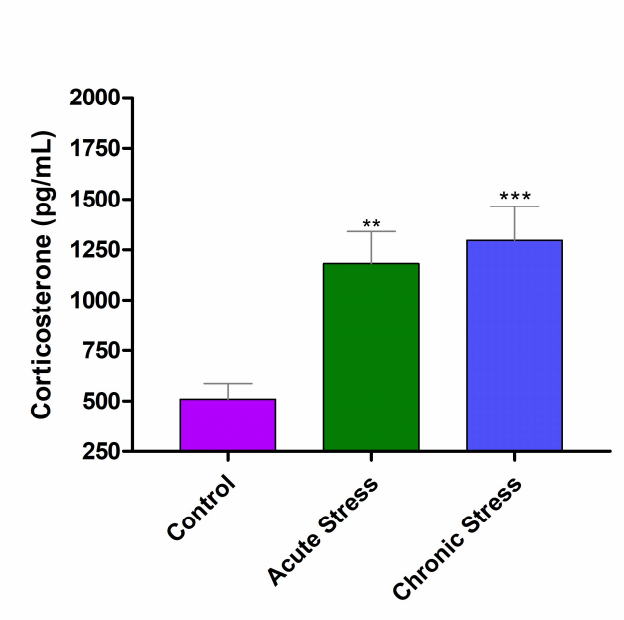

Figure 10: Plasma corticosterone in acute and chronic stress. The levels of 1,182 ± 158.8 pg/ml in acute stress and 1,296 pg/ml ± 167.9 pg/ml in chronic stress are very highly significant versus control mice (508 ± 77.21 pg/ml). The data are expressed as mean ± Standard Error of the Mean (SEM). The data were analyzed by One-Way ANOVA and Bonferroni´s Multiple Comparison Post-hoc Test. *** indicate statistically significant differences with $p<0.001$ vs. control; ** indicate statistically significant differences with $p<0.01$ vs. control.

In addition, the reduction in body weight is indicative of stress (Krahn *et al.*, 1990; Jeong *et al.*, 2013). Body weight gradually increased in controls but dropped in chronic stress (Figure 11A). However, it there was an increase in the last day of the chronic stress (1.96 ± 1.85 %; n=13) with respect to controls (12.24 ± 1.63 %; n=13) (Figure 11B).

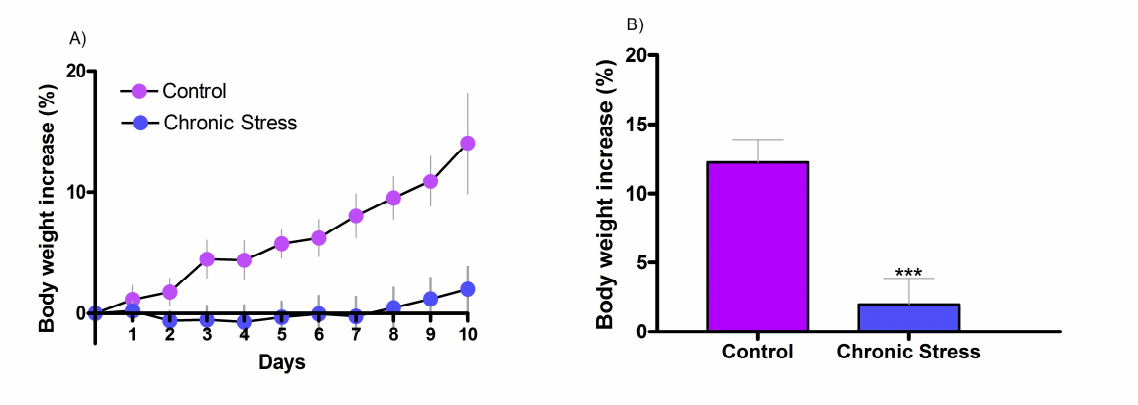

Figure 11: Chronic stress reduces body weight. A) The percentage of the body weight increases per day in control but not in chronically stressed mice. **B)** Mice with chronic stress have a significant lower body weight (1.96 ± 1.85 %) vs control mice (12.24 ± 1.63 %). Data are expressed as mean ± SEM. Data were analyzed by Student unpaired t test. *** indicate statistically significant differences with $p<0.001$ vs. control.

5.2 Western Blot

5.2.1 Expression of Gαi/o subunits in hippocampal membranes from control and stress mice

Next step was to determine the expression of $G_{i/o}$ protein subunits in hippocampal membranes. As shown in the graph, no changes in $G_{i/o}$ isoforms were detected in stress vs. control mice (Figure 12).

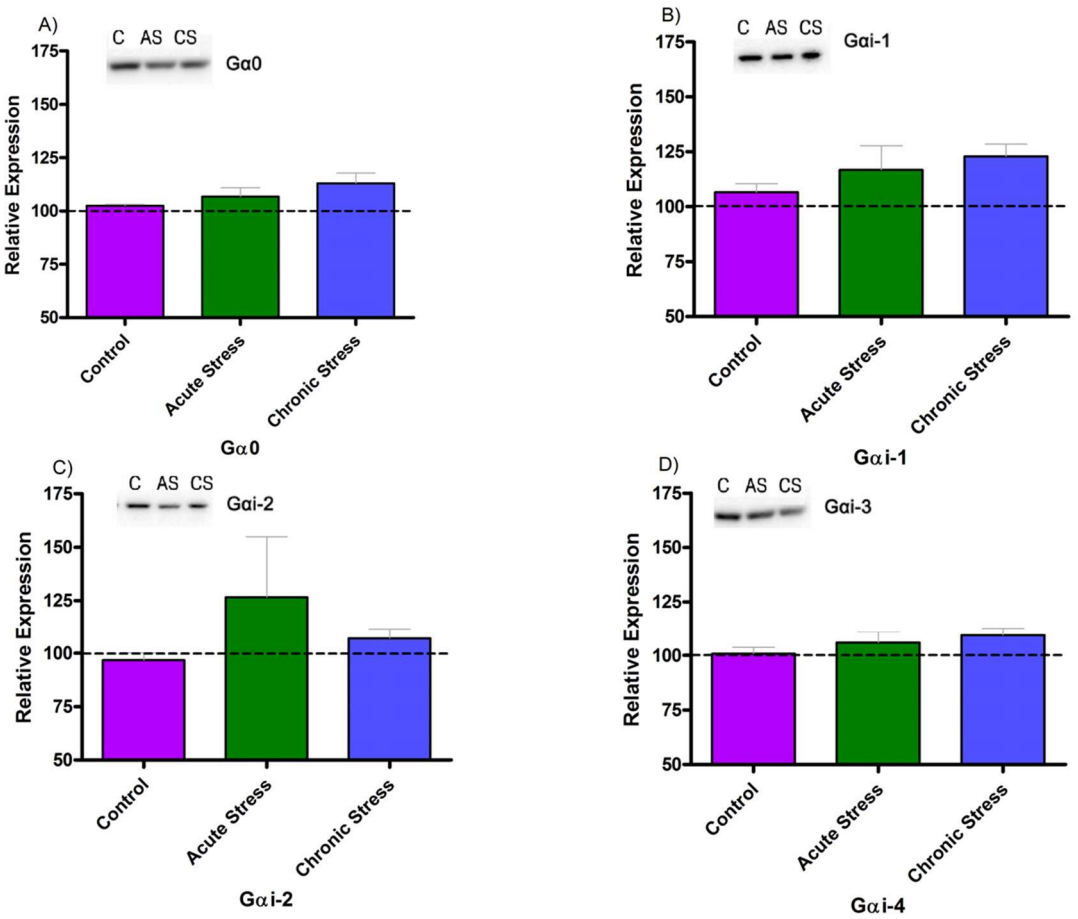

Figure 12: No significant differences in the relative expression of Gα protein isoforms detected by immunoblotting **in hippocampal (P2) membrane fractions . A)** Gα0 isoform. C: 102.40 ± 0.65 %; AS: 106.76 ± 4.06 %; CS: 113.00 ± 4.78 %. **B)** Gαi-1 isoform. C: 106.60 ± 3.86 %; AS: 116.76 ± 11.05 %; CS: 123.00 ± 5.51 %. **C)** Gαi-2 isoform. C: 96.70 ± 3.38 %; AS: 126.55 ± 28.30 %; CS: 107.00 ± 4.65 %. **D)** Gαi-3 isoform. C: 100.75 ± 3.05 %; AS: 106.00 ± 5.01 %; CS: 109.41 ±3.30 %. Data are expressed as mean ± SEM and were analyzed by One-Way ANOVA and Bonferroni´s Multiple Comparison Post-hoc Test.

5.2.2 Expression of eCB system components in hippocampal membranes from control and stress mice

Western blotting was used to study CB_1R, DAGL-α, PLCβ1, MAGL proteins and the associated and potential modulator protein of CB_1R activity Crip1a (Smith *et al.*, 2010; Guggenhuber *et al.*, 2016). In acute stress, a decrease in hippocampal CB_1R was found (values: 78.4 ± 7.42 %; $p<0.05$ vs. control; n=4) but not changes in CB_1R were

detected in chronic stress. Also, DAGL-α and PLCβ1 had a similar decrease in acute stress vs. control (DAGL-α values: 82.6 ± 7.50 %; p<0.01; n=3, PLCβ1 values: 85.52 ± 4.71 %; p<0.05; n=2). In chronic stress, DAGL-α decreased 15.69% (values: 84.31 ± 7.14 %; p<0.01; n =3) and PLCβ1 16.5% (values: 83.50 ±4.57 %; p<0.05; n=2). In contrast, MAGL (AS values: 94.08 ±1.25 %; p>0.05; n=3, CS values: 91.79 ± 7.05 %; p>0.05; n=3) and Crip1a (AS values: 106.20 ± 1.93 %; p<0.05; n=3, CS values: 102.30 ± 5.92 %; p<0.05; n=3) did not change neither in acute nor in chronic stress vs. control mice (Figure 13).

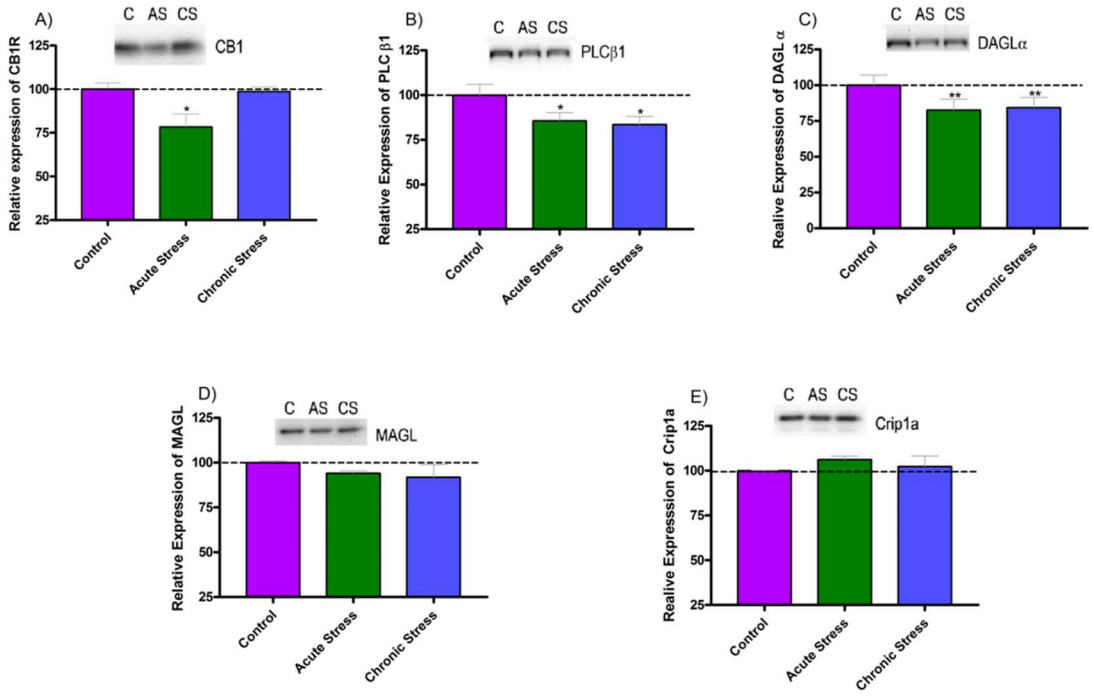

Figure 13: Relative expression of components of the eCB system in isolated hippocampi. A) Immunoblot of CB_1R (50 KDa). Acute stress shows a significant decrease in CB_1R protein (values: 78.4 ± 7.42 %) vs. control. There are no changes in in chronic stress. **B)** PLCβ1 (150 KDa) expression decreases in acute (values: 85.52 ± 4.71 %) and chronic stress (values: 83.50 ± 4.57 %). **C)** DAGLα (115 KDa) expression is reduced about 17.4% in acute stress (values: 82.6 ± 7.50 %), and about 15.69% in chronic stress (values: 84.31 ± 7.14 %). **D)** MAGL protein (33 KDa) does not change significantly between groups (CS values: 100.0 ± 0.92 %; AS values: 94.08 ± 1.25 %; CS values: 91.79 ± 7.05 %). **E)** Neither Crip1a (18 KDa) shows significant changes between groups (CS values: 100.0 ± 0.24 %; AS values: 106.20 ± 1.93 %; CS values: 102.30 ± 5.92 %). Data are expressed as mean ± SEM and analyzed by One-Way ANOVA and Bonferroni´s Multiple Comparison Post-hoc Test. ** indicate statistically significant differences with p<0.01 vs. control; * indicate statistically significant differences with p<0.05 vs. control.

5.3 [^{35}S] GTPγS binding assays

[^{35}S] GTPγS binding assays were performed with the CB_1 cannabinoid receptor agonist CP55940 in hippocampal membranes from control and stress mice.

A significant reduction in [^{35}S] GTPγS basal binding (the binding in the absence of agonist) was observed in hippocampal membranes of both acute and chronic stress. Moreover, CP55940 stimulated [^{35}S] GTPγS binding in a concentration dependent manner in all conditions, but only a significant increase in efficacy (Emax) was observed in chronic stress vs. control. The EC_{50} was similar between groups (Table below and Figure 14).

	Control	Acute Stress	Chronic Stress
Emax (%)	100 ± 0.4	113 ± 4.9	118 ± 2.2*
pEC50	100 ± 0.4	100 ± 0.4	100 ± 0.4
Basal (%)	100 ± 1.5	66.11 ± 4.13**	74.92 ± 2.17**

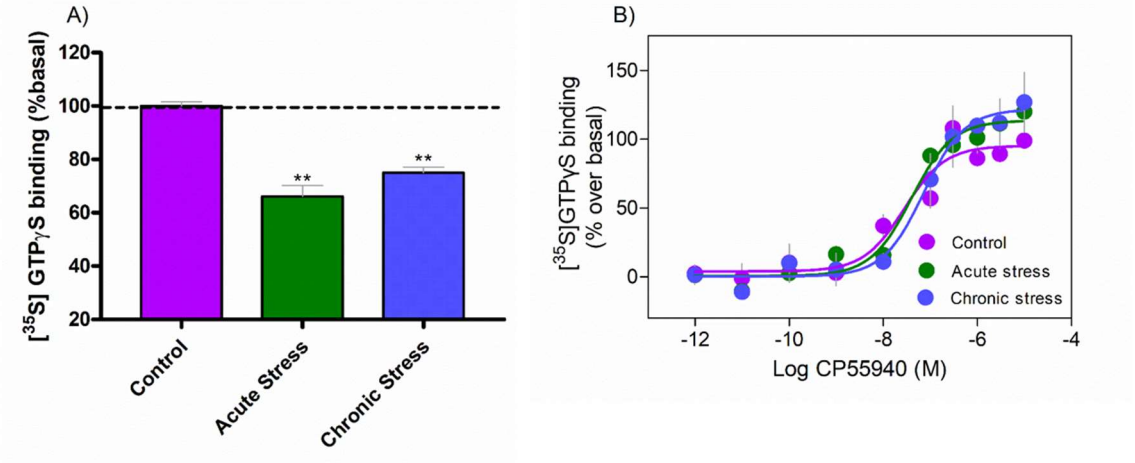

Figure 14: [^{35}S]GTPγS binding. Summary of the means ± SEM and the significances vs control. **A)** Significant impairment of the basal [^{35}S] GTPγS binding in both acute and chronic stress. **B)** A significant increase (18%) in the Emax of [^{35}S] GTPγS in chronic stress is seen. Data are expressed as mean ± SEM and were analyzed by One-Way ANOVA and Bonferroni´s Multiple Comparison Post-hoc Test. ** indicate statistically significant differences with $p<0.01$ vs. control; * indicate statistically significant differences with $p<0.05$ vs. control.

5.4 Measurement of endogenous 2-AG

The basal 2-AG levels were quantified in hippocampal samples of control and restraint mice by liquid chromatography and mass spectrometry. In order to get an accurate quantification, we have developed a strategy based on isotope dilution combined with standard addition techniques (García del Caño *et al.*, 2015). We spiked into each aliquot of hippocampal homogenate the same amount of the internal standard solution (2-AG-d_5), and 2-AG in their natural form was spiked with increased amounts (2-AG standard additions: 20, 40, 60, 80, and 120 nM) into the series of subsamples tubes except the first one. In these conditions, it is possible to find a linear relationship with an excellent correlation coefficient between the 2-AG concentrations spiked to the homogenate and the ratio of the obtained areas for 2-AG and 2-AG-d_5. The intercept on the x-axis provides the endogenous level of 2-AG in the aliquot of the hippocampal homogenate. Moreover, given than 2-AG undergoes rapid isomerization to 1-AG under common experimental conditions (Zoerner *et al.*, 2011), it is necessary to pay attention to their extent during the analytical procedures. Therefore, all the samples were spiked with the internal standard 1-AG-d_5 [100 nM]. In our hands, 1-AG usually represents 5% of 2-AG and was not included in the total amount of 2-AG. Basal 2-AG in control mice was 6.99 ± 0.60 nm/g hippocampal tissue (n=4). In acute stress, 2-AG was significantly higher (9.06 ± 0.90 nm/g; 30%; n=4) with respect to non-stress mice (Figure 15). By contrast, 2-AG levels in chronic stress were 43% lower than in control mice (3.99 ± 0.41 nm/g; n=4). Altogether, these data indicate that there is a 2-AG imbalance between control and restraint mice.

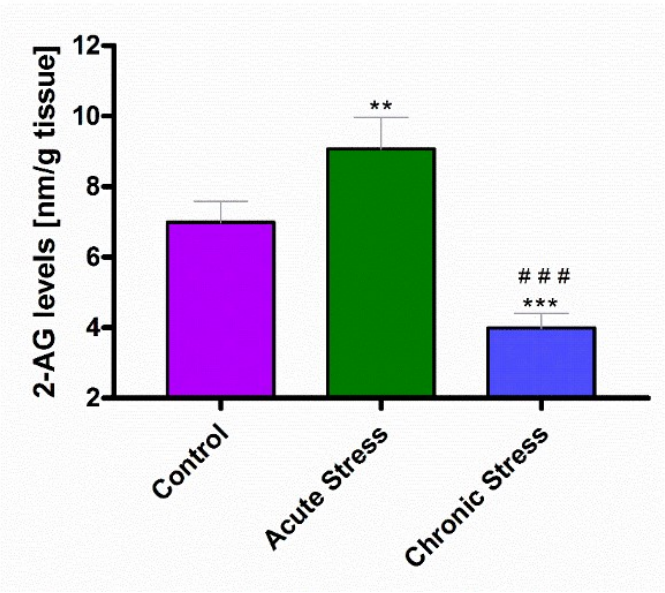

Figure 15: Measurement of endogenous 2-AG. Stress induces a significant alteration of 2-AG. In acute stress, 2-AG significantly increases (9.06 ± 0.90 nm/g) vs. control (6.99 ± 0.60 nm/g). However, chronic stress strongly decreases 2-AG (3.99 ±0.41 nm/g) vs. control. Data are expressed as mean ± SEM and were analyzed by One-Way ANOVA and Bonferroni´s Multiple Comparison Post-hoc Test. *** indicate statistically significant differences with p<0.001 vs. control;** indicate statistically significant differences with p<0.01 vs. control; # # # indicate statistically significant differences with p<0.001 vs. acute stress.

5.5 Light Microscopy

5.5.1 Immunohistochemical localization of CB_1 and TRPV1 receptors in the dentate molecular layer of the dorsal hippocampus

The DML was heavily CB_1 receptor immunoreactive showing a conspicuous band of immunoreactivity in its innermost third which corresponds to the termination zone of the commissural/associational axon fibers (Monory et al., 2006; Ruehle et al., 2013). Less prominent but remarkable CB_1 receptor immunostaining was observed in the outer 2/3 of the ML where the MPP and LPP ends. TRPV1-like immunoreactivity was detected in the Ammon´s horn regions and in the dentate gyrus. In the latter, the granule cell bodies and astrocytic-like processes were immunostained. In addition, a faint TRPV1 staining was observed in the termination zone of the perforant path (outer 2/3) and

association and commissural fiber synapses (inner 1/3) of the ML. Importantly, the hippocampal TRPV1 pattern disappeared in the TRPV1 knock-out tissue (Puente *et al.*, 2015). Altogether, both CB_1 and TRPV1 receptors show a distinct staining pattern (Figures 16A and 16B).

The proportion of CB_1R inmunoreactivity analyzed by optical density was estimated to be 100.4 ± 0.55 % in control mice (n=3). Under stress conditions, CB_1R immunostaining decreased more prominently in acute than chronic stress (AS values: 89.35 ± 0.44 %; $p<0.001$; n=3; CS values: 95.61 ± 0.60 %; $p<0.001$; n=3) particularly in the termination area of the perforant path. In contrast, TRPV1 immunoreactivity increased in both acute and chronic stress (AS values: 134.9 ± 3.10 %; $p<0.001$; n=3, CS values: 176.0 ± 2.58 %; $p<0.001$; n=3) vs. control (100.0 ± 2.56 %; n=3). (Figures 16C and 16D).

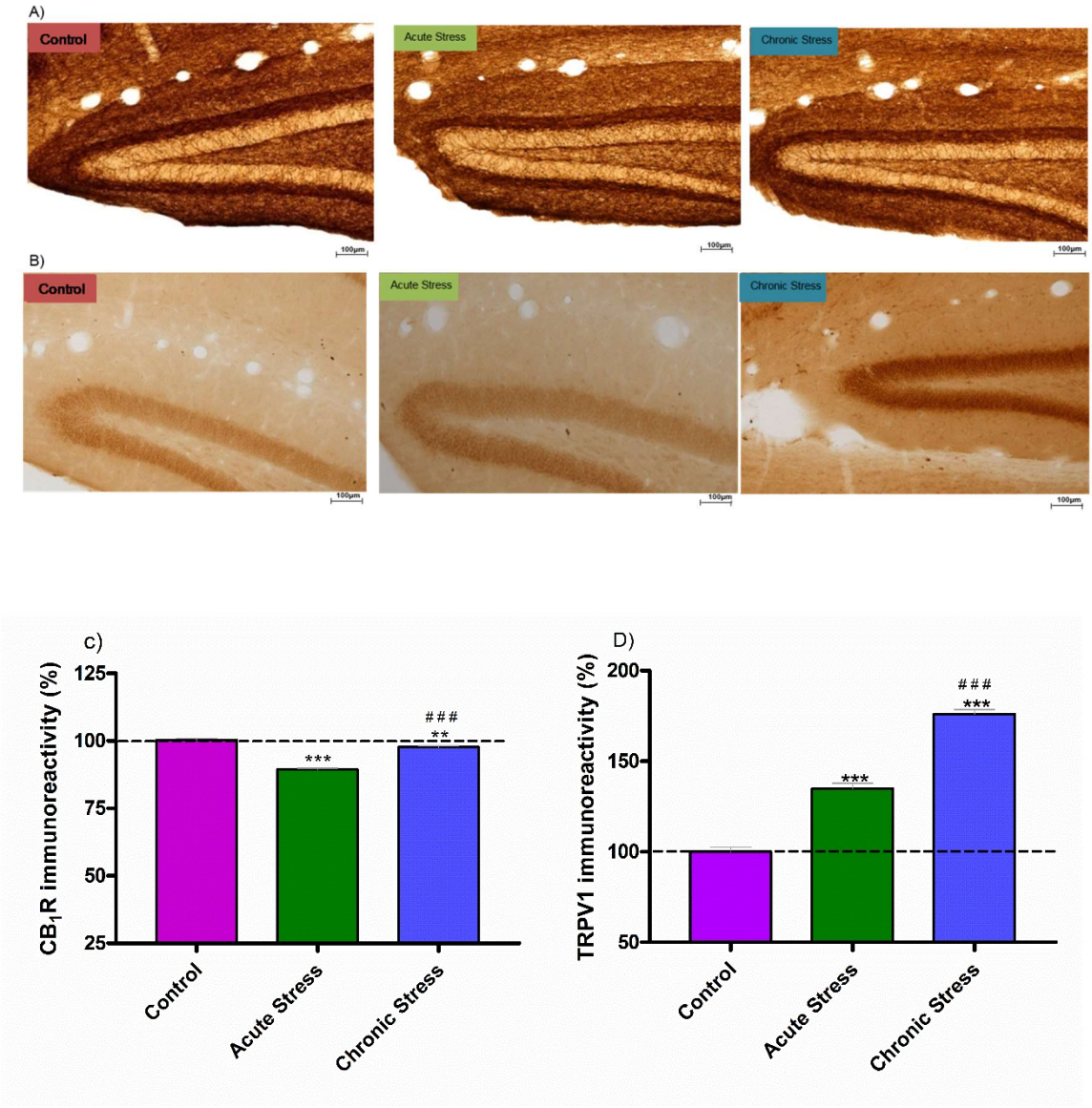

Figure 16: CB_1R and TRPV1 immunostaining in control and stress mice. CB_1R **(A)** and TRPV1 immunoreactivity **(B)** in the DML. **C)** Mean of the percentage of CB_1R immunoreactivity assessed by optical density. Acute stress shows a higher decrease in CB_1R immunostaining (10.65 ± 0.44 %) than chronic stress (4.39 ± 0.60 %) vs. control mice. **D)** Summary data of the percentage of TRPV1 immunoreactivity by optical density. Both acute and chronic stress mice show a highly significant increase in TRPV1 immunostaining (AS values: 134.9 ± 3.10 %; CS values: 176.0 ± 2.58 %) vs. control. The data are expressed as mean ± SEM and were analyzed by One-Way ANOVA and Bonferroni´s Multiple Comparison Post-hoc Test. *** indicate statistically significant differences with $p<0.001$ vs. control; ** indicate statistically significant differences with $p<0.01$ vs. control. ### indicate statistically significant differences with $p<0.001$ vs. acute stress.

5.6 High Resolution Electron Microscopy

5.6.1 Subcellular localization of the CB_1 receptor in excitatory and inhibitory axon terminals in the hippocampal dentate molecular layer

Control, acute and chronic stress mice were used to determine the subcellular localization of CB_1R. As expected in control mice, CB_1R labeling was low in presynaptic excitatory terminal membranes making asymmetric synapses, and high in presynaptic inhibitory terminals forming symmetric synapses. CB_1R immunoparticles were located at a distance from the active zone of both symmetric and asymmetric synapses with dendritic spines and postsynaptic dendrites, respectively (Figures 17-19). The CB_1R distribution was maintained in all experimental groups.

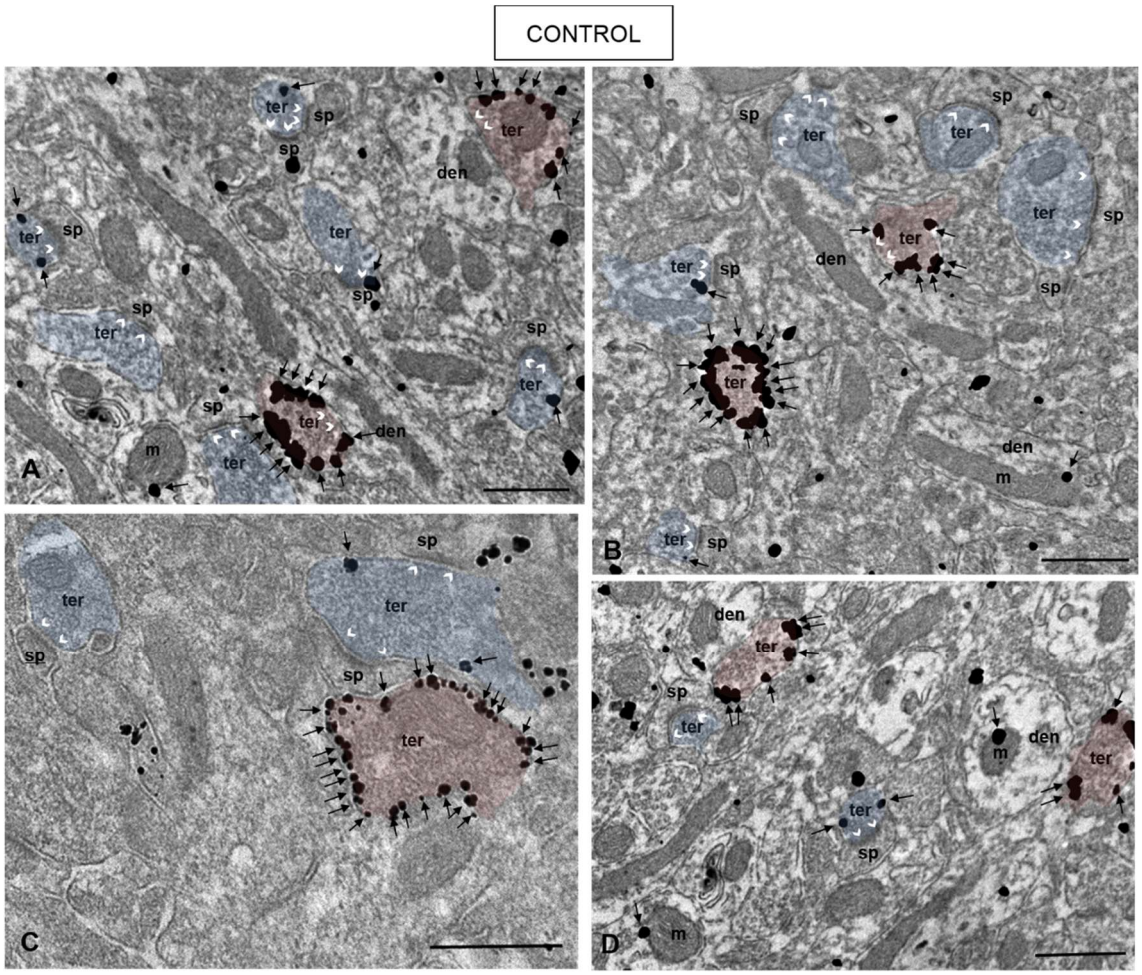

Figure 17: Subcellular CB_1 receptor localization in synaptic terminals of the MPP in the DML. Pre-embedding immunogold method for electron microscopy. A-D) In control mice, CB_1 receptor immunoparticles are localized to excitatory (asymmetric synapses) and inhibitory (symmetric synapses) terminal membranes making synaptic contacts with dendritic spines and dendrites, respectively. Red outline: inhibitory terminals and preterminals; Blue outline: excitatory terminals; White arrowheads: excitatory and inhibitory synapses; Black arrows: CB1 receptor immunoparticles. ter: terminal; den: dendrite; sp: dendritic spine; m: mitochondria. Scale bars: 0.5 µm.

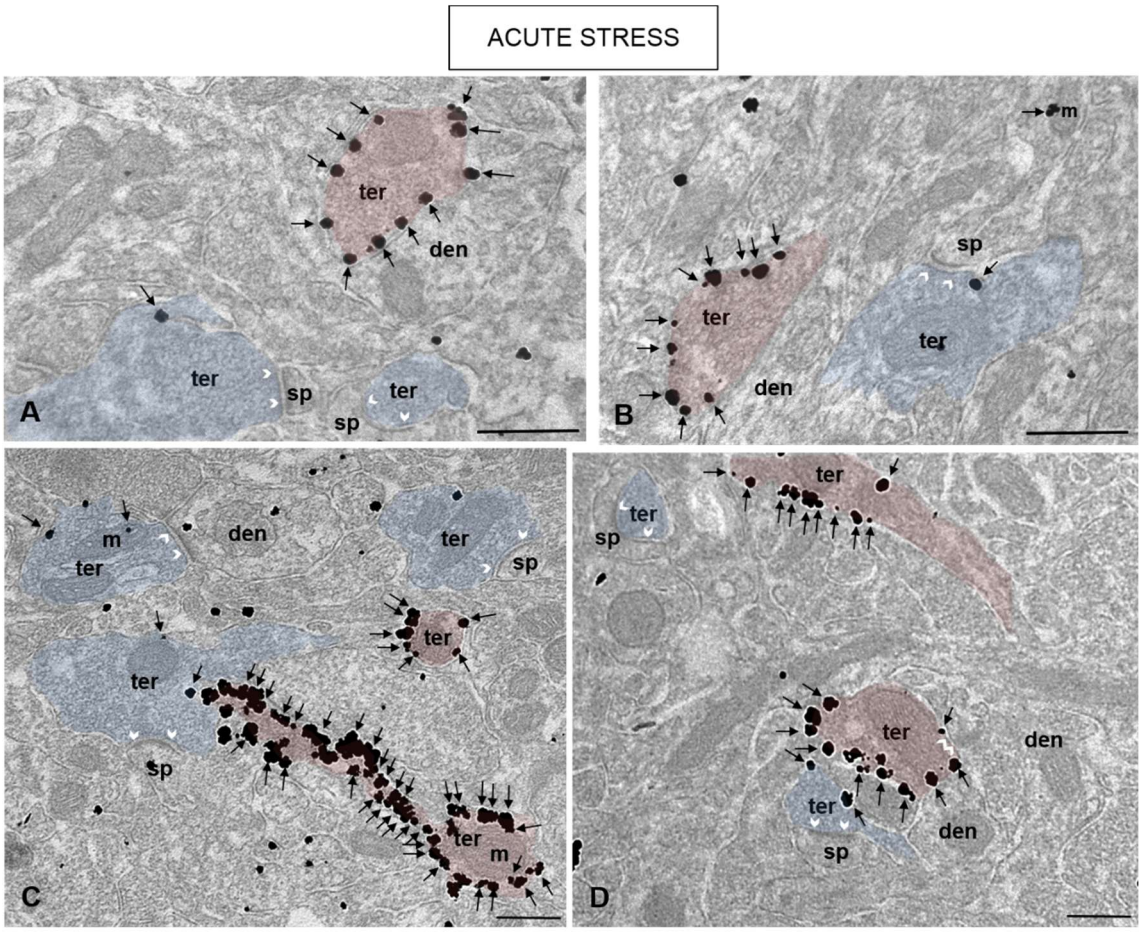

Figure 18: Subcellular CB_1 receptor localization in synaptic terminals of the MPP in the DML after acute stress. Pre-embedding immunogold method for electron microscopy. A-D) CB_1 receptor immunoparticles on presynaptic terminals of asymmetric synapses with dendritic spines but numerous/abundant metal particles at inhibitory terminals are seen. Red outline: inhibitory terminals and preterminals; Blue outline: excitatory terminals; White arrowheads: synapses; Black arrows: CB_1 receptor immunoparticles. ter: terminal; den: dendrite; sp: dendritic spine; m: mitochondria. Scale bars: 0.5 µm.

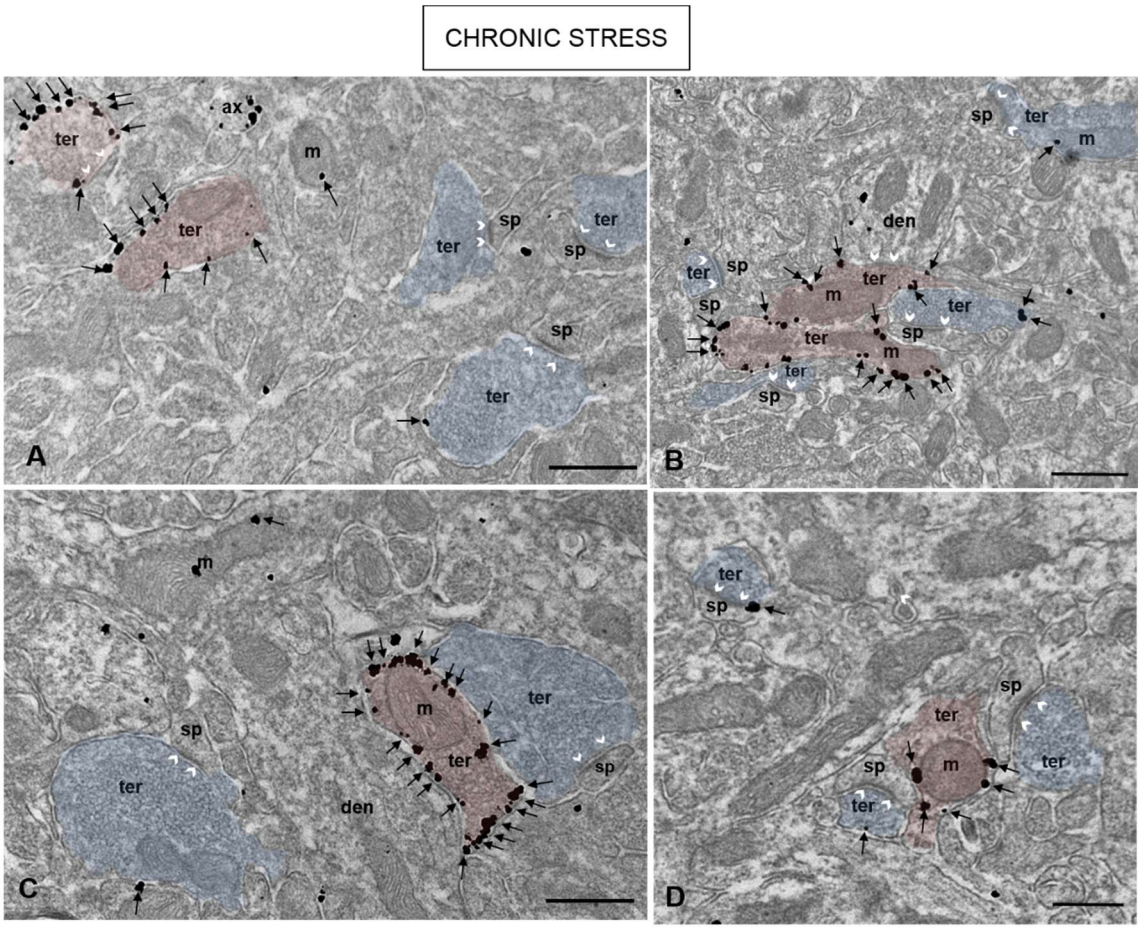

Figure 19: Subcellular CB_1 receptor localization in synaptic terminals of the MPP in the DML after chronic stress. Pre-embedding immunogold method for electron microscopy. A-D) CB_1 receptor immunoparticles are localized on excitatory (asymmetric synapses) and inhibitory (symmetric synapses) terminal membranes making synaptic contacts with dendritic spines and dendrites, respectively. Red outline: inhibitory terminals and preterminals; Blue outline: excitatory terminals; White arrowheads: synapses; Black arrows: CB_1 receptor immunoparticles. ter: terminal; den: dendrite; sp: dendritic spine; m: mitochondria. Scale bars: 0.5 µm.

5.6.2 Statistical analysis of the CB_1 receptors distribution in excitatory terminals of acute and chronic stress

In controls, 40.83 ± 1.61 % of the excitatory synaptic terminals in the target zone of the MPP in the DML were CB_1R immunopositive. There were not statistical differences with the proportions found in acute (38.36 ± 1.70 %; $p>0.05$) and chronic stress (36.03 ± 2.29 %; $p>0.05$) (Figure 20A). Furthermore, the CB_1R density in the excitatory terminals was not significantly different between controls (0.68 ± 0.02 part/µm; $p>0.05$) and after acute (0.63 ± 0.02 part/µm) or chronic stress (0.72 ± 0.03 part/µm; $p<0.05$). However, the somehow higher CB_1R density detected after chronic stress was statistically significant with respect to acute stress (Figure 20B).

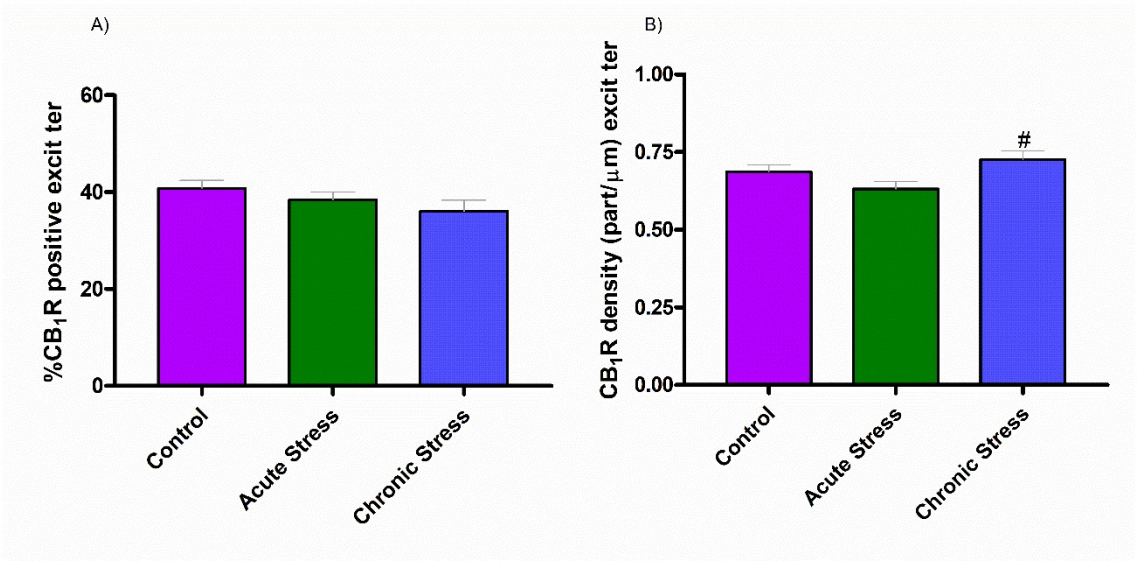

Figure 20: Statistical assessment of the CB_1R immunopositive glutamatergic terminals of the MPP in the DML in controls and after acute and chronic stress. A) The proportions of 40.83 ± 1.61 % in control, 38.36 ± 1.70 % in acute and 36.03 ± 2.29 % in chronic stress are not statistically different. **B)** Mean CB_1R density (part/µm) in CB_1R immunopositive excitatory terminals. The density in chronic stress is statistically higher (0.72 ± 0.03 part/µm) than in acute stress (0.63 ± 0.02 part/µm) but there are not differences with respect to controls. The data are expressed as mean ± SEM and were analyzed by One-Way ANOVA and Dunn´s Multiple Comparison Post-hoc Test. # indicate statistically significant differences with $p<0.05$ vs. acute stress.

5.7 Electrophysiology in Acute and Chronic Stress

The minimum intensity needed to obtain the maximal signal in the experimental groups was first established (Figure 21). As a result, around 40% below that intensity was used in both synaptic transmission and plasticity protocols.

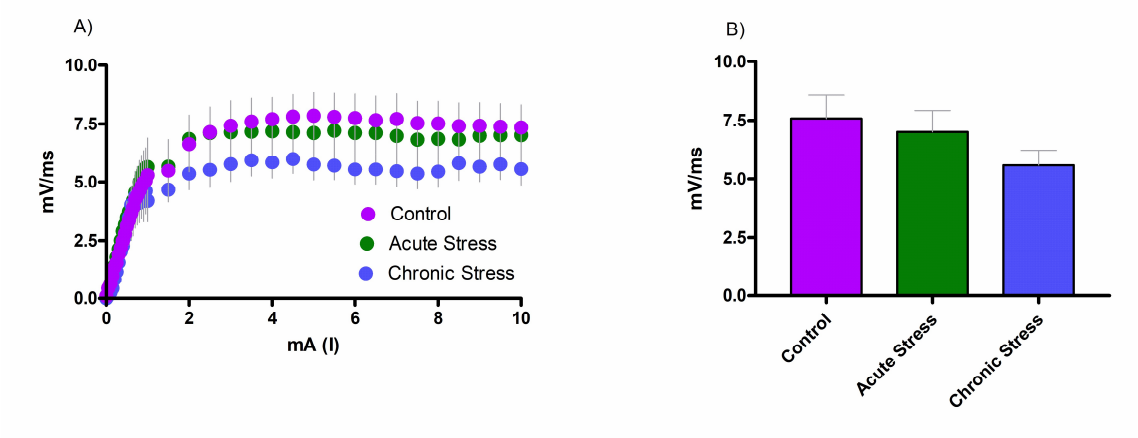

Figure 21: Effect of stress on basal activity frequency. **A)** Blot diagram of the frequency. **B)** Histogram of the means in controls (7.58 ± 0.98 mV/ms), acute (7.01 ± 0.91 mV/ms) and chronic stress (5.59 ± 0.64 mV/ms). There are not significant differences between the groups. Data are expressed as mean ± SEM and were analyzed by One-Way ANOVA and Bonferroni´s Multiple Comparison Post-hoc Test.

5.7.1 Synaptic transmission

We first tested the hypothesis that field excitatory post-synaptic potentials (fEPSP) responses in the MPP were CB_1R-dependent. Hence, bath application of the CB_1R agonist CP55940 to the hippocampal slices caused an inhibition of the postsynaptic excitatory transmission in the MPP (values: 83.08 ± 3.95 %; 16.92 % of inhibition; n=12) that was abolished by the CB_1R antagonist AM251 (4μM) (values: 100.4 ± 3.79 %; n=7) (Figures 22C and 22D). In addition, the $GABA_BR$ antagonist CGP55845 (5μM) blocked the CP55940-induced fEPSP inhibition (values: 105.7 ± 6.23 %; n=10) supporting the existence of a $GABA_B$ and CB_1 receptor interaction (Cinar R. *et al*., 2008) (Figures 22E and 22F).

The fEPSPs decrease observed after CP55940 application in acute (values: 87.94 ± 3.71 %; 12.06% decrease; n=7) and chronic stress (values: 90.72 ± 6.62 values:; 9.72% decrease; n=10) was not significant relative to controls (Figures 22A and 22B).

Furthermore, AM251 increased the fEPSPs in controls (values: 136.7 ± 3.14 %; n=7), acute (values: 117.6 ± 4.84 %; 17.6% increase, n=7) and chronic stress (values: 118.5 ± 2.98 %; 18.5% increase, n=10). However, the fEPSP increase in both stress conditions was significantly lower than in controls (Figure 23).

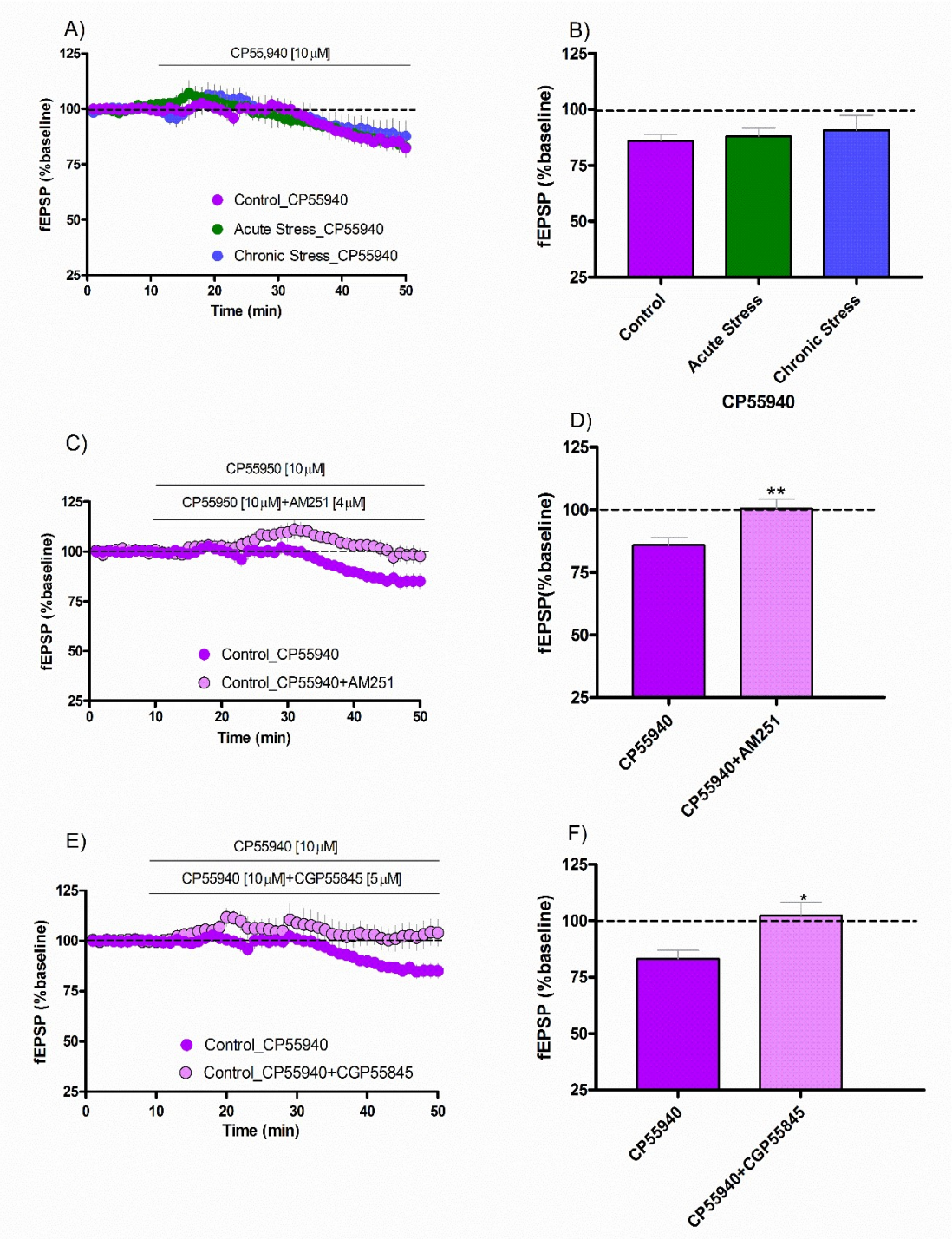

Figure 22: Field excitatory postsynaptic potentials (fEPSP) in the MPP. A) CP55940 induces fEPSP inhibition in all experimental groups. **B)** fEPSP (mean) in control (83.08 ± 3.95 %), acute (87.94 ± 3.71 %) and chronic stress (90.72 ± 6.62%). No significant differences are found between conditions. **C)** fEPSP average areas with CP55940 and AM251 in control. **D)** CP55940 plus AM251 in control produces a statistically significant recovery of the fEPSP area inhibition (100.4 ± 3.79 %). **E)** The GABABR antagonist CGP55845 blocks the CP55940 effect on baseline synaptic transmission in control mice. **F)** Graph representation of the fEPSP area upon application of CP55940 plus CGP55845 (105.7 ± 6.23 %). The cocktail does not induce fEPSP inhibition in controls. Data are expressed as mean ± SEM and were analyzed by One-Way ANOVA and Bonferroni´s Multiple Comparison Post-hoc Test and by Student unpaired t-test. ** indicate statistically significant differences with $p<0.01$; * indicate statistically significant differences with $p<0.05$.

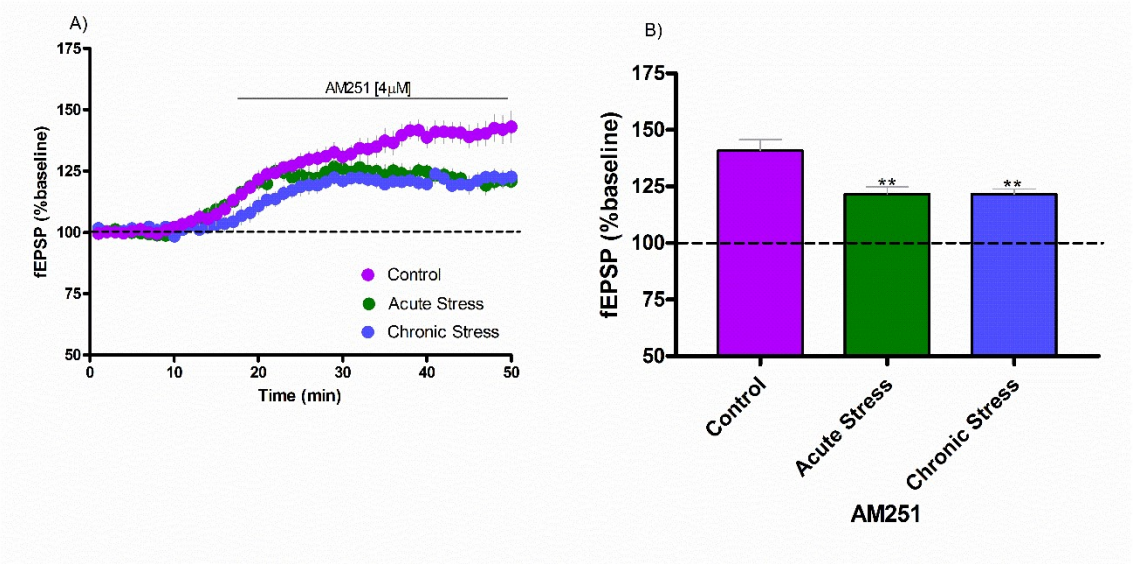

Figure 23: Imbalance of the endocannabinoid system. **A)** The fEPSP increase after bath application of AM251 is affected by stress. **B)** Summary data of the experiments performed. The fEPSP increase observed in controls is significantly reduced in both acute (117.6 ± 4.84 %) and chronic stress (118.5 ± 2.98 %). Data are expressed as mean ±SEM and were analyzed by One-Way ANOVA and Bonferroni´s Multiple Comparison Post-hoc Test. ** indicate statistically significant differences with p<0.01 vs. control.

5.7.2 eCB- eLTD in control mice

In this thesis work, I was able to confirm the novel eCB-dependent LTD of the excitatory synaptic transmission at the MPP synapses in the DML that has been very recently reported by our laboratory (Peñasco *et al*. 2019, submitted) in control mice. Previous studies reported that the extracellular field configuration allows long-term stable recordings in the brain of mature mice (Gredeman *et al*., 2002; Robbe *et al*., 2002; Wang *et al*., 2010; Puente N. *et al*., 2010). Hence, the excitatory fibers raising from the entorhinal cortical layers II-III were stimulated in the medial 1/3 of the DML to evoke baseline fEPSP in the MPP. Repetitive stimulation of the MPP fibers at moderate frequency (10Hz) for 10 min triggered LTD of the fEPSP (86.64 ± 2.27 %, p<0.001; n=16) that was completely abolished by the CB_1 receptor antagonist AM251 ([4 µM]; 103.6 ± 4.16 %; p<0.01; n=8.), the TRPV1 antagonist AMG9810 ([3µM]; 103.7 ± 4.40 %; p<0.01;

n=5) and the $GABA_B$ receptor antagonist CGP55845 ([5μM]; 103.0 ± 3.92 %; p<0.01; n=7) (Figures 24A-B and 25C). Furthermore, this LTD required the participation of the mGluR5 (mGluR5 antagonist MPEP: [10μM]; 110.5 ± 2.6 %; p<0.001; n=9), the 2-AG degrading and synthesizing enzymes MAGL (MAGL inhibitor JZL184: [50μM]; 101.7 ± 5.56 %; p<0.01; n=13) and DAGL (DAGL inhibitor RHC80267: [100μM]; 97.19 ± 2.8 %; p<0.01; n=14) respectively, as well as L-type voltage gated Ca^{2+}channels (L-VGCC) (the L-type Ca^{2+}channel blocker nimodipine: [1μM]; 105.3 ± 3.51 %; p<0.001; n=7) (Figures 24C, 24E-F and 25B). Furthermore, the LTD was unaffected by the FAAH inhibitor URB597 (2μM; 82.4 ± 4.48 %; p>0.05; n=9) and the NMDAR antagonist DL-APV ([100μM]; 90.27%±4.62%; p>0.05; n=6) (Figures 24D and 25A). Taken together, the data indicate that mGluR5 and TRPV1 activity together with Ca^{2+} entry through L-type Ca^{2+} channels combine with CB_1R activation by 2-AG are necessary to generate the eCB-LTD at the excitatory MPP synapses (Figures 24G and 25D).

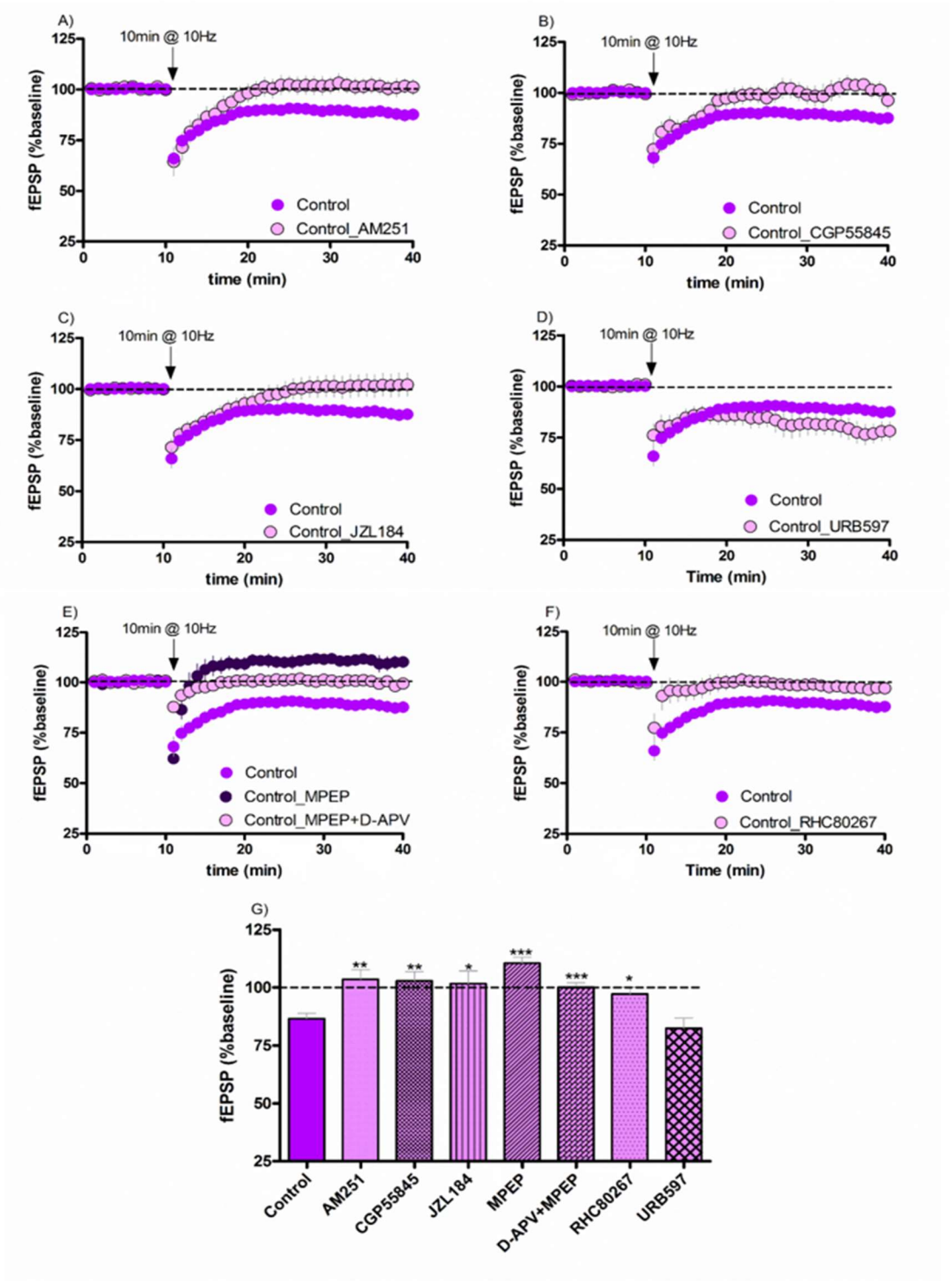

Figure 24: eCB-LTD in control mice. The LTD triggered by MPP stimulation (10Hz, 10´) is blocked by AM251 (103.6 ± 4.16 %; n=8) **(A)** and CGP55845 (103.3 ± 3.92 %; n=7) **(B). C)** Time course plot illustrating that the MAGL inhibitor JZL184 occludes the LTD (101.7 ± 5.56 %; n=13), but is unaffected by the FAAH inhibitor URB597 (82.4 ± 4.48 %; n=9) **(D). E)** The LTD is also blocked by MPEP (110.5 ± 2.6%; n=9) and the DAGL inhibitor RHC80267 (97.19 ± 2.8 %; n=14) **(F). G)** Summary data of the experiments performed. Data are expressed as mean ± SEM and were analyzed by Student´s unpaired t test. *** p<0.001 vs. control. ** p<0.01 vs. control.* p<0.05 vs. control.

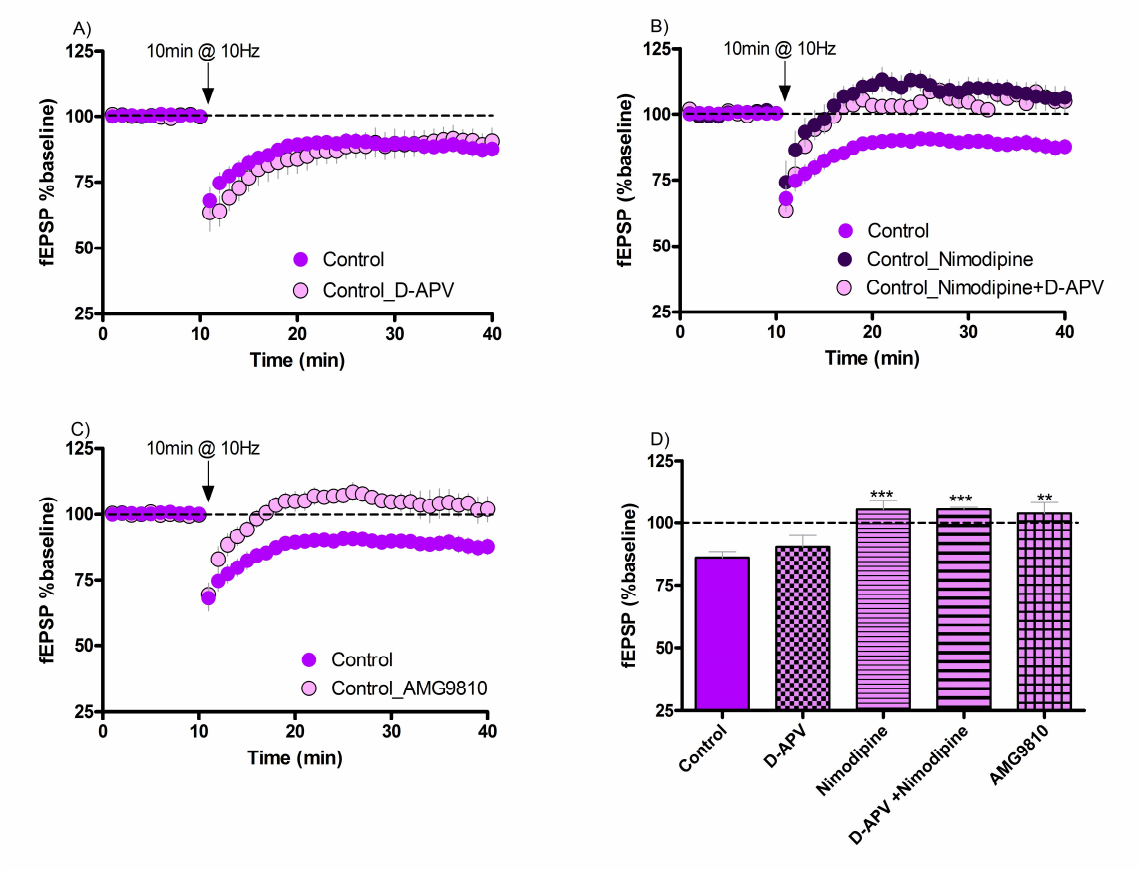

Figure 25: LTD in control mice. A) The NMDA receptor antagonist D-APV has no effect on the MPP-LTD (90.27 ± 4.62 %; n=6), while the L-type Ca^{2+} channel blocker nimodipine (105.3 ± 3.51 %; n=7) **(B)** and the TRPV1 antagonist AMG9810 (103.7 ± 4.40 %; n=5) **(C)** abolish the LTD. **D)** Summary data of the experiments performed. Data are expressed as mean ± SEM and were analyzed by Student unpaired t test. $^{***}p<0.001$ vs. control. $^{**}p<0.01$ vs. control.

5.7.3 eCB-eLTD in acute stress

In conditions of acute stress, 10 Hz MPP stimulation during 10 min triggered a long-term potentiation (LTP) of the fEPSP at the MPP synapses (113.3 ± 2.89 %; p<0.001; n=12) (Figure 26). To study the underlying mechanisms supporting the switch from LTD to LTP in acute stress, we started doing pharmacological manipulations of the receptors involved in LTD under normal conditions. Hence, LTP of fEPSP was blocked by AM251 ([4μM]; 102.3 ± 3.11 %; p<0.05 vs. AS; n=10) but not by CGP55845 ([5μM]; 109.7 ± 2.59 %; p>0.05 vs. control; n=7) (Figures 27A-B). However, AMG9810 slightly reduced (5.57%) the fEPSP ([3μM]; 94.43 ± 3.08 %; n=12). This synaptic depression was abolished by AM251 ([4μM]; 102.1 ± 4.57 %; p<0.01 vs. control; n=8) (Figure 28B). In addition, LTP was elicited in the presence of JZL184 ([50μM]; 111.9 ± 4.78 %; p<0.001 vs. control; n=14) and RHC80267 ([100μM]; 105.2 ± 5.16 %; p<0.05 vs. control; n=9) (Figures 27D-E). However, LTD was observed with URB597 (93.59 ± 6.10 %; p<0.01 vs. AS; n=7) (Figure 27F). Thus, the changes in synaptic plasticity in acute stress involve AEA but not 2-AG. Furthermore, the switch from LTP to LTD was more significant in the presence of nimodipine ([1μM]; 87.87 ± 4.26 %; p<0.001 vs. AS; n=8). Similarly, when D-APV was applied, the LTD recovered in a significant manner ([100μM]; 88.46 ± 4.35 %; p<0.001 vs. AS; n=7). Interestingly, the activity-dependent LTD elicited in the presence of AMG9810, D-APV and nimodipine was fully abolished by AM251 (Figure 28). However, only the LTD block was statistically significant vs AS+D-APV when both the NMDA and CB_1 receptor antagonists were present in the bath solution (D-APV+AM251: 104.6 ± 2.14%; p<0.05 vs. drug; n=4) (Figure 28).

We also wanted to know whether the intensity threshold of synaptic plasticity was altered. Hence, we modified the time of the stimulus (1 min at 10 Hz and 5 min at 10Hz. We observed a slightly reduction of the fEPSP (2.82%) after 1 min at 10 Hz (values: 97.18 ± 2.66 %; p<0.01; n=7). However, 5min at 10Hz elicited eLTD (6.5% fEPSP inhibition; values: 93.50 ± 4.08 %; p<0.01; n=5) (Figure 29). Overall, LTP was AEA and

Ca^{2+} dependent but independent of 2-AG, while LTD was CB_1Rmediated, suggesting that CB_1R worked properly. Moreover, acute stress alters the intensity threshold of the excitatory synaptic plasticity.

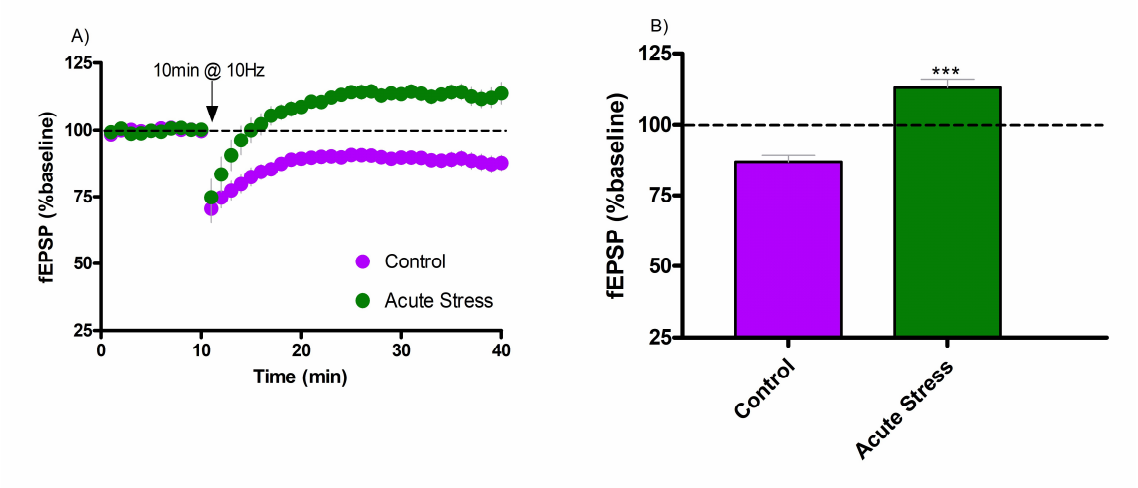

Figure 26: Acute stress switches LTD to LTP. A) Kinetic of the mean percentage change. The 10 min at 10 Hz stimulation has opposite effects on MPP plasticity in control and acute stress mice. **B)** LTD switches to LTP (113.3 ± 2.89 % fEPSP; n=10). Data are expressed as mean ± SEM and were analyzed by Student unpaired t test. *** $p<0.001$.

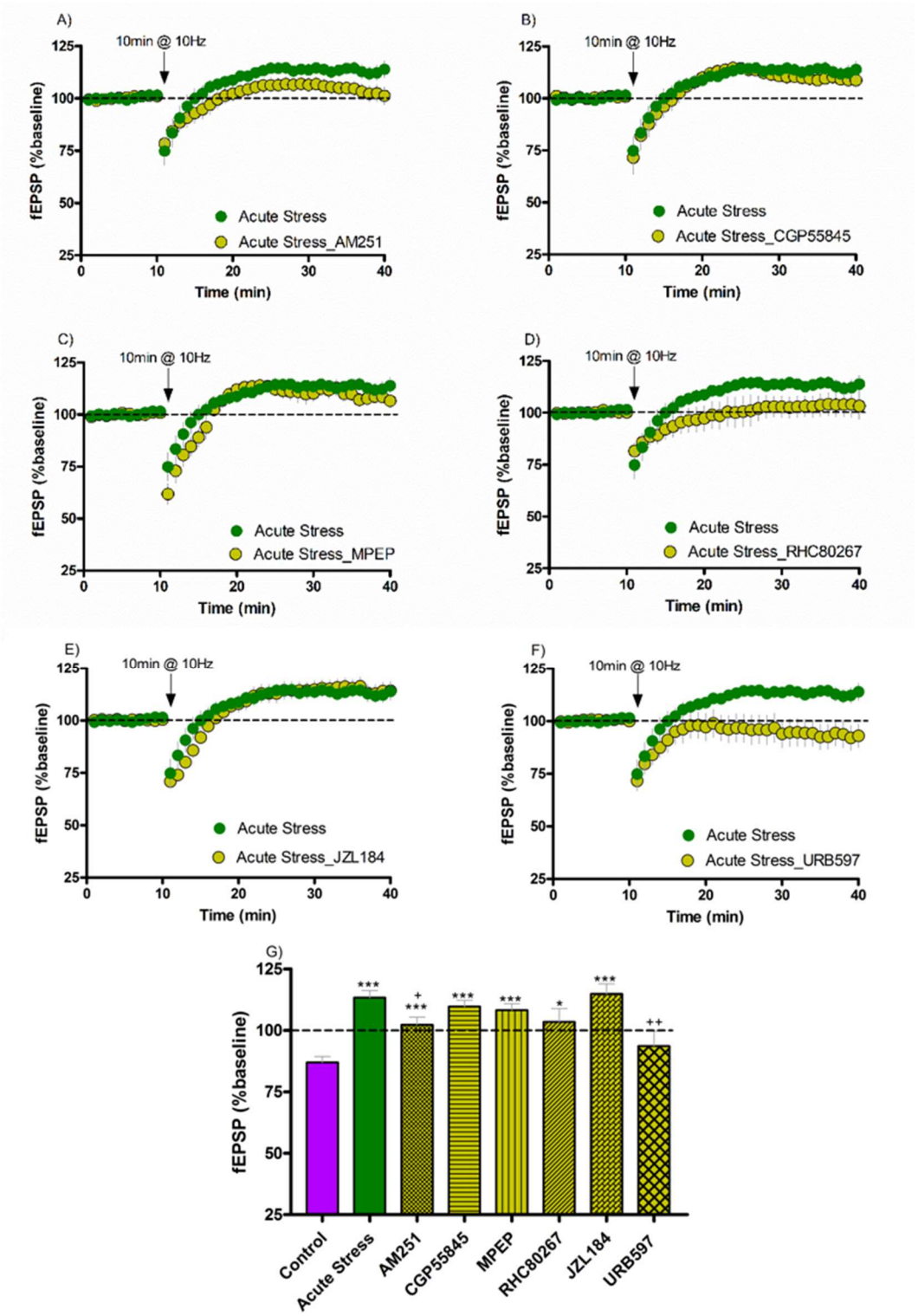

Figure 27: Acute stress displays AEA-dependent LTD. A) LTP was CB_1R-mediated (102.3 ± 3.11 %; n=10). However, $GABA_BR$ (109.7 ± 2.59%, n=7) **(B),** mGluR5 (108.2 ± 2.68 %; n=6) **(C),** DAGL (105.2 ± 5.16 %, n=9) **(D)** and MAGL (111.9 ± 4.78 %, n=14) **(E)** are not involved in the LTP-MPP upon 10 min at 10Hz in acute stress**. F)** LTD is elicited in the presence of URB597 (93.59 ± 6.10 %; n=7). **G)** Summary data illustrating the changes observed. Data are expressed as mean ± SEM and were analyzed by One-Way ANOVA and Bonferroni´s Multiple Comparison Post-hoc Test. *** p<0.001 vs. control. * p<0.05 vs. control. $^{++}$ p<0.01 vs. acute stress; $^{+}$ p<0.05 vs. acute stress.

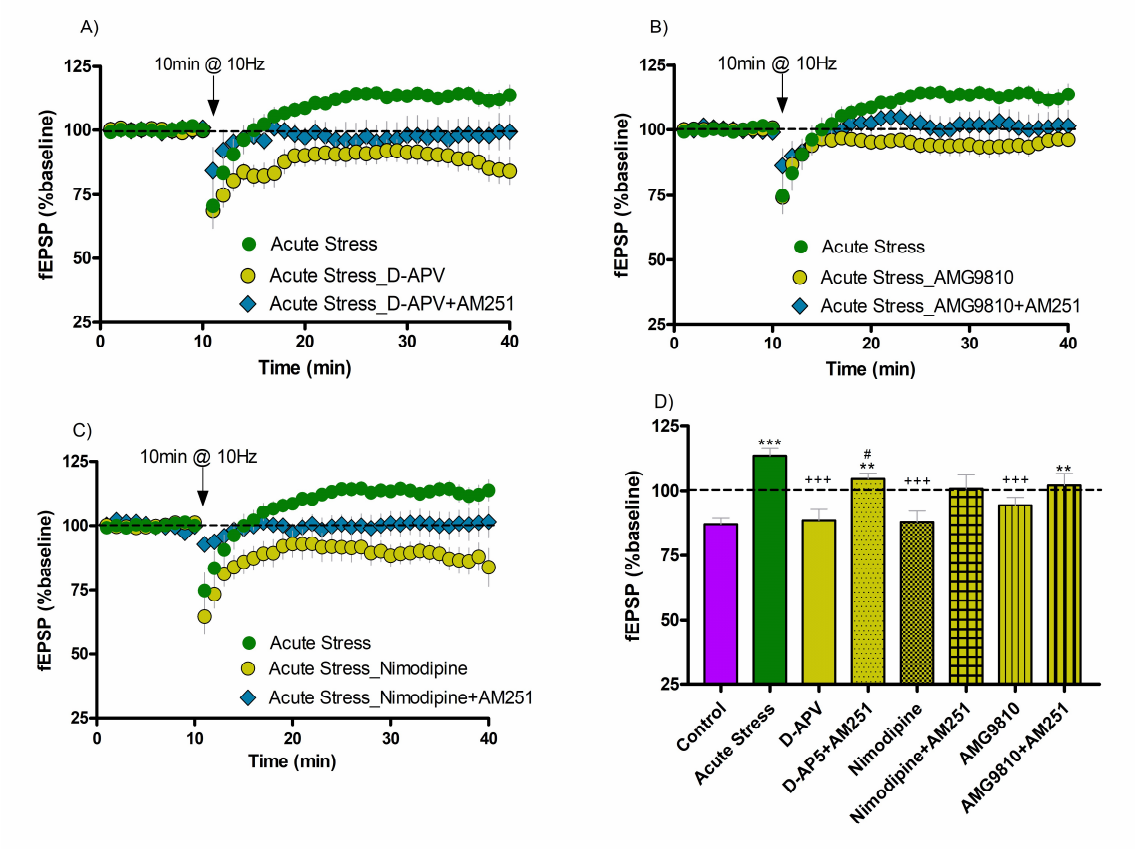

Figure 28: Changes in long-term synaptic plasticity under acute stress. A) The fEPSP increase induced by 10 Hz/10´ stimulation of the MPP synapses under acute stress (109.7 ± 2.59 %) is significantly reduced by D-APV (88.46 ± 4.35 %), AMG9810 (**B)** and nimodipine (87.87 ± 4.26 %) **(C)**. In the three cases, the fEPSP depression disappears with the concomitant application of AM251 (D-APV+AM251: 104.6 ± 2.14 %) **(A),** (AMG9810+AM251: 102.1 ± 4.57 %) **(B),** (nimodipine+AM251: 100.8 ± 5.34 %) **(C). D)** Summary data illustrating in percentage the means of the fEPSP changes. Data are expressed as mean ± SEM and were analyzed by One-Way ANOVA and Bonferroni´s Multiple Comparison or Dunn´s Multiple Comparison Post-hoc Test. *** p<0.001 vs. control. **p<0.01 vs. control. +++p<0.001 vs. acute stress. #p<0.05 vs drug.

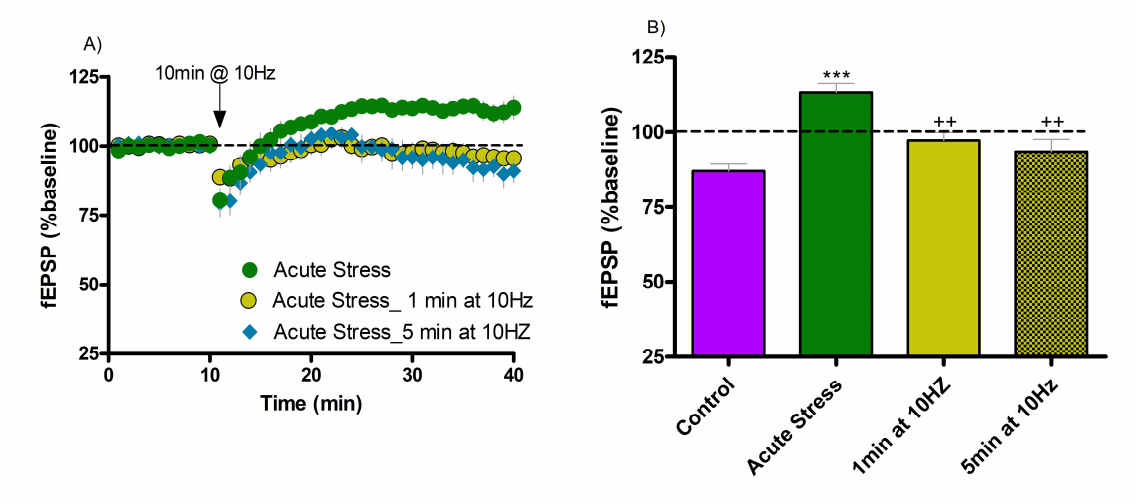

Figure 29: Acute stress disrupts LTD intensity threshold. **A)** Kinetics of the intensity fEPSP changes elicited by 10Hz during 1 min and 5 min. LTD is generated by short intensity times a. **B)** Quantification of the mean percentage change of 10HZ at 1 min (97.18 ± 2.66 %, n=7) and 5 min (93.50 ± 4.04 %, n=5). Data are expressed as mean ± SEM and were analyzed by One-Way ANOVA and Bonferroni´s Multiple Comparison Post-hoc Test. *** p<0.001 vs. control. $^{++}$ p<0.01 vs. acute stress.

5.7.4 Characterization of the eCB-eLTD in chronic stress

In chronic stress conditions, the repetitive MPP stimulation (10Hz, 10´) was not able to induce LTD of the fEPSP (101.7 ± 3.85 %; p<0.01; n=10) (Figure 30). Furthermore, the CB_1R and TRPV1 receptor antagonists did not have any effect (AM251: 108.10 ± 2.78 %; p>0.05 vs. CS; n=4. AMG9810: 110.8 ± 8.72 %; p>0.05 vs CS; n=4) (Figure 31). However, the fEPSP increase was observed when the endocannabinoid tone was enhanced by extracellular administration of JZL184 (121.4 ± 4.08 %; p<0.01 vs. CS; n=8) or URB597 (123.4 ± 5.75 %; p<0.01 vs. CS; n=7) (Figures 32A and 33A). Conversely, concomitant application of AM251 with JZL184 blocked the fEPSP potentiation observed after JZL184 administration (102.9 ±4.35 %; p>0.05 vs. CS; n=7). Also, bath application of JZL184 with AMG9810 reduced fEPSP potentiation (102.3 ± 2.50 %; p>0.05 vs. CS; n=10) (Figures 32B-C). Similarly, fEPSP potentiation was reduced in the presence of URB597 plus AM251 (107.1 ± 2.10 %; p>0.05 vs. control;

n=8) or URB597 plus AM251 plus AMG9810 (108.8 ± 4.95 %; p>0.05; n=8) (Figures 33B- C). Additionally, slight fEPSP depression of 8.41% and 8.77% was observed with superfusion of JZL184 plus AM251 plus AMG9810 (91.59 ± 4.96 %; p<0.001 vs. CS_JZL184; n=8) and URB597 plus AMG9810 (91.23 ± 4.21 %; p<0.001 vs. CS_URB597; n=7), respectively (Figures 32D and 33D). Altogether, these results demonstrate the imbalance settled in the endocannabinoid control of the MPP synapses upon chronic stress.

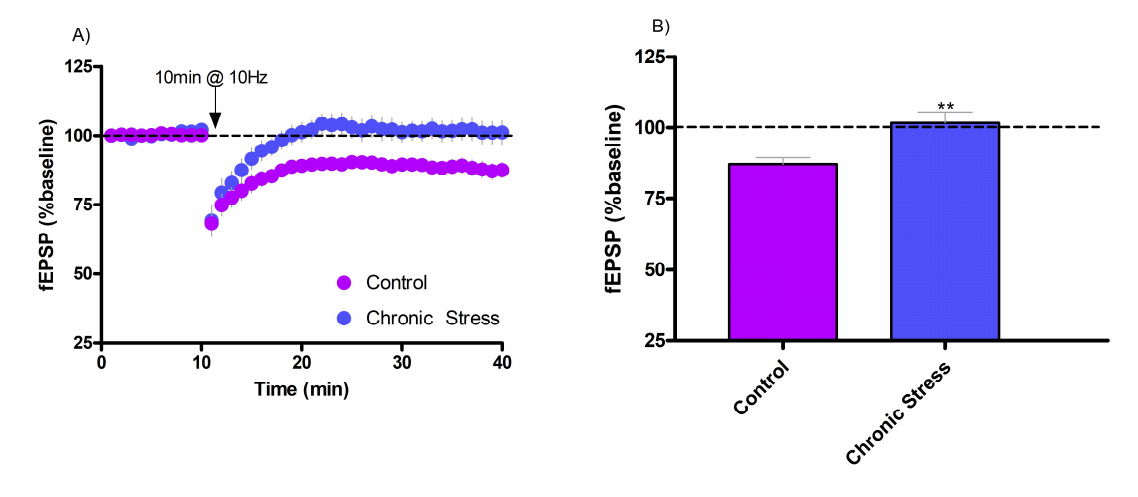

Figure 30: Chronic stress impairs LTD at the MPP synapses. A) LTD is not seen after 10Hz/10´ MPP stimulation. **B)** The value of fEPSP relative to baseline is 101.7 ± 3.85 % in chronic stress. Data are expressed as mean ± SEM and were analyzed by Student unpaired t test.** p<0.01.

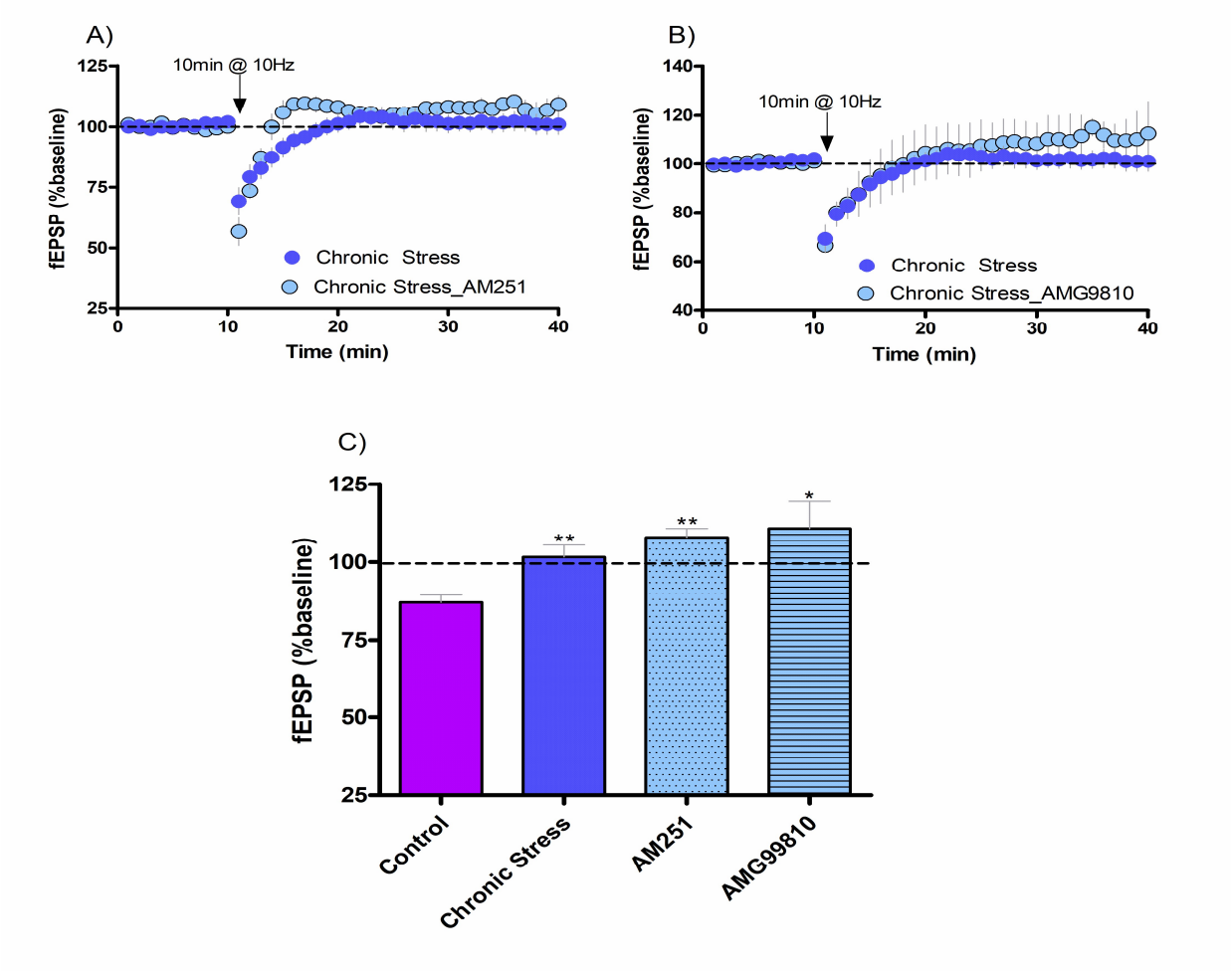

Figure 31: Chronic stress alters CB_1 and TRPV1 receptors at MPP synapses. fEPSPs elicited by 10 Hz/10´ MPP stimulation significantly increase upon AM251 (108.10 ± 2.78 %) **(A)** and AMG9810 (110.8 ± 8.72 %) **(B). C)** Summary data representing the mean percentage change in fEPSP. Data are expressed as mean ± SEM and were analyzed by One-Way ANOVA and Dunn´s Multiple Comparison Post-hoc Test. $^{**}p<0.01$ vs. control. $^{*}p<0.05$ vs. control.

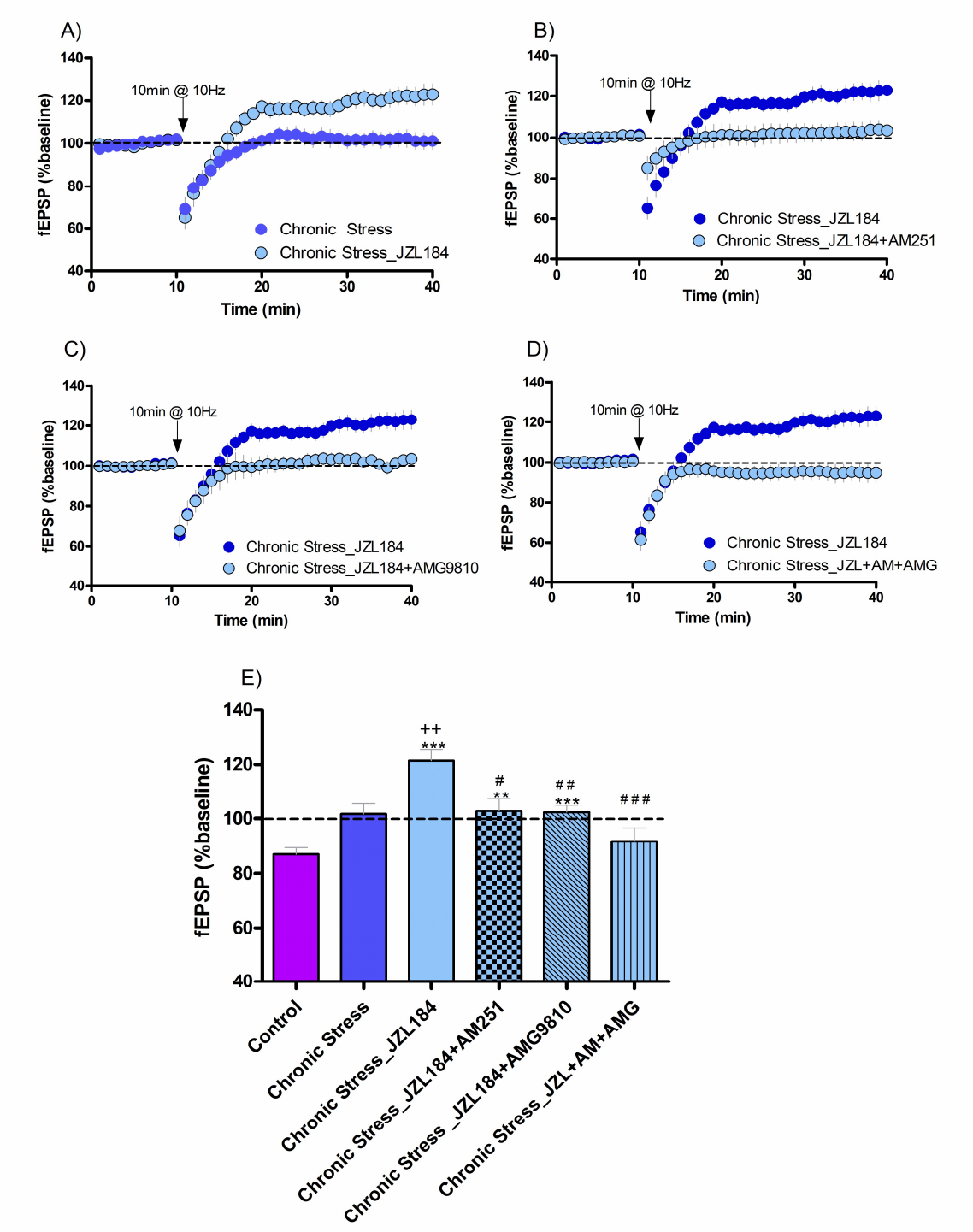

Figure 32: Chronic stress generates an imbalance in the regulation of eCB system at MPP synapses. A) JZL184 elicits a drastic increase in fEPSP upon MPP stimulation (121.4 ± 4.08 %). This effect is abolished by AM251 (102.9 ± 4.3 %) **(B)** and AMG9810 (102.3 ± 2.50 %) **(C). D)** Simultaneous bath application of AM251 and AMG9810 shows a more drastic reduction in the JZL184-mediated increase in fEPSP (91.59 ± 4.96 %). **E)** Summary data illustrating the means of the percentage changes in fEPSP. Data are expressed as mean ± SEM and were analyzed by One-Way ANOVA and Bonferroni´s Multiple Comparison Post-hoc Test. ***p<0.001 vs. control. ** p<0.05 vs. control. $^{++}$ p<0.01 vs. chronic stress. $^{\#\#\#}$p<0.001 vs. JZL184.$^{\#\#}$ p<0.01 vs. JZL184.$^{\#}$ p<0.05 vs. JZL184.

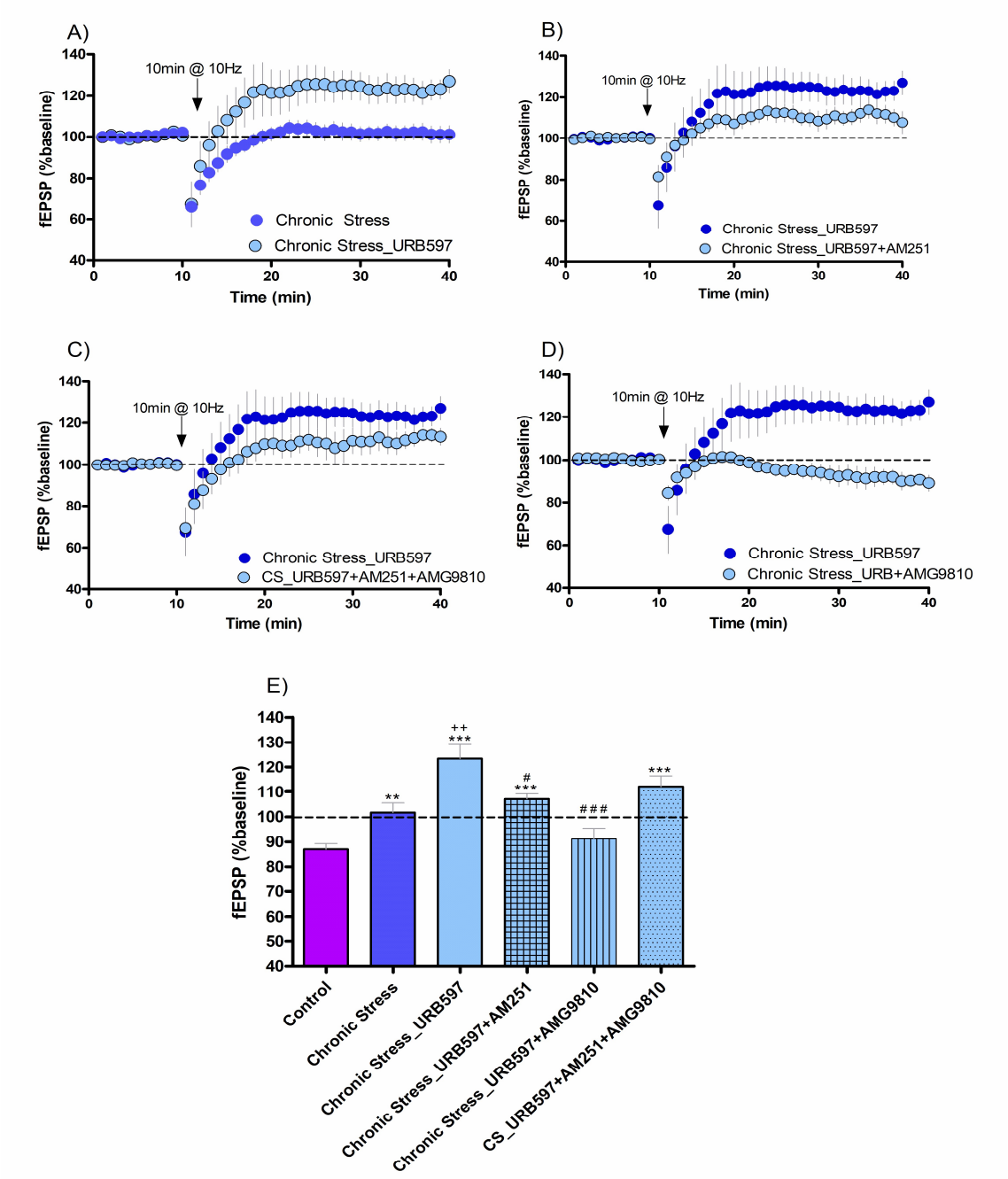

Figure 33: Chronic stress generates an imbalance in the regulation of eCB system at the MPP synapses. **A)** URB597 elicits a drastic increase in fEPSP upon MPP stimulation: (123.4 ± 5.75 %). **(B)** This effect is abolished by AM251 (107.1 ± 2.10 %). **C)** Simultaneous bath application of AM251 and AMG9810 shows a reduction in the URB597-mediated increase in fEPSP (108.8 ± 4.95 %). **D)** However, AMG9810 alone reduces further the fEPSP increase (91.23 ± 4.21 %). **E)** Summary data illustrating the means of the percentage changes in fEPSP. Data are expressed as mean ±SEM. and were analyzed by One-Way ANOVA and Bonferroni´s Multiple Comparison Post-hoc Test. *** p<0.001 vs. control. ** p<0.05 vs. control. $^{++}$ p<0.01 vs. CS. $^{###}$ p<0.001 vs. URB597. $^{#}$ p<0.05 vs. URB597.

5.8 Behavior Test

5.8.1 Elevated plus maze test

The time of latency shown by the mice in conditions of acute stress was shorter (1.17 ± 0.50 s, $p<0.05$ vs. control; n=15) than in controls (3.10 ± 0.60 s; n=28) but not differences were detected in mice under chronic stress (2.50 ± 0.62 s; $p>0.05$ vs. control; n=15). Furthermore, the time spent in the open arms was not significant different between the experimental groups (control: 3.17 ± 1.03 s; n=28. Acute stress: 0.81 ± 0.55 s; $p>0.05$ vs. control; n=15. Chronic stress: 2.59 ± 1.2 s; $p>0.05$ vs. control; n=15). However, the time of controls in the crossroad (129.7 ± 6.88 s; n=28) significantly decreased in acute (90.69 ± 11.13 s; $p<0.01$ vs. control; n=15) but not in chronic stress (132.0 ± 7.63 s; $p<0.05$ vs. control; n=15) (Figure 34). Altogether, these data suggested that mice under conditions of acute stress, but not chronic stress, have a slight anxiety behavior.

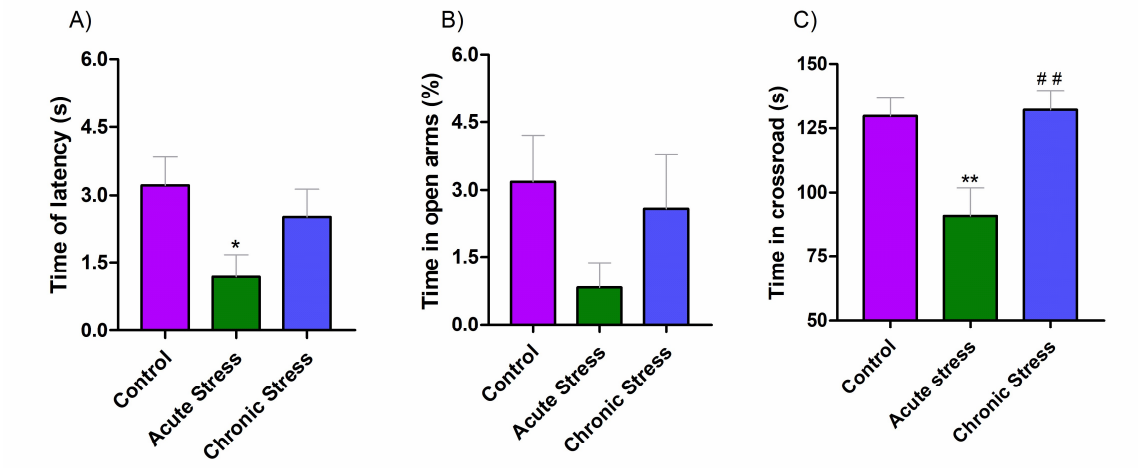

Figure 34: Acute stress causes anxiety-like behavior in mice. A) The latency time displayed by mice with acute stress is significantly lower (1.17 ± 0.50 s) than mice with chronic stress (3.10 ±0.60 s). **B)** No statistical differences are found in the time spent by the mice in the open arms. **C)** Mice with acute stress spend significantly less time in the crossroad (90.69 ± 11.13 s) than mice with chronic stress (129.7 ± 6.88 s). Data are expressed as mean ± SEM and were analyzed by One-Way ANOVA and Dunn´s Multiple Comparison Post-hoc Test. $^{**}p<0.01$ vs. control.$^{*}p<0.05$ vs. control. $^{\#\#}p<0.01$ vs. acute stress.

6. DISCUSSION

The eCB system is a critical component of the body´s homeostatic regulation (Hill *et al*., 2010; Hillard *et al*., 2014; Lutz *et al*., 2015; Morena *et al*., 2016). The endocannabinoid-CB_1R signaling primarily dampens stress reducing both endocrine and neural responses to stress. CB_1R signaling participates in habituation to stress exposure, which is a protective mechanism designed to reduce responses to a non-threatening stimulus. Given the important role of CB_1 receptors in maintaining hedonia and reducing anxiety, the reduction of CB_1R signaling contribute to the negative consequences of stress (McEwen, 2007; Hillard *et al*., 2014; Lutz *et al.,* 2015).

The main results of my Doctoral Thesis were that acute and chronic restraint stress during adolescence severely and differentially disrupt the eCB-eLTD that takes place at the MPP-granule cell synapses under normal conditions after application of a low frequency stimulation (LFS) protocol known to elicit eCB-eLTD at these MPP synapses (Peñasco *et al.*, under review) and at CB_1 receptor-containing excitatory synapses in the BNST (Puente *et al*., 2010, 2011).

6.1 eCB-eLTD at MPP-granule cell synapses in adolescent Swiss male mice.

In this Doctoral Thesis, we have found that a LFS induces CB_1 receptor-dependent inhibition of MPP-granule cell excitatory synaptic transmission in adolescent Swiss male mice. This study confirms the existence of CB_1 receptor-dependent excitatory LTD at the MPP synapses in the DG of adolescent Swiss male mice that requires postsynaptic activation of group I mGluR5, calcium increase and 2-AG synthesis acting on presynaptic CB_1 receptors localized to glutamatergic presynaptic terminals of the MPP. We found a CB_1 receptor-dependent inhibition of MPP-granule cell excitatory synaptic transmission. In addition, a LFS protocol (10 Hz for 10 min) that has previously been used to consistently induce eCB-dependent LTD in other brain regions (Lafourcade *et al*., 2007; Puente *et al*., 2011; Cui *et al*., 2015) elicited a eCB-eLTD at MPP synapses in C57 adult

mice (Peñasco *et al.*, under review) as well as in male adolescent Swiss mice. We also observed that the magnitude of eCB-eLTD was unaffected by the NMDA receptor antagonist D-APV suggesting that NMDA receptors were not involved in the eCB-eLTD despite the fact that eCB-eLTD may require NMDA receptor activity at other synapses (Sjöström *et al*., 2003; Bender *et al*., 2006; Lantè *et al.,*2006).

The stimulation paradigm applied could be a critical factor for the eCB-eLTD induction at the MPP-granule cell synapses. Furthermore, a TRPV1-dependent LTD at these same synapses was previously shown to require mGluR5 activation, but not mGluR1, and involved postsynaptic AMPA receptor internalization (Chávez *et al*., 2010). In my Doctoral Thesis, TRPV1-LTD was also revealed as LFS-induced LTD was abolished in the presence of the TRPV1 antagonist AMG9810. Despite the fact that this eLTD was not AEA-mediated, TRPV1 can modulate synaptic transmission by altering synaptic calcium levels and neurotransmitter release. As a calcium cation channel, TRPV1 has been implicated in synaptic plasticity, especially in facilitating LTD (Ho *et al*., 2012). According to this, our findings showed a TRPV1-dependent eLTD but AEA-independent in hippocampal MPP. This TRPV1-dependent LTD could also be induced by the same stimulation protocol in the BNST that was mediated by postsynaptic mGluR5-dependent release of AEA acting on postsynaptic TRPV1 receptors, and was strongly inhibited by depletion of intracellular calcium stores (Puente *et al.*, 2011). We found that the eCB-eLTD at MPP synapses was 2-AG dependent and activates CB_1 receptors distributed on presynaptic excitatory terminals in the middle 1/3 of the DML. In the BNST, however, dendritic L-type calcium channels and the subsequent release of 2-AG acting on presynaptic CB1 receptors triggered retrograde short-term depression (Puente *et al*., 2011).

In our previous study in adult c57BL/6J mice (Peñasco *et al*., under review) the different kinetics of recovery after LFS following MPEP and CPCCoEt suggest that mGluR1 and mGluR5 contribute differentially to the eCB-eLTD shown at the MPP-

granule cell synapses. That is, while MPEP has an effect on both the induction and late phase, CPCCoEt only affects the late phase of this form of plasticity. Furthermore, both mGluR1 and mGluR5 activation was critically required for persistent eCB-LTD at the MPP-granule cell synapses; however, only mGluR5, and not mGluR1, is required for the initial depression (Peñasco *et al.*, under review). Previous studies in the CA1 hippocampus have shown that differences between both group I mGluR subtypes have distinct effects on synaptic plasticity and memory processes (Neyman and Manahan-Vaughan, 2008). Mechanistically, the activation of mGluR1 causes an intracellular calcium rise, neuronal depolarization and increase in the frequency of spontaneous inhibitory postsynaptic potentials (Mannaioni *et al.*, 2001). However, mGluR5 activation leads to the suppression of calcium-activated potassium currents (IAHP) and the potentiation of N-methyl-d-aspartate (NMDA) receptor currents (Attucci *et al*., 2001; Jia *et al*., n.d.; Mannaioni *et al*., 2001).

The differences observed among studies could be due to several critical factors like rodent species (rat/mouse), mouse strain (c57/Swiss), mouse age (PND 74-80/adolescence of PND 35-42), temperature of the in vitro experiments (32-35ºC) and/or the stimulation paradigm. Significantly, the eCB-LTD can be induced at either presynaptic (our work) or postsynaptic loci (Chávez *et al*., 2010a, and this Thesis work) of the MPP-granule cell synapses depending on the stimulation, recruiting either presynaptic CB1 receptors or postsynaptic TRPV1 and mobilizing 2-AG or AEA, respectively. Together, our findings further suggest that the precise subcellular localization of the eCB components in specific cell types and synapses are key players for the induction of diverse forms of synaptic plasticity through distinct signaling mechanisms (Castillo *et al*., 2012; Puente *et al*., 2011).

We also revealed in this Doctoral Thesis that LFS (10 Hz for 10 min) elicited $GABA_B$-dependent LTD which was blocked by the $GABA_B$ receptor antagonist CGP55845. The CB_1 and metabotropic $GABA_B$ receptors display similar

pharmacological effects in pathways involved in anxiety, learning and memory, cognition, and co-localize in some brain regions (Ameri, 1999; Hampson and Deadwyler, 1999; File *et al.*, 2000; Cannistraro and Rauch, 2003; Freund, 2003; Cinar *et al.*, 2008). Actually, Cinar *et al*. (2008) showed that both receptors localization overlaps in hippocampal membranes. Thus, activation of presynaptic $GABA_B$ receptors decreases neurotransmitter release by VGCC inhibition and vesicular release (Lafourcade and Alger, 2008; Foster *et al.*, 2013; Li *et al.*, 2014) and their presence at excitatory and inhibitory synapses induces inhibitory and disinhibitory effects, respectively (Foster *et al.,* 2013; Nazari *et al.,* 2016). We confirmed that both CB_1 and $GABA_B$ receptors are necessary for the inhibition of MPP-granule cell excitatory synaptic transmission and for the eLTD in hippocampal DG. These results support the existence of a co-localization of both receptors as well as indicate that there are functional interactions between them in MPP synapses during adolescence.

6.1.1 Functional context of the eCB-eLTD at MPP-granule cell synapses

Brain functions regulated by the eCB system rely on its distribution in cerebral tissue (Busquets-Garcia *et al*., 2018; Castillo *et al*., 2012; Hu and Mackie, 2015; Katona and Freund, 2012). The hippocampus is required for declarative/episodic memory and is involved in spatial and context-dependent learning (Eichenbaum *et al*., 2012). Inputs from the postrhinal cortex convey spatial information to the dorsolateral medial entorhinal cortex that projects to the dorsal hippocampus through the MPP (Fyhn *et al*., 2004; Hargreaves *et al*., 2005). On the other hand, the perirhinal cortex projects to the lateral entorhinal cortex which gives rise to the LPP (Burwell, 2000). The LPP pathway transmits non-spatial information, and, together with information about spatial clues forwarded by the MPP into the DG, representations for object-place or event-place scenarios are thought to be built (Suzuki *et al*., 1997; Gaffan, 1998; Hargreaves *et al*., 2005). At the same time, signal integration by granule cells related to environment or context is under control of hilar mossy cells which are critical in the learning of information sequences

(Lisman *et al*., 2005). The mossy cells receive glutamatergic granule mossy fiber collaterals, and in turn send commissural/associational fibers that travel long distances giving innervation to multiple DG cells forming mossy-granule cell synapses (Amaral and Witter, 1989; Scharfman and Myers, 2013). The glutamatergic synapses of the three excitatory pathways targeting the dentate granule cells contain CB_1 receptors (Marsicano and Lutz, 1999; Katona *et al*., 2006; Kawamura *et al*., 2006; Monory *et al*., 2006; Uchigashima *et al*., 2011; Katona and Freund, 2012; Wang *et al*., 2016; Gutiérrez-Rodríguez *et al*., 2017) and display different forms of eCB dependent-synaptic plasticity (Chiu and Castillo, 2008; Chávez *et al*., 2010; Wang *et al*., 2016, 2018) which correlate with the distinct information processed by each pathway.

As previously shown in single BNST neurons (Puente *et al*., 2011), either the 2-AG and CB_1 receptor-dependent eLTD here with described, or the AEA and TRPV1-dependent eLTD at the MPP synapses (Chávez *et al*., 2010b, also observed in this Thesis) might each be switched on by distinct patterns of neural activity conveying spatial information. At the same time, high frequency stimulation of the LPP in the outer 1/3 of the DML leads to 2-AG production and CB1 receptor-dependent eLTP at these LPP synapses which have been associated with memories related to odor discrimination, and semantic information and representation (Wang *et al*., 2016, 2018).

Altogether, the spatial and non-spatial information transmitted by granule cells to CA3 pyramidal neurons that provides sequence learning and sequence prediction (Hunt *et al*., 2013) would involve perforant path inputs and different forms of cannabinoid-dependent plasticity recruited upon the type of information processed, all being modulated by mossy cell activity. Learning and memory processes that involve the hippocampus can be affected by some pathological conditions. For instance, impaired recognition, spatial, and associative memories can be observed in the adult brain after high ethanol exposure (binge drinking) during adolescence (Rico-Barrio *et al*., 2018). This also correlates with a decrease in CB_1 receptor expression in astrocytes (Bonilla-

Del Río *et al*., 2017), as well as with changes in CB_1 receptor expression at the perforant path synapses (Peñasco *et al*., 2015). Interestingly, the memory impairment observed after adolescent binge drinking is recovered in adults exposed to enriched environmental conditions (Rico-Barrio *et al*., 2018). It is plausible that changes in different forms of CB_1 receptor-dependent plasticity in the DG underlie the memory deficits observed in adults after adolescent binge drinking, as well as in the distortion of space perception experienced as a psychoactive effect of cannabis use.

Stress during adolescence might also affect the brain development and maturation (Spear, 2000; Giedd, 2004; Sisk, Foster, 2004; Crews *et al.*, 2007; McCormick, Mathews 2010) through changes in eCB-dependent synaptic plasticity as in this study was demonstrated, leading to psychiatric conditions such as anxiety and depression. The eCBs travel retrogradely across the synaptic cleft to activate pre-synaptic CB_1 receptors on glutamatergic terminals (homosynaptic eCB-LTD) or nearby GABAergic terminals (heterosynaptic eCB-LTD) (Chevaleyre *et al.*, 2006; Castillo, 2012). The eCB release happens via two different post-synaptic processes: activation of Gq protein-coupled group I mGluRs and depolarization-induced calcium influx via VGCC, like L-Type VGCC. The metabotropic pathway engages the activation of PLC and DAGL which generates 2-AG. Most forms of eCB-LTD require postsynaptic calcium increase released from intracellular stores, which likely facilitates eCB production by activating calcium-dependent enzymes, including PLC. The signaling cascade leads to postsynaptic eCB release and activation of presynaptic CB_1 receptors consequently, eliciting LTD. The metabotropic and calcium-driven mechanisms can act independently or synergistically, to promote eCB release and eCB-mediated plasticity (Robbe *et al.*, 2002: Hashimotodani *et al.*, 2007; Heifets and Castillo, 2009; Castillo, 2012). Our data support the hypothesis that these two mechanisms are underlying the eCB-eLTD at the MPP synapses of adolescent Swiss mice. Thus, we demonstrated that this eCB-eLTD is mGluR5- and L-type VGCCs-dependent as it was prevented by bath application of the

mGluR5 antagonist MPEP and nimodipine, respectively. Additionally, we found that in this plasticity 2-AG dependent but AEA-independent.

6.2 Effects of stress on the eCB-eLTD at MPP-granule cell synapses in adolescent Swiss male mice

Restraint conditions do not modify the distribution pattern and functionality of the CB_1 receptors in the hippocampus. In control mice, the eCB-eLTD was 2-AG-mediated, L-type VGCC- and TRPV1-dependent, but AEA and NMDA-independent. However, in acute restraint stress the plasticity switch from LTD to LTP is probably due to a modification in calcium levels and/or eCBs. Furthermore, acute restraint stress disrupts the synaptic intensity threshold which might contribute to the observed changes in synaptic plasticity. On the other hand, the imbalance between both CB_1R and TRPV1 is pronounced in chronic restraint stress that could reflect an adjustment of the organism to recover the control status. Nevertheless, the absence of synaptic plasticity elicited by the LFS applied could be due to eCB disruption. In this scenario, to recover a slight eLTD is necessary CB_1R activation by AEA increase associated with TRPV1 blocking.

6.2.1 Acute stress impairs intracellular calcium and endocannabinoids

Our findings have shown noticeable anatomical, biochemical and physiological changes in the eCB system after acute restraint stress, in particular:

1) The LFS applied (10Hz/10´) (Puente *et al.*, 2011; Peñasco *et al.*, under review) elicits potentiation of the fEPSP instead of LTD that appears to be CB_1 receptor-, 2-AG- and AEA- dependent. Also, LTP switches to LTD by D-APV, AMG9810 and nimodipine; LTD in the three instances is blocked by AM251.

2) Shorter LFS protocols (10Hz / 1 min; 10Hz / 5 min) do not elicit LTP.

3) There are significant decreases in the CB_1 receptor, PLCβ1 and DAGLα proteins.

4) There is a significant decrease in CB_1 receptor immunoreactivity.

5) A remarkable increase in TRPV1 immunoreactivity occurs.

6) The CB_1 receptor localization and expression (%, density) in excitatory terminals are maintained at control values.

7) A very significant increase in 2-AG accompanies the condition.

In both acute and chronic stress conditions, no significant differences in Gα subunits and a significant reduction in [^{35}S] GTPγS basal binding were detected.

Our findings support that acute restraint stress in adolescent mice alters synaptic plasticity through two main ways. One is through the alteration of calcium levels by disrupted calcium channels and receptors. Another is through rapid FAAH mobilization which depletes the AEA signaling, increasing excitability and driving anxiety. Finally, the data suggest that the acute restraint stress increases 2-AG excessively. Hence, alteration of both 2-AG and AEA is involved in the switch from LTD to LTP.

We have found that acute restraint stress does not modify significantly the CB_1 receptor-dependent inhibition of the excitatory synaptic transmission at the MPP-granule cell synapses. Nevertheless, the CB_1 receptor antagonism modifies the inhibition of the excitatory synaptic transmission, indicating an alteration of the eCB system. As we have already discussed LFS triggered eCB-eLTD at the MPP synapses in control mice. However, a single episode of restraint stress seems to have a significant impact on this form of synaptic plasticity. The findings indicate that acute restraint stress generates a bidirectional change in plasticity switching from eCB-dependent LTD to LTP in the MPP synapses in response to LFS. The eCB system through the activation of CB_1 receptors located on

glutamatergic terminals regulate stress responses (Gangletas *et al*., 2013; Lutz *et al*., 2015). Acute homotypic stress reverses the long-term depressive impact of mPFC stimulation onto BNST neurons into LTP. Also, this stress-induced LTP upon 10Hz stimulus was controlled by CB_1 receptors located on glutamatergic terminals (Gangletas *et al*., 2013). We got some data about the effect of an acute restraint stress with a different LFS protocols (10Hz during 1 or 5 min). We observed in these conditions that time is sufficient to change the bidirectionality of the excitatory synapses. These findings support bidirectionality of the hippocampal MPP glutamatergic synapses when acute restraint stress was applied. These data further suggest that acute restraint stress modify the intensity threshold of excitatory synapses, thus enabling the necessary adaptive transformations of the synaptic strength. Moreover, we demonstrated that the switch in the long-term plasticity was not dependent of CB_1 receptor alterations, since the LTP was blocked by the CB_1 receptor antagonist- AM251.

The eCBs can trigger LTP of synaptic transmission in the hippocampus through stimulation of astrocytes (Gómez-Gonzalo *et al*., 2014). This LTP requires activation of group I mGluRs by glutamate released from astrocytes after being stimulated by eCBs. Thus, astrocytic CB_1 receptors elevate calcium and stimulate glutamate release that activates type I mGluRs persistently enhancing synaptic transmitter release when it coincides with a postsynaptic signal through activation of presynaptic PKC (Navarrete *et al*., 2012; Gómez-Gonzalo *et al*., 2014).

In this Thesis work, our data suggest that calcium could underlie the changes in synaptic plasticity at the MPP-granule cell synapses under acute restraint stress conditions. In this sense, the LTP observed in acute stress after LFS could be triggered by an increase in glutamate release and calcium channels activation (TRPV1, NMDA, L-type VGCC), as LTP disappeared after bath perfusion of AMG9820, D-APV and nimodipine, TRPV1 and NMDA antagonists and L-type VGCC blocker, respectively.

Acute restraint stress appears to produce divergent effects on AEA and 2-AG levels in the basolateral amygdala, mPFC and hippocampus. An episodic exposure to restraint stress generates an elevation in 2-AG and a rapid induction of FAAH activity and a resultant decline in the pool of AEA (Patel *et al.*, 2005; Rademacher *et al*., 2008; Hill *et al*., 2009; Dubreucq *et al*., 2012; Wang *et al*, 2012; Guzun-Cinar *et al*., 2013; Morena *et al*., 2016). These findings are according with our results in the MPP synapses as the inhibition of FAAH, therefore, rising AEA levels, generated a slight recovery of the eLTD. On the other hand, our biochemical results have shown an increase in 2-AG after acute restraint stress. However, the perfusion with the MAGL antagonist JZL 184 did not modify the LTP. Moreover, the inhibition of 2-AG synthesis reduced the LTP but the eLTD was not recovered. Overall, the results suggest that acute stress increases 2-AG, nevertheless MAGL could not be functional or is insufficient to degrade the excess of 2-AG. Accordingly, our findings evidence that in the MPP synapses of adolescent mice subjected to acute restraint stress, a rise in AEA might activate CB_1 receptors and /or TRPV1, leading to the recovery of eLTD; however, the 2-AG control is not sufficient to rescue the eLTD.

Our immunohistochemical experiments revealed an increase in the TRPV1 labeling and, as we have already mentioned, our quantitative biochemical experiments demonstrated a 2-AG increase in the hippocampus, suggesting an anatomical and/or functional imbalance between both CB_1 and TRPV1 receptors. TRPV1 is a good stress response candidate because its polymodal nature and sensitivity to noxious stimuli (Caterina *et al.*, 1997; Ross, 2003). By integrating multiple signaling pathways, TRPV1 can modulate intracellular calcium levels to mobilize the cell's response to stress and injury (Ho *et al*., 2012). Moreover, this imbalance between both CB_1 receptors and TRPV1 generated by acute stress could increase intracellular calcium which activates PLC. Consequently, PLC

generates 2-AG through postsynaptic DAGL. As stated in the introduction, when 2-AG suffers a spontaneous acylmigration to yield 1-AG, the balance between the effects on TRPV1 and CB_1 receptors could be changed in systems that contain both receptors. This fact occurs because 1-AG activates TRPV1 but not the CB_1 receptor (Sugiura *et al*., 2006; Zygmunt *et al*., 2013).

Collectively, these data suggest that bidirectionality mediated by calcium and eCB-control could be a defense mechanism of the organism to confront acute restraint stress. Bidirectionality is of paramount functional importance since allows LTD and LTP to reverse each other with time at a single synapse, thus enabling adaptive changes of the synaptic strenght. Both the levels and timing of eCB release control strength changes in synaptic connections. Thus, electrical stimulations that produce moderate amounts of eCBs over a prolonged period lead to synaptic depression. However, stimulations that produce short but large eCB peaks cause synaptic potentiation (Cui *et al*., 2015; Cui *et al*., 2016). The eCBs are major players in learning and memory because of their powerful influence on synaptic plasticity (Chevaleyre *et al.*, 2006; Heifets and Castillo, 2009; Kano *et al.*, 2009; Katona and Freund, 2012). Moreover, there exist a growing body of evidence that paves the way for a bidirectional action of eCBs in synaptic plasticity depending on the activity pattern on either side of the synapse. In the case of glutamate terminals, the principal mechanism proposed to account for bidirectionality is the calcium-control, which states that postsynaptic calcium levels and/or time courses decide the outcome of plasticity (LTP or LTD) (Shouval *et al*., 2002; Graupner and Brunel, 2012; Cui *et al*., 2016). The spike-timing dependent plasticity in the striatum also exhibits eCB-dependent bidirectionality; thus, a prolonged release and moderate levels of eCBs lead to LTD, and a brief release of high eCB concentration yields LTP (Cui *et al*., 2015).

6.2.2 Chronic stress impairs 2-AG levels and the endocannabinoid system

The changes observed in acute restraint stress, however, do not correlate with the effects produced by chronic stress. Thus:

1) LFS protocol (10Hz/10 min) does not elicit LTD nor LTP. However, AM251 and AMG9810 can slightly increase fEPSP.
2) The 2-AG increase by JZL184 switches to LTP blocked by AM251 and AMG9810. Furthermore, AM251+AMG9810 display LTD.
3) URB597 and LFS (10Hz/10 min) elicit LTP reduced by AM251and fully blocked (and beyond: LTD) by AMG9810.
4) The PLCβ1 and DAGLα proteins decrease.
5) There is a little (but significant) decrease in CB_1 receptor immunoreactivity.
6) TRPV1 immunoreactivity increases drastically.
7) There is a significant increase in CB_1 receptor density in excitatory terminals.
8) There is a significant increase in the CP55940 efficacy to stimulate [^{35}S] GTPγS binding.
9) The 2-AG levels decrease significantly.

As already said, in both acute and chronic stress conditions no significant differences in Gα subunits and a significant reduction in [^{35}S] GTPγS basal binding were detected.

We observed in our study a high increase in TRPV1 immunolabeling in the DML of the chronic stress mice. This rise could affect to the balance between both CB_1 receptors and TRPV1 and, as a consequence, the functionality of the MPP synapses are modified. Furthermore, chronic restraint stress do not alter significantly the CB_1 receptor-dependent inhibition of MPP-granule cell synaptic transmission. Nevertheless, the CB_1R antagonism modifies the inhibition of the excitatory synaptic transmission, indicating an alteration of the eCBs levels or their functionality.

Similar to what has been described in acute stress, repeated exposure to homotypic stress reliably reduces AEA levels in the hippocampus, amygdala, hypothalamus and mPFC. This reduction in AEA is associated to an increase in FAAH activity (Patel *et al.*, 2005; Rademacher *et* al., 2008; Hill *et al*., 2010, 2013; Dubreucq *et al*., 2012). These effects of chronic homotypic stress on FAAH and AEA signaling are likely mediated by sustained exposure to corticosterone produced by stress, as some models of chronic corticosterone exposure have similarly found an increase in FAAH activity and a reduction in AEA content. However, these effects of corticosterone appear to be mediated by a CRH mechanism as the ability of chronic corticosterone to increase FAAH and reduce AEA levels are reversed by CRHR1 antagonist and mimicked by the forebrain overexpression of CRH (Bowles *et al*., 2012; Morena *et al*., 2016). These common CRH mechanisms mediated both the acute and chronic stress effects on FAAH and AEA (Morena *et al.,* 2016). By contrast, the literature describes a 2-AG increase in the hippocampus, mPFC, hypothalamus and amygdala in chronic stress (Patel *et al*, 2004, 2005, 2009; Rademacher *et al*, 2008; Hill *et al*, 2010; Dubreucq *et al*, 2012). Actually, the MAGL downregulation in the amygdala contributes to enhance 2-AG signaling after chronic stress (Sumislawski *et al*., 2011). However, our findings show a decrease in hippocampal 2-AG. These different results could be due to several factors: age and mouse strain, type and duration of stress.

We did not find plasticity at the MPP synapses after LFS in adolescent mice with chronic restraint stress. This finding suggests that chronic stress could impair eCBs and/or the functionality of their receptors. Moreover, the pharmacological increase of 2-AG or AEA through the perfusion of a MAGL or FAAH inhibitor, respectively, generated a pharmacological LTP (2-AG-LTP and AEA-LTP). Even though the pharmacological rise of 2-AG generated LTP, neither CB_1R nor TRPV1 blocking recovered eLTD. Despite this, 2-AG-LTP was abolished with either CB_1R or TRPV1 antagonism. However, 2-AG-LTP switched to eLTD when both CB_1R and TRPV1 were blocked simultaneously. A

recently study described a 2-AG-mediated LTP through CB_1R activation in the mouse LPP (Wang *et al*., 2016). This eCB-mediated LTP initiates postsynaptically and requires the activation of mGluR5 and NMDA receptors. Consequently, the increase in postsynaptic calcium activates DAGL-α and 2-AG production causing a long-lasting increase in glutamate release (Wang *et al*., 2016). The study also revealed that the eCB-LTP is due to the reorganization of actin filaments in the glutamatergic axons (Wang *et al*., 2016). In our study, we found that a pharmacological increase of AEA through the inhibition of FAAH causes AEA-LTP. These results suggest that the AEA reduction at the MPP synapses would generate the opposite. However, TRPV1 antagonism suppresses the eLTP induced by pharmacological rise of AEA showing at the same time a slight recovery of eLTD. Furthermore, this eLTD is abolished by CB_1 receptor antagonism. Altogether, these results indicate that the increase in TRPV1 expression is not sufficient to recover the eLTD, and that AEA activates the CB_1 receptor in order to recover a slight eLTD. This fact supports the idea of an eLTD depends on AEA (and not 2-AG) in adolescent Swiss male mice under chronic stress.

7. CONCLUSIONS

The conclusions of this Doctoral Thesis are:

1. Adolescent mice subjected to acute and chronic restraint stress display a highly significant increase in TRPV1 immunostaining.
2. The CB_1 receptor in glutamatergic terminals in the middle 1/3 of DML maintains the same expression and localization after stress as the control mice.
3. CB_1 receptor activation inhibits field excitatory postsynaptic potentials evoked by MPP stimulation in the DML in acute and chronic restraint stress to the same extent as controls. However, CB_1R antagonism reveals an alteration in the eCBs levels and/or functionality in acute or chronic restraint stress.
4. Low frequency stimulation (10 min, 10 Hz) of the MPP in adolescent Swiss mice triggers a CB_1-eLTD at the MPP-granule cell synapses which requires 2-AG, but not AEA, as well as L-type voltage-gated calcium channels, $GABA_B$, mGluR5 and TRPV1, but not NMDA receptors.
5. LFS of the MPP synapses under acute restraint stress triggers an AEA- and calcium-dependent LTP which involves NMDA and TRPV1 receptors.
6. Inhibition of the NMDA-TRPV1 receptor-dependent LTP elicits eCB-LTD at the MPP-granule cell synapses after acute restraint stress.
7. Acute restraint stress disrupts the intensity threshold of the MPP synapses.
8. Acute restraint stress generates anxiogenic-like behavior in adolescent mice.
9. Chronic restraint stress abolishes LFS-induced long-term synaptic plasticity at MPP-granule cell synapses in adolescent mice.
10. LFS-MPP associates with an increase in 2-AG or AEA, and produces LTP, but not LTD, at the MPP-granule cell synapses which involves CB_1 and TRPV1 receptors.

8. ABBREVIATIONS

- AA: Arachidonic acid.
- ABC: Avidin-biotin peroxidase.
- ABHD6: α/β-hydrolase domain containing 6.
- ABHD12: α/β-hydrolase domain containing 12.
- ACSF: Artificial cerebrospinal fluid.
- ACTH: Adrenocorticotropin hormone
- AEA: Arachidonoyl-ethanolamine or anandamide
- AEA-LTP: Pharmacological Long Term Potentiation mediated by AEA
- 1-AG: 1-arachidonoyl glycerol
- 2-AG: 2-arachidonoyl glycerol
- 2-AG-LTP: Pharmacological Long Term Potentiation mediated by 2-AG.
- AMPA: α-amino-3-hydroxy-5-methyl-isoxazole propionic acid.
- ANOVA: Analysis of variance.
- AS: Acute stress

- BNST: Bed nucleus of the stria terminalis.
- BSA: Bovine serum albumin.

- C: Control
- CB_1-eLTD: CB_1 receptor-dependent excitatory long-term depression.
- CB_1R: Cannabinoid Receptor Type-1.
- CB_2R: Cannabinoid Receptor Type-2.
- CNS: Central Nervous System.
- CPCCoEt: Selective non-competitive mGlu1 antagonist.
- CRH: corticotrophin-release-hormone.
- CRIP1a: Cannabinoid receptor associated protein 1a.
- CS: Chronic stress.

- DAB: 3,3'-diaminobenzidine
- DAG: Diacylglycerol.
- DAGL: Diacylglycerol lipase.
- DG: Dentate Gyrus.
- DML: dentate molecular layer
- DMSO: Dimethyl sulfoxide.
- DSE: depolarization-induced suppression of excitation
- DSI: depolarization-induced suppression of inhibition

- EC: Entorhinal Cortex.
- EC_{50}: Half maximal effective concentration
- eCB: Endocannabinoid.
- EM: Electron microscopy.
- Emax: Efficacy maximum.

- FAAH: Fatty acid amide hydrolase.
- fEPSPs: Field excitatory postsynaptic potentials.

- GABA: Gamma-Aminobutyric acid.
- $GABA_A$: Gamma-Aminobutyric acid Type A.
- $GABA_B$: Gamma-Aminobutyric acid Type B.
- GPCRs: G-protein-coupled receptors.
- GPR55: G protein-coupled receptor 55.

- h: Hours
- HF: Hippocampal formation
- HPA: Hypothalamic-pituitary-adrenocortical
- HF: Hippocampal Formation.

- IAHP: calcium-activated potassium currents.

- LC-MS/MS: Liquid chromatography tandem mass spectrometry.
- LFS: Low-frequency stimulation.
- LM: Light microscopy.
- LPP: Lateral perforant pathway.
- LTD: Long-Term Depression.
  LTP: Long-Term Potentiation.
- L-VGCC: L-type Voltage gated Calcium Channels

- MAGL: Monoacylglicerol lipase.
- MCF: Mossy Cell Fiber.
- mGluR: Group I metabotropic glutamate receptor.
- mGluR5: Metabotropic glutamate receptor 5.
- mGluR1: Metabotropic glutamate receptor 1.
- min: Minutes.
- ML: Molecular layer.
- MO: Medulla Oblongata.

- mPFC: Medial Prefrontal Cortex.
- MPP: Medial Perforant Pathway.
- MRM: multiple-reaction monitoring.

- NAPE: N-arachidonoyl phosphatidylethanolamine.
- NAPE-PLD: N-acyl phosphatidylethanolamine hydrolyzing phospholipase D.
- NMDA: N-methyl-D-aspartate receptor.

- OD: Optical density.

- PB: Phospate buffer.
- PBS: Phosphate buffered saline.
- PFC: Prefrontal cortex.
- PKA: Protein kinase type A.
- PLC: Phospholipase C.
- PND: Postnatal day.
- PPAR-α: Peroxisome Proliferator-Activated Receptors.
- PTX: Picrotoxin.
- PVDF: polyvinylidene fluoride.
- PVN: Paraventricular Nuclei.

- RT: Room temperature.

- s: Seconds.
- SDS: Sodium dodecyl sulfate.
- SDS-PAGE: SDS–polyacrylamide.
- SEM: Standard error mean.
- [^{35}S] GTPγS: [^{35}S] Guanosine-5*-O-(3-thiotriphosphate).

- TBS: Tris-HCl buffered saline.
- THC: (−)-trans-Δ9-tetrahydrocannabinol.
- TRPA1: Transient receptor potential ankyrin 1.
- TRPV1: Transient Receptor Potential Vanilloid 1
- TRPV1-LTD: Long term depression mediated by TRPV1 receptor.

- WB: Western blot.

9. BIBLIOGRAPHY

- **Aguado T**, Monory K, Palazuelos J, Stella N, Cravatt B, Lutz B *et al.* (2005). The endocannabinoid system drives neural progenitor proliferation. FASEB J 19:1704–1706.
- **Aguado T**, Romero E, Monory K, Palazuelos J, Sendtner M, Marsicano G *et al*. (2007). The CB1 cannabinoid receptor mediates excitotoxicity-induced neural progenitor proliferation and neurogenesis. J Biol Chem 282 (33): 23892-23898.
- **Ahn K**, McKinney MK, Cravatt, BF (2008). Enzymatic pathways that regulate endocannabinoid signaling in the nervous system. Chem Rev 108:1687-1707.
- **Alger BE** (2002). Retrograde signaling in the regulation of synaptic transmission: focus on endocannabinoids. Prog Neurobiol 68(4):247–286.
- **Araque A**, Castillo PE, Manzoni OJ, Tonini R (2017). Synaptic functions of endocannabinoid signaling in health and disease. Neuropharmacology 124:13-24.
- **Alhouayek M**, Masquelier J, Muccioli GG (2014). Controlling 2-arachidonoylglycerol metabolism as an anti-inflammatory strategy. Drug Discov Today 19:295-304.
- **Amaral DG**, Witter MP (1989). The three-dimensional organization of the hippocampal formation: a review of anatomical data. Neurosci 31:571-591.
- **Amaral DG**, Scharfman HE, Lavenex P (2007). The dentate gyrus: fundamental neuroanatomical organization (dentate gyrus for dummies). Prog Brain Res 163:3-22.
- **Ameri A** (1999). The effects of cannabinoids on the brain. Prog Neurobiol 58:315–48.
- **Attucci S**, Carlà V, Mannaioni G, Moroni F (2001). Activation of type 5 metabotropic glutamate receptors enhances NMDA responses in mice cortical wedges. Br J Pharmacol 132(4):799-806.
- **Azad SC**, Kurz J, Marsicano G, Lutz B, Zieglgansberger W, Rammes G (2008). Activation of CB1 specifically located on GABAergic interneurons inhibits LTD in the lateral amygdala. Learn Mem 15:143–152.

- **Balsevich G**, Petrie GN, Hill MN (2017). Endocannabinoids: effectors of glucocorticoid signaling. Front Neuroendocrinol 47:86–108.
- **Barrondo S**, Sallés J (2009). Allosteric modulation of 5-HT1A receptors by zinc: Binding studies. Neuropharmacol 56:455-462.
- **Bénard G**, Massa F, Puente N, Lourenço J, Bellocchio, L, Soria-Gómez E, Marsicano G (2012). Mitochondrial CB 1 receptors regulate neuronal energy metabolism. Nature Neurosci *15*(4):558–564.
- **Bender VA**, Bender KJ, Brasier DJ, Feldman DE (2006): Two coincidence detectors for spike timing-dependent plasticity in somatosensory cortex. J Neurosci. 26:4166-4177.
- **Bishop SJ** (2008). Neural mechanisms underlying selective attention to threat. Ann NY Acad Sci 1129:141–152.
- **Bisogno T**, Howell F, Williams G, Minassi A, Cascio MG, Ligresti A et al (2003). Cloning of the first sn1-DAG lipases points to the spatial and temporal regulation of endocannabinoid signaling in the brain. J Cell Biol 163:463–468.
- **Boccara CN**, Kjonigsen LJ, Hammer IM, Bjaalie JG, Leergaard TB, Witter MP (2015). A three-plane architectonic atlas of the rat hippocampal region. *Hippocampus 25*(7):838–857.
- **Bonilla-Del Río I**, Puente N, Peñasco S, Rico I, Gutiérrez-Rodríguez A, Elezgarai I, Grandes P (2017). Adolescent ethanol intake alters cannabinoid type-1 receptor localization in astrocytes of the adult mouse hippocampus. Addiction Biology.
- **Bowles NP**, Hill MN, Bhagat SM, Karatsoreos IN, Hillard CJ, McEwen BS (2012). Chronic, noninvasive glucocorticoid administration suppresses limbic endocannabinoid signaling in mice. Neurosci 204:83 –89.
- **Castillo PE** (2012). Presynaptic LTP and LTD of excitatory and inhibitory synapses. Cold Spring Harbor Perspectives in Biology 4:a005728.

- **Campos AC**, Ferreira FR, Guimarães FS, Lemos JI (2010). Facilitation of endocannabinoid effects in the ventral hippocampus modulates anxiety-like behaviors depending on previous stress experience. Neurosc 167(2):238-46.
- **Canduela MJ**, Mendizabal-Zubiaga J, Puente N, Reguero L, Elezgarai I, Ramos-Uriarte A, Grandes, P (2015). Visualization by high resolution immunoelectron microscopy of the transient receptor potential vanilloid-1 at inhibitory synapses of the mouse dentate gyrus. PLoS ONE 10(3):15–20.
- **Cannistraro PA**, Rauch SL (2003). Neural circuitry of anxiety: evidence from structural and functional neuroimaging studies. Psychopharmacol. Bull. 37: 8–25.
- **Cappaert NLM**, Van Strien NM, Witter MP (2015). Hippocampal Formation. The Rat Nervous System: Fourth Edition (Fourth Edition). Elsevier Inc.
- **Caterina MJ**, Schumacher MA, Tominaga M, Rosen TA, Levine JD, Julius D (1997). The capsaicin receptor: a heat-activated ion channel in the pain pathway. Nature 389(6653):816-24.
- **Charil A**, Laplante DP, Vaillancourt C, King S (2010). Prenatal stress and brain development. Brain Res Rev 65 (1): 56-79.
- **Chávez AE**, Grimes WN, Diamond JS (2010a). Mechanisms underlying lateral GABAergic feedback onto rod bipolar cells in rat retina.
- **Chávez AE**, Chiu CQ, Castillo PE (2010b). TRPV1 activation by endogenous anandamide tirggers postsynaptic LTD in dentate gyrus. Nat Neurosci 13:1511-1518.
- **Chevaleyre V**, Takahashi KA, Castillo PE (2006). Endocannabinoid-mediated synaptic plasticity in the CNS. Annu Rev Neurosci 29:37–76.
- **Chiu CQ**, Castillo PE (2008). Input-specific plasticity at excitatory synapses mediated by endocannabinoids in the dentate gyrus. Neuropharmacology 54:68-78.
- **Cinar R**, Freund TF, Katona I, Mackie K, Szucs M (2008). Reciprocal inhibition of G-protein signaling is induced by CB1 cannabinoid and GABAB receptor interactions in rat hippocampal membranes. Neuroch Intern 52:1402–1409.

- **Cota D**, Marsicano G, Tschop M, Grubler Y, Flachskamm C, Schubert M, *et al.,*(2003). The endogenous cannabinoid system affects energy balance via central orexigenic drive and peripheral lipogenesis. J Clin Investig 112:423–431.
- **Cota D,** Steiner MA, Marsicano G, Cervino C, Herman JP, Grubler Y, *et al.,* (2007). Requirement of cannabinoid receptor type 1 for the basal modulation of hypothalamic-pituitary-adrenal axis function. Endocrinology 148:1574–1581.
- **Cravatt BF**, Giang DK, Mayfield SP, Boger DL, Lerner RA, Gilula NB (1996). Molecular characterization of an enzyme that degrades neuromodulatoryfatty-acidamides. Nature 384:83–87.
- **Crews F**, He J, Hodge C (2007). Adolescent cortical development: a critical period for vulnerability for addiction. Pharmacol Biochem Behav 26:189–99.
- **Cristino L**, Starowicz K, De Petrocellis L, Morishita J, Ueda N, Guglielmotti V *et al.* (2008). Immunohistochemical localization of anabolic and catabolic enzymes for anandamide and other putative endovanilloids in the hippocampus and cerebellar cortex of the mouse brain. Neurosci 151:955–968.
- **Cui Y**, Paillé V, Xu H, Genet S, Delord B, Fino E, *et al.,* (2015). Endocannabinoids mediate bidirectional striatal spike-timing-dependent plasticity. J Physiol 593(13):2833–2849.
- **Cui Y**, Prokin I, Xu H, Delord B, Genet S, Venance L, *et al.,* (2016). Endocannabinoid dynamics gate spike timing dependent depression and potentiation. eLife 5:e13185.
- **Dahl RE** (2004). Adolescent development and the regulation of behavior and emotion: introduction to part VIII. Ann N Y Acad Sci 1021:294-5.
- **De Petrocellis L**, Vellani V, Schiano-Moriello A, Marini P, Magherini PC, Orlando P, *et al.,* (2008). Plant-derived cannabinoids modulate the activity of transient receptor potential channels of ankyrin type-1 and melastatin type-8. J Pharmacol Exp Ther 325:1007-1015.

- **De Petrocellis L**, Di Marzo V (2009). Role of endocannabinoids and endovanilloids in Ca2+ signaling. Cell Calcium 45:611-624.
- **Devane WA**, Hanus L, Breuer A, Pertwee RG, Stevenson LA, Griffin G, *et al.,* (1992). Isolation and structure of a brain constituent that binds to the cannabinoid receptor. Science 258:1946–1949.
- **Di S**, Malcher-Lopes R, Halmos KC, Tasker JG (2003). Nongenomic glucocorticoid inhibition via endocannabinoid release in the hypothalamus: a fast feedback mechanism. J Neurosci 23:4850–4857.
- **Di S**, Malcher-Lopes R, Marcheselli VL, Bazan NG, Tasker JG (2005). Rapid glucocorticoid-mediated endocannabinoid release and opposing regulation of glutamate and gamma-aminobutyric acid inputs to hypothalamic magnocellular neurons. Endocrinology 146:4292–4301.
- **Dubreucq S**, Matias I, Cardinal P, Haring M, Lutz B, Marsicano G *et al.* (2012). Genetic dissection of the role of cannabinoid type-1 receptors in the emotional consequences of repeated social stress in mice. Neuropsychopharmacol 37:1885-1900.
- **Egertová M**, Elphick MR (2000). Localization of cannabinoid receptors in the rat brain using antibodies to the intracellular C-terminal tail of CB. J Comp Neurol 422:159–71.
- **Eiland L**, Romeo RD (2013). Stress and the developing adolescent brain. Neurosci 249:162–171.
- **Evanson NK**, Tasker JG, Hill MN, Hillard CJ, Herman JP (2010). Fast feedback inhibition of the HPA axis by glucocorticoids is mediated by endocannabinoid signaling. Endocrinology 151:4811–4819.
- **Fanselow MS**, Dong HW (2010). Are the dorsal and ventral hippocampus functionally distinct structures?. Neuron 65:7–19.

- **File SE**, Kenny PJ, Cheeta S (2000). The role of the dorsal hippocampal serotonergic and cholinergic systems in the modulation of anxiety. Pharmacol. Biochem. Behav. 66: 65–72.
- **Foster JD**, Kitchen I, Bettler B, Chen Y (2013). $GABA_B$ receptor differentially modulate synaptic inhibition in the dentate gyrus to enhance granule cell output. Br. J. Pharmacol 168 (8): 1808-1819.
- **Fraguas-Sánchez AI**, Fernández-Carballido AM, Torres-suárez AI (2014). Cannabinoides: una prometedora herramienta para el desarrollo de nuevas terapias. An. Real Acad. Farm. 80 (4): 555-577.
- **Freund TF**, Katona I, Piomelli D (2003). Role of endogenous cannabinoids in synaptic signaling. Physiol Rev 83(3):1017–1066.
- **Galiègue S**, Mary S, Marchand J, Dussossoy D, Carrière D, Carayon P, *et al*. (1995). Expression of central and peripheral cannabinoid receptors in human immune tissues and leukocyte subpopulations. Eur J Biochem 232:54-61.
- **Gangletas C**, Girard D, Groc L, Marsicano G, Chaouloff F, Georges F (2013). Stress switches cannabinoid type-1(CB1) receptor-dependent plasticity from LTD to LTP in the Bed Nucleus of the Stria Terminalis. J Neurosci 33(50):19657–19663.
- **Gaoni Y**, Mechoulam R (1964). Isolation structure and partial synthesis of an active constituent of hashish. J Am Chem Soc 86:1646–1647.
- **García del Caño G**, Aretxabala X, González-Burguera I, Montaña M, López de Jesús M, Barrondo S, *et al*. (2015). Nuclear diacylglycerol lipase-α in rat brain cortical neurons: evidence of 2-arachidonoylglycerol production in concert with phospholipase C-β activity. J Neurochem 132:489-503.
- **Gerdeman GL**, Lovinger DM (2003). Emerging roles for endocannabinoids in long-term synaptic plasticity. Br J Pharmacol 140 (5): 781-785.
- **Giedd JN** (2004). Structural magnetic resonance imaging of the adolescent brain. Ann NY Acad Sci 1021:77–85.

- **Golech SA**, McCarron RM, Chen Y, Bembry J, Lenz F, Mechoulam R, *et al* (2004). Human brain endothelium: coexpression and function of vanilloid and endocannabinoid receptors. Brain Res Mol Brain Res 132 (1): 87-92.
- **Gómez-Gonzalo M**, Navarrete M, Perea G, Covelo A, Martín-Fernández M, Shigemoto R, *et al.,* (2014). Endocannabinoids induce lateral Long-Term Potentiation of transmitter release by stimulation of gliotransmission. Cereb Cortex 25(10):3699-712.
- **Graupner M**, Brunel N (2012). Calcium-based plasticity model explains sensitivity of synaptic changes to spike pattern rate and dendritic location. Proc Natl Acad Sci USA 109:3991–3996.
- **Guggenhuber S**, Romo-Parra H, Bindila L, Leschik J, Lomazzo E, Remmers F, *et al.,* (2016). Impaired 2-AG signaling in hippocampal glutamatergic neurons: Aggravation of anxiety-like behavior and unaltered seizure susceptibility. Intern J Neuropsychopharm 1–13.
- **Gutiérrez-Rodríguez A**, Puente N, Elezgarai I, Ruehle, S, Lutz B, Reguero L *et al.,* (2017). Anatomical characterization of the cannabinoid CB $_1$ receptor in cell-type-specific mutant mouse rescue models. J Comp Neurol *525*(2):302–318.
- **Gutiérrez-Rodríguez A**, Bonilla-Del Río I, Puente N, Gómez-Urquijo SM, Fontaine CJ, Egaña-Huguet J *et al.,* (2018). Localization of the cannabinoid type-1 receptor in subcellular astrocyte compartments of mutant mouse hippocampus. *GLIA 66*(7).
- **Gunduz-Cinar O**, Hill MN, McEwen BS, Holmes A (2013a). Amygdala FAAH and anandamide: mediating protection and recovery from stress. Trends Pharmacol Sci 34:637–644.
- **Gunduz-Cinar O**, MacPherson KP, Cinar R, Gamble-George J, Sugden K, Williams B *et al*., (2013b). Convergent translational evidence of a role for anandamide in amygdala-mediated fear extinction threat processing and stress-reactivity. Mol Psychiatry 18:813–823.

- **Hampson RE**, Deadwyler SA (1999). Cannabinoids, hippocampal function and memory. Life Sci 65:715–23.
- **Han J**, Kesner P, Metna-Laurent M, Duan T, Xu L, Georges F (2012). Acute cannabinoids impair working memory through astroglial CB1 receptor modulation of hippocampal LTD. Cell 148:1039–50.
- **Haring M**, Marsicano G, Lutz B, Monory K (2007). Identification of the cannabinoid receptor type 1 in serotonergic cells of raphe nuclei in mice. Neuroscience 146:1212–1219.
- **Hashimotodani Y**, Ohno-Shosaku T, Kano M (2007). Ca(2+)-assisted receptor-driven endocannabinoid release: mechanisms that associate presynaptic and postsynaptic activities. Curr Opin Neurobiol 17(3):360-365.
- **Hebert-Chatelain E**, Reguero L, Puente N, Lutz B, Chaouloff F, Rossignol R, *et al.,* (2014a). Cannabinoid control of brain bioenergetics: Exploring the subcellular localization of the CB1 receptor. Molec Metabolism *3*(4):495–504.
- **Hebert-Chatelain E**, Reguero L, Puente N, Lutz B, Chaouloff, F, Rossignol R, *et al.,* (2014b). Studying mitochondrial CB1 receptors: Yes we can. Molec Metabolism 3(4):339-343.
- **Hebert-Chatelain E**, Desprez T, Serrat R, Bellocchio L, Soria-Gomez E, Busquets-Garcia A, *et al.,* (2016). A cannabinoid link between mitochondria and memory. *Nature 539*(7630):555–559.
- **Heifets BD**, Castillo PE (2009). Endocannabinoid signaling and long-term synaptic plasticity. Annu Rev Physiol 71:283e306.
- **Herkenham M**, Lynn AB, Little MD, Johnson MR, Melvin LS, Decosta BR, *et al.,* (1990). Cannabinoid receptor localization in brain. Proc Natl Acad Sci USA 87:932–1936.

- **Herkenham M**, Lynn AB, Johnson MR, Melvin LS, Decosta BR, Rice KC (1991). Characterization and localization of cannabinoid receptors in rat-brain: a quantitative in vitro autoradiographic study. J Neurosci 11:563–583.
- **Herman JP**, Figueiredo H, Mueller NK, Ulrich-Lai Y, Ostander MM, Choi DC *et al.,* (2003). Central mechanisms of stress integration: hierarchicalcircuitry controlling hypothalamic-pituitary-adrenocortical responsiveness. Front Neuroendocrinol 24:151–180.
- **Herman JP**, Ostrander MM, Mueller NK, Figueiredo H (2005). Limbic system mechanisms of stress regulation: Hypothalamo-pituitary-adrenocortical axis. Prog Neuropsychopharmacol Biol Psychiatry 29:1201–1213.
- **Hermann H**, Marsicano G, Lutz B (2002). Coexpression of the cannabinoid receptor type 1 with dopamine and serotonin receptors in distinct neuronal subpopulations of the adult mouse forebrain. Neuroscie 109:451–460.
- **Hermans EJ**, Battaglia FP, Atsak P, de Voogd LD, Fernandez G, Roozendaal B, (2014). How the amygdala affects emotional memory by altering brain network properties. Neurobiol Learn Mem 112:2–16.
- **Hill MN**, McLaughlin RJ, Morrish AC, Viau V, Floresco SB, Hillard CJ *et al.,* (2009). Suppression of amygdalar endocannabinoid signaling by stress contributes to activation of the hypothalamic-pituitary-adrenal axis. Neuropsychopharmacol 34:2733–2745.
- **Hill MN**, McLaughlin RJ, Bingham B, Shrestha L, Lee TT, Gray JM *et al.,* (2010). Endogenous cannabinoid signaling is essential for stress adaptation. Proc Natl Acad Sci USA 107:9406–9411.
- **Hill MN**, Kumar SA, Filipski SB, Iverson M, Stuhr KL, Keith JM *et al.,* (2013). Disruption of fatty acid amide hydrolase activity prevents the effects of chronic stress on anxiety and amygdalar microstructure. Mol Psychiatry 18:1125–1135.

- **Hillard CJ** (2014). Stress regulates endocannabinoid-CB1 receptor signaling. Semin Immunol 26:380–388.
- **Hillard CJ**, Beatka M, Sarvaideo J (2016). Endocannabinoid signaling and the Hypothalamic-Pituitary Adrenal axis. Compr Physiol 7(1):1–15.
- **Ho KW,** Ward NJ, Calkins DJ (2012). TRPV1: a stress response protein in the central nervous system. Am J Neurodegener Dis 2012;1(1):1-14.
- **Howlett AC**, Barth F, Bonner TI, Cabral G, Casellas P, Devane WA, *et al*., (2002). International Union of Pharmacology. XXVII. Classification of Cannabinoid Receptors. Pharmacol Rev 54:161-202.
- **Hu SS-J**, Mackie K (2015). Distribution of the Endocannabinoid System in the Central Nervous System. Handb Exp Pharmacol, Endocannabinoids. Springer International Publishing 231:59-93.
- **Hunt DL**, Puente N, Grandes P, Castillo PE (2013). Bidirectional NMDA receptor plasticity controls CA3 output and heterosynaptic metaplasticity. Nat Neurosci 16(8):1049-1059.
- **Ishac EJ**, Jiang L, Lake KD, Varga K, Abood ME, Kunos G (1996). Inhibition of exocytotic noradrenaline release by presynaptic cannabinoid CB1 receptors on peripheral sympathetic nerves. Br J Pharmacol 118:2023-2028.
- **Jeong JY**, Lee DH, Kang SS (2013). Effects of chronic restraint stress on body weight, food intake, and hypothalamic gene expressions in mice. Endocrinol Metab 28:288-296.
- **Kano M** (2014). Control of synaptic function by endocannabinoid-mediated retrograde signaling. Proc Japan Acad Series B: Physic and Biol Scienc *90*(7):235–250.
- **Kano M**, Ohno-Shosaku T, Hashimotodani Y, Uchigashima M, Watanabe M (2009). Endocannabinoid-mediated control of synaptic transmission. Physiol Rev 89:309-380.

- **Katona I**, Urban GM, Wallace M, Ledent C, Jung KM, Piomelli D *et al*., (2006). Molecular composition of the endocannabinoid system at glutamatergic synapses. J Neurosci 26:5628-5637.
- **Katona I**, Freund TF (2012). Multiple functions of endocannabinoid signaling in the brain. Annu Rev Neurosci 35:529–58.
- **Kawamura Y**, Fukaya M, Maejima T, Yoshida T, Miura E, Watanabe M *et al.,* (2006). The CB1 cannabinoid receptor is the major cannabinoid receptor at excitatory presynaptic sites in the hippocampus and cerebellum. J Neurosci 26:2991–3001.
- **Koch M**, Varela L, Kim JG, Kim JD, Hernández-Nuño F, Simonds SE, *et al*., (2015). Hypothalamic POMC neurons promote cannabinoid-induced feeding. Nature 519:45-50.
- **Krahn DD**, Gosnell BA, Majchrzak MJ (1990).The anorectic effects of CRH and restraint stress decrease with repeated exposures. Biol Psychiatry 27:1094-102.
- **Lafourcade M**, Elezgarai I, Mato S, Bakiri Y, Grandes P, Manzoni OJ (2007). Molecular components and functions of the endocannabinoid system in mouse prefrontal cortex. PLoS One 2:e709.
- **Lafourcade CA**, Alger BE (2008). Distinctions among $GABA_A$ and $GABA_B$ responses revealed by calcium channel antagonists, cannabinoids, opioids, and synaptic plasticity in rat hippocampus. Psychopharmacol (Berl) 198(4): 539–549.
- **Lanté F**, Cavalier M, Cohen-Solal C, Guiramand J, Vignes M (2006). Developmental switch from LTD to LTP in low frequency-induced plasticity. Hippocampus 16: 981-989.
- **Li CJ**, Lu Y, Zhou M, Zong XG, Li C, Xu XI *et al.,* (2014). Activation of $GABA_B$ receptors ameliorates cognitive imapirment via restoring the balance of HCN1/HCN2 surface expression in the hippocampal CA1 area in rats with chronic cerebral hypoperfusion. Mol. Neurobiol 50 (2): 704-720.

- **Likhtik E**, Paz R (2015). Amygdala-prefrontal interactions in (mal)adaptive learning. Trends Neurosci 38:158–166.
- **Lutz B**, Marsicano G, Maldonado R, Hillard CJ (2015). The endocannabinoid system in guarding against fear, anxiety and stress. Nat Rev Neurosci 16:705–18.
- **Maccarrone M**, Rossi S, Bari M, De Chiara V, Fezza F, Musella A, *et al.,* (2008). Anandamide inhibits metabolism and physiological actions of 2-arachidonoylglycerol in the striatum. Nat Neurosci 11:152-159.
- **Maccarrone M**, Guzmán M, Mackie K, Doherty P, Harkany T (2014). Programming of neural cells by (endo)cannabinoids: from physiological rules to emerging therapies. Nat Rev Neurosci 15:786–801.
- **Maccarone R**, Rapino C, Zerti D, di Tommaso M, Battista N, Di Marco S, *et al.,* (2016). Modulation of Type-1 and Type-2 Cannabinoid Receptors by Saffron in a Rat Model of Retinal Neurodegeneration. PLoS One 11:e0166827.
- **Mackie K** (2005). Distribution of cannabinoid receptors in the central and peripheral nervous system. Handb Exp Pharmacol. Springer Berlin Heidelberg 168:299-325.
- **Mailleux P**, Vanderhaeghen J-J (1992). Distribution of neuronal cannabinoid receptor in the adult rat brain: A comparative receptor binding radioautography and in situ hybridization histochemistry. Neurosci 48:655–68.
- **Mannaioni G**, Marino MJ, Valenti O, Traynelis SF, Conn PJ (2001). Metabotropic glutamate receptors 1 and 5 differentially regulate CA1 pyramidal cell function. J Neurosci 21(16):5925-5934.
- **Marsicano G**, Goodenough S, Monory K, Hermann H, Eder M, Cannich A, *et al*., (2003). CB1 cannabinoid receptors and on-demand defense against excitotoxicity. Science 302: 84-88.
- **Marsicano G**, Lutz B (1999). Expression of the cannabinoid receptor CB1 in distinct neuronal subpopulations in the adult mouse forebrain. Eur J Neurosci 11: 4213–4225.

- **Marsicano G**, Lutz B (2006). Neuromodulatory functions of the endocannabinoid system. J Endocrinol Invest 29: 27-46.
- **Matsuda LA**, Lolait SJ, Brownstein MJ, Young AC, Bonner TI (1990). Structure of a cannabinoid receptor and functional expression of the cloned cDNA. Nature 346: 561–564.
- **Matsuda LA**, Bonner TI, Lolait SJ (1993). Localization of cannabinoid receptor mRNA in rat brain. J Comp Neurol 327: 535–50.
- **McCormick CM**, Mathews IZ (2010). Adolescent development, hypothalamic-pituitary-adrenal function, and programming of adult learning and memory. Prog Neuro-Psychopharmacol Biol Psychiatry 34: 756–765.
- **McEwen BS** (2002). Sex, stress and the hippocampus: allostasis, allostatic load and aging pocces. Neurobiol Ag 23 (5): 921-939.
- **McEwen BS** (2006). Protective and damaging effects of stress mediators: central role of the brain. Dial in Clin Neurosci 8: 367–381.
- **McEwen BS** (2007). Physiology and neurobiology of stress and adaptation: Central role of the brain. Physiol. Rev. 87: 873–904.
- **McEwen BS** (2008). Central effects of stress hormones in health and disease: understanding the protective and damaging effects of stress and stress mediators. Eur J Pharmacol 583 (2-3): 174–185.
- **McEwen BS** (2012). Brain on stress: how the social environment gets under the skin. Proc Natl Acad Sci USA 109(Suppl 2):17180–17185.
- **McEwen BS**, Alves SE (1999). Estrogen actions in the central nervous system. Endos Rev 20 (3): 279-307.
- **McEwen BS**, Bowles PN, Gray, JD, Hill MN, Hunter RG, Karatsoreos IN, *et al.,* (2015). Mechanisms of stress in the brain. Nat Rev Neurosci 18(10):1353–1363.
- **Mechoulam R**, Ben-Shabat S, Hanus L, Lingumski NE, Schatz AR, Gopher A *et al.,* (1995). Identification of an endogenous 2-monoglyceride, present in canine gut, that binds to cannabinoid receptors. Biochem Pharmacol 50:83–90.

- **Mechoulam R**, Parker LA (2013). The endocannabinoid system and the brain. Annu Rev Psychol 64:21–47.
- **Mendizabal-Zubiaga J**, Melser S, Bénard G, Ramos A, Reguero L, Arrabal S *et al.,* (2016). Cannabinoid CB1 Receptors Are Localized in Striated Muscle Mitochondria and Regulate Mitochondrial Respiration. *Frontiers in Physiology 7*.
- **Moldrich G**, Wenger T (2000). Localization of the CB1 cannabinoid receptor in the rat brain. An immunohistochemical study. Peptides 21: 1735-1742.
- **Monory K**, Massa F, Egertová M, Eder M, Blaudzun H, Westenbroek R *et al.,* (2006). The endocannabinoid system controls key epileptogenic circuits in the hippocampus. Neuron 51:455–66.
- **Montaña M**, García del Caño G, López de Jesús M, González-Burguera I, Echeazarra L, Barrondo S *et al.,* (2012). Cellular neurochemical characterization and subcellular localization of phospholipase C β1 in rat brain. Neurosci 222:239-268.
- **Morena M**, Patel S, Bains JS, Hill MN (2016). Neurobiological interactions between stress and the endocannabinoid system. Neuropsychopharmacol *41*(1):80–102. -
- **Morozov YM**, Torii M, Rakic P (2009). Origin, early commitment, migratory routes, and destination of cannabinoid type 1 receptor-containing interneurons. Cereb Cortex Suppl 1:i78-89.
- **Munro S**, Thomas KL, Abu-Shaar M (1993). Molecular characterization of a peripheral receptor for cannabinoids. Nature 365:61–65.
- **Navarrete M**, Araque A (2008). Endocannabinoids mediate neuron-astrocyte communication. Neuron 57:883-893.
- **Navarrete M**, Araque A (2010). Endocannabinoids potentiate synaptic transmission through stimulation of astrocytes. *Neuron 68*(1):113–126.

- **Navarrete M**, Perea G, Fernandez de Sevilla D, Gómez-Gonzalo M, Núñez A, Martín ED *et al.,* (2012). Astrocytes mediate in vivo cholinergic-induced synaptic plasticity. PLoS Biol 10(2):e1001259.
- **Nazari M**, Komaki A, Karamian R, Shahidi S, Sarihi A, Asadbegi M (2016). The interactive role of CB_1 and $GABA_B$ receptors in hippocampal synaptic plasticity in rats. Br Research Bul 120:123-130.
- **Neyman S** and Manahan-Vaughan D (2008). Metabotropic glutamate receptor 1 (mGluR1) and 5 (mGluR5) regulate late phases of LTP and LTD in the hippocampal CA1 region in vitro. Eur J Neurosci 27(6):1345-1352.
- **Ohno-Shosaku T**, Kano M (2014). Endocannabinoid-mediated retrograde modulation of synaptic transmission. Curr Opin Neurobiol 29:1 –8.
- **Oropeza VC**, Mackie K, Van Bockstaele EJ (2007). Cannabinoid receptors are localized to noradrenergic axon terminals in the rat frontal cortex. Brain Res 1127:36–44.
- **Pagotto U**, Marsicano G, Fezza F, Theodoropoulou M, Grübler Y, Stalla J *et al.,* (2001). Normal human pituitary gland and pituitary adenomas express cannabinoid receptor type 1 and synthesize endogenous cannabinoids: first evidence for a direct role of cannabinoids on hormone modulation at the human pituitary level. J Clin Endocrinol Metab 86:2687–2696.
- **Patel S**, Roelke CT, Rademacher DJ, Cullinan WE, Hillard CJ (2004). Endocannabinoid signaling negatively modulates stress-induced activation of the hypothalamicpituitary-adrenal axis. Endocrinology 145:5431–5438.
- **Patel S**, Roelke CT, Rademacher DJ, Hillard CJ (2005). Inhibition of restraint stress-induced neural and behavioural activation by endogenous cannabinoid signalling. Eur J Neurosci 21:1057–1069.
- **Patel S**, Hillard CJ (2008). Adaptation in endocannabinoid signaling in response to repeated homotypic stress: A novel mechanism for stress habituation. Eur J Neurosci 27(11):2821-2829.

- **Patel S**, Kingsley PJ, Mackie K, Marnett LJ, Winder DG (2009). Repeated homotypic stress elevates 2-arachidonoylglycerol levels and enhances short-term endocannabinoid signaling at inhibitory synapses in basolateral amygdala. Neuropsychopharmacol 34:2699–2709.
- **Patton GC**, Viner R (2007). Pubertal transitions in health. Lancet Mar 31; 369(9567):1130-1139.
- **Peñasco S**, Mela V, López-Moreno JA, Viveros MP, Marco EM (2015). Early maternal deprivation enhances voluntary alcohol intake induced by exposure to stressful events later in life. Neural Plast 2015:342761.
- **Peñasco S**, Rico-Barrio I, Puente N, Gómez-Urquijo SM, Fontaine CJ, Egaña-Huguet J *et al.,* (2019). Endocannabinoid Long-Term Depression Revealed at Medial Perforant Path Excitatory Synapses in the Dentate Gyrus. Neuropharmacol Under Review.
- **Pertwee RG** (2001). Cannabinoid receptors and pain. Prog Neurobiol 63:569-611.
- **Pertwee RG** (2005). Pharmacological actions of cannabinoids. Handb Exp Pharmacol 168:1 –51.
- **Pertwee RG** (2015). Endocannabinoids and their pharmacological actions, in: Handb Exp Pharmacol pp. 1–37.
- **Piomelli D** (2003). The molecular logic of endocannabinoid signaling. Nat Rev Neurosci 4:873–84.
- **Piomelli D** (2014). More surprises lying ahead. The endocannabinoids keep us guessing. Neuropharmacol. 76 Pt B 228–34.
- **Puente N**, Elezgarai I, Lafourcade M, Reguero L, Marsicano G *et al*., (2010a) Localization and Function of the Cannabinoid CB1 Receptor in the Anterolateral Bed Nucleus of the Stria Terminalis. PLoS ONE 5(1):e8869.
- **Puente N**, Mendizabal-Zubiaga J, Elezgarai I, Reguero L, Buceta I, Grandes P (2010b). Precise localization of the voltage-gated potassium channel subunits

Kv3.1n and Kv3.3 revealed in the molecular layer of the rat cerebellar cortex by a pre-embedding immunogold method. Histochem Cell Biol 134(4):403-409.

- **Puente N**, Cui Y, Lassalle O, Lafourcade M, Georges F, Venance L *et al.,* (2011). Polymodal activation of the endocannabinoid system in the extended amygdala. Nature Neurosci *14*(12):1542–1547.
- **Puente N**, Reguero L, Elezgarai I, Canduela MJ, Mendizabal-Zubiaga J, Ramos-Uriarte A *et al.,* (2015). The transient receptor potential vanilloid-1 is localized at excitatory synapses in the mouse dentate gyrus. Brain Structure and Function 220(2):1187–1194.
- **Puente N**, Bonilla-Del Río I, Achicallende S, Nahirney PC, Grandes P (2019). High-resolution Immunoelectron Microscopy Techniques for Revealing Distinct Subcellular Type 1 Cannabinoid Receptor Domains in Brain. Bio-Protoc 9(2):1-18.
- **Rademacher DJ**, Meier SE, Shi L, Ho WS, Jarrahian A, Hillard CJ (2008). Effects of acute and repeated restraint stress on endocannabinoid content in the amygdala, ventral striatum, and medial prefrontal cortex in mice. Neuropharmacology 54:108–116.
- **Razzoli M**, Bartolomucci A (2016). The dichotomous effect of chronic stress on obesity. Trends Endocrinol Metab 27:504–515.
- **Razzoli M**, Pearson C, Crow S, Bartolomucci A (2017). Stress, overeating and obesity: Insights from human studies and preclinical models. Neurosci Biobehav Rev 76(A):154-162.
- **Reguero L**, Puente N, Elezgarai I, Mendizabal-Zubiaga J, Canduela MJ, Buceta I, *et al*. (2011). GABAergic and cortical and subcortical glutamatergic axon terminals contain CB_1 cannabinoid receptors in the ventromedial nucleus of the hypothalamus. PLoS One 6:e26167.
- **Reguero L**, Puente N, Elezgarai I, Ramos-Uriarte A, Gerrikagoitia I, Bueno-López JL *et al.,* (2014). Subcellular localization of NAPE-PLD and DAGL-α in the

ventromedial nucleus of the hypothalamus by a preembedding immunogold method. Histochem Cell Biol 141(5):543-550.

- **Rico-Barrio I**, Peñasco S, Puente N, Ramos A, Fontaine C, Reguero L *et al.,* (2018). Cognitive and neurobehavioral benefits of an enriched environment on young adult mice after chronic ethanol consumption during adolescence. Addict Biol Aug 14.
- **Robbe D**, Kopf M, Remaury A, Bockaert J, Manzoni OJ (2002). Endogenous cannabinoids mediate long-term synaptic depression in the nucleus accumbens. Proc Natl Acad Sci USA 99:8384-8388.
- **Robertson Blackmore EK**, Stansfeld SA, Weller I, Munce S, Zagorski BM, Stewart DE (2007). Major depressive episodes and work stress: Results from a national population survey. Am J Public Health 97:2088–93.
- **Romeo R** (2017). The impact of stress on the structure of the adolescent brain: Implications for adolescent mental health. Brain Research. 1654:185-191.
- **Roozendaal B**, McEwen BS, Chattarji S (2009). Stress, memory and the amygdala. Nat Rev Neurosci 10:423–433.
- **Ross RA** (2003). Anandamide and vanilloid TRPV1 receptors. Br J Pharmacol 140(5):780-801.
- **Rossi S**, Motta C, Musella A, Centonze D (2015). The interplay between inflammatory cytokines and the endocannabinoid system in the regulation of synaptic transmission. Neuropharmacol 96:105-112.
- **Rubino T**, Guidali C, Vigano D, Realini N, Valenti M, Massi P *et al.,* (2008). CB1 receptor stimulation in specific brain areas differently modulate anxiety-related behaviour. Neuropharmacol 54:151–160.
- **Ruehle S**, Remmers F, Romo-Parra H, Massa F, Wickert M, Wortge S *et al.,* (2013). Cannabinoid CB1 receptor in dorsal telencephalic glutamatergic neurons: distinctive sufficiency for hippocampus-dependent and amygdala-dependent synaptic and behavioral functions. J Neurosci 33:10264–10277.

- **Ryberg E**, Larsson N, Sjögren S, Hjorth S, Hermansson N-O, Leonova J, *et al*. (2007). The orphan receptor GPR55 is a novel cannabinoid receptor. Br J Pharmacol 152:1092-1101.
- **Salio C**, Doly S, Fischer J, Franzoni MF, Conrath M (2002). Neuronal and astrocytic localization of the cannabinoid receptor-1 in the dorsal horn of the rat spinal cord. Neurosci Lett 329(1):13-6.
- **Sapolsky RM**, Romero LM, Munck AU (2000). How do glucocorticoids influence stress responses? Integrating permissive, suppressive, stimulatory, and preparative actions. Endocr Rev 21:55–89.
- **Scarante FF**, Vila-Verde C, Detoni VL, Ferreira-Junior NC, Guimarães FS, Campos AC (2017). Cannabinoid Modulation of the Stressed Hippocampus. Front Molec Neurosci, 10(December), 1–17.
- **Schulte K**, Steingrüber N, Jergas B, Redmer A, Kurz CM, Buchalla R, *et al*. (2012). Cannabinoid CB1 receptor activation, pharmacological blockade, or genetic ablation affects the function of the muscarinic auto- and heteroreceptor. Naunyn Schmiedebergs Arch Pharmacol 385:385-396.
- **Schultz C**, Engelhardt M (2014). Anatomy of the hippocampal formation. The Hippocampus in Clinical Neuroscience. Front Neurol Neurosci Basel Karger 34:6-17.
- **Senst L**, Bains J (2014). Neuromodulators, stress and plasticity: a role for endocannabinoid signaling. J Exp Biol 217:102-108.
- **Shouval HZ**, Bear MF, Cooper LN (2002). A unified model of NMDA receptor-dependent bidirectional synaptic plasticity. Proc Natl Acad Sci USA 99:10831–10836.
- **Sisk CL**, Foster DL (2004). The neural basis of puberty and adolescence. Nat Neurosci 7:1040–1047.

- **Sjöström PJ**, Turrigiano GG, Nelson SB (2003): Neocortical LTD via coincident activation of presynaptic NMDA and cannabinoid receptors. Neuron 39:641-654.
- **Spear LP** (2000). The adolescent brain and age-related behavioral manifestations. Neurosci Biobehav Rev 24:417–63.
- **Steindel F**, Lerner R, Häring M, Ruehle S, Marsicano G, Lutz B *et al.,* (2013). Neuron-type specific cannabinoid-mediated G protein signaling in mouse hippocampus. J Neurochem 124:1–13.
- **Sticht MA**, Lau DJ, Keenan CM, Cavin JB, Morena M, Vemuri VK *et al.,* (2018). Endocannabinoid regulation of homeostatic feeding and stress-induced alterations in food intake in male rats. British J Pharmacol 16(July).
- **Sugiura T**, Kishimoto S, Oka S, Gokoh M (2006). Biochemistry, pharmacology and physiology of 2-arachidonoylglycerol, an endogenous cannabinoid receptor ligand. Prog Lipid Res 45:405-446.
- **Sumislawski JJ**, Ramikie TS, Patel S (2011). Reversible Gating of Endocannabinoid Plasticity in the Amygdala by Chronic Stress: A Potential Role for Monoacylglycerol Lipase Inhibition in the Prevention of Stress-Induced Behavioral Adaptation. Neuropsychopharmacol 36:2750-2761.
- **Sun Y**, Alexander SPH, Kendall DA, Bennett AJ (2006). Cannabinoids and PPAR alpha signaling. Biochem Soc Trans 34:1095-1097.
- **Tordera RM**, Totterdell S, Wojcik SM, Brose N, Elizalde N, Lasheras B *et al* (2007). Enhanced anxiety, depressive-like behaviour and impaired recognition memory in mice with reduced expression of the vesicular glutamate transporter 1 (VGLUT1). Eur J Neurosci 25(1):281-290.
- **Tóth A**, Blumberg PM, Boczán J (2009). Anandamide and the vanilloid receptor (TRPV1). Vitam Horm 81:389-419.
- **Tsou K**, Brown S, Sañudo-Peña M, Mackie K, Walker J (1998). Immunohistochemical distribution of cannabinoid CB1 receptors in the rat central nervous system. Neurosci 83:393–411.

- **Uchigashima M**, Narushima M, Fukaya M, Katona I, Kano M, Watanabe M (2007). Subcellular arrangement of molecules for 2-arachidonoyl-glycerol-mediated retrograde signaling and its physiological contribution to synaptic modulation in the striatum. J Neurosci 27:3663-3676.
- **Ulrich-Lai YM**, Ryan KK (2014). Neuroendocrine circuits governing energy balance and stress regulation: Functional overlap and therapeutic implications. Cell Metab 19:910–925.
- **Wamsteeker JI**, Kuzmiski JB, Bains JS (2010). Repeated stress impairs endocannabinoid signaling in the paraventricular nucleus of the hypothalamus. J Neurosci 30:11188–11196.
- **Wang M**, Hill MN, Zhang L, Gorzalka BB, Hillard CJ, Alger BE (2012). Acute restraint stress enhances hippocampal endocannabinoid function via glucocorticoid receptor activation. J Psychopharmacol 26:56 –70.
- **Wang W**, Sun D, Pan B, Roberts CJ, Sun X, Hillard CJ *et al*., (2010). Deficiency in endocannabinoid signaling in the nucleus accumbens induced by chronic unpredictable stress. Neuropsychopharmacol 35:2249–2261.
- **Wang W**, Trieu BH, Palmer LC, Jia Y, Pham DT, Jung KM *et al.,* (2016). A primary cortical input to hippocampus expresses a pathway-specific and endocannabinoid-dependent form of Long-Term Potentiation. eNeuro. 3(4):e0160-16.2016.
- **Wittmann G**, Deli L, Kallo I, Hrabovszky E, Watanabe M, Liposits Z *et al.,* (2007). Distribution of type 1 cannabinoid receptor (CB1)-immunoreactive axons in the mouse hypothalamus. J Compd Neurol 503:270–279.
- **Yoshida T**, Uchigashima M, Yamasaki M, Katona I, Yamazaki M, Sakimura K *et al.,* (2011). Unique inhibitory synapse with particularly rich endocannabinoid signaling machinery on pyramidal neurons in basal amygdaloid nucleus. Proc Natl Acad Sci USA 108:3059–3064.

- **Ziegler CG**, Mohn C, Lamounier-Zepter V, Rettori V, Bornstein SR, Krug AW *et al.,* (2010). Expression and function of endocannabinoid receptors in the human adrenal cortex. Horm Metab Res 42:88–92.
- **Zou S**, Kumar U (2018). Cannabinoid receptors and the endocannabinoid system: Signaling and function in the central nervous system. Int J Mol Sci 19:833.
- **Zygmunt PM**, Ermund A, Movahed P, Andersson DA, Simonsen C, Jönsson BAG (2013). Monoacylglycerols activate TRPV1 - A link between phospholipase C and TRPV1. *PLoS ONE 8*(12).